TRANSPORTATION RESEARCH RECORD 692

Adhesive Materials, Paints, and Corrosion

TRANSPORTATION RESEARCH BOARD

COMMISSION ON SOCIOTECHNICAL SYSTEMS
NATIONAL RESEARCH COUNCIL

NATIONAL ACADEMY OF SCIENCES
WASHINGTON, D.C. 1978

Transportation Research Record 692
Price $3.00

modes
1 highway transportation
3 rail transportation
4 air transportation

subject areas
32 cement and concrete
34 general materials
40 maintenance

Transportation Research Board publications are available by ordering directly from the board. They may also be obtained on a regular basis through organizational or individual supporting membership in the board; members or library subscribers are eligible for substantial discounts. For further information, write to the Transportation Research Board, National Academy of Sciences, 2101 Constitution Avenue, N.W., Washington, DC 20418.

Library of Congress Cataloging in Publication Data
National Research Council. Transportation Research Board.
Adhesive materials, paints, and corrosion.

(Transportation research record; 692)
Six reports prepared for the 57th annual meeting of the Transportation Research Board.
1. Road materials—Congresses. 2. Corrosion and anti corrosives—Congresses. 3. Paint—Testing—Congresses. 4. Road markings—Materials—Testing—Congresses. I. Title. II. Series.
TE7.H5 no. 692 [TE200] 380.5'08s [625.8]
ISBN 0-309-02838-8 79-17217

Sponsorship of the Papers in This Transportation Research Record

GROUP 2—DESIGN AND CONSTRUCTION OF TRANSPORTATION FACILITIES
Eldon J. Yoder, Purdue University, chairman

Concrete Section
Carl F. Crumpton, Kansas Department of Transportation, chairman

Committee on Curing of Concrete
Richard E. Hay, Federal Highway Administration, chairman
Edward A. Abdun-Nur, Cecil H. Best, E. J. Breckwoldt, E. R. Davis, Ben E. Edwards, William E. Elmore, Roderick R. Harris, Samuel B. Helms, Paul Klieger, William L. Kubie, Bryant Mather, Harry H. McLean, Alvin H. Meyer, V. Ramakrishnan, Floyd O. Slate, Don L. Spellman, Val Worona

General Materials Section
Roger V. LeClerc, Washington State Department of Transportation, chairman

Committee on Coatings, Signing, and Marking Materials
K. K. Moore, Texas State Department of Highways and Public Transportation, chairman
Harold C. Rhudy, North Carolina Department of Transportation, secretary
Carroll E. Caltrider, Jr., Robert L. Davidson, William E. Douglas, Clarence W. Gault, Edward T. Harrigan, John S. Humphries, William B. Isaacson, John D. Keane, John C. Moore, E. W. Myers, A. J. Permoda, James R. Ritter, Burton M. Rudy, Lothar S. Sander, Frank D. Shepard, Leroy W. Shuger, W. R. Tooke, Jr.

Committee on Corrosion
Harold J. Fromm, Ministry of Transportation and Communications, chairman
Kenneth J. Boedecker, Jr., Robert P. Brown, John F. Cavanaugh, Kenneth C. Clear, Seymour K. Coburn, Israel Cornet, Carl F. Crumpton, William J. Ellis, E. T. Franzen, William F. Gerhold, John D. Keane, Ray I. Lindberg, Robert A. Manson, A. H. Roebuck, Arnold M. Rosenberg, Joseph E. Ross, Richard F. Stratful, F. O. Waters, Frank O. Wood, Leonard E. Wood

William G. Gunderman and Bob H. Welch, Transportation Research Board staff

Sponsorship is indicated by a footnote at the end of each report. The organizational units and officers and members are as of December 31, 1977.

Contents

Improving Thermoplastic Stripe Adhesion on Concrete Pavements

Steven D. Hofener, Texas Transportation Institute, Texas A&M University, College Station

Thermoplastic striping material can be used as a pavement-marking system and has several advantages over other systems; however, it also has the disadvantage that, in some cases, the entire system is lost prematurely. These failures have been attributed to faulty application procedures. This paper examines four important possible application criteria—the temperature of the molten thermoplastic material, the air temperature, the pavement temperature, and the moisture condition of the pavement—for inclusion in a specification. A minimum bond strength necessary to ensure an acceptable service life of the material of 862 kPa (125 lbf/in^2) is suggested. It was concluded that (a) the temperature of the thermoplastic material at application is important, and a small range should be specified based on test results; (b) the air temperature does not affect the bond strength and should not be included in a specification; (c) the temperature of the pavement is an important criterion, and no thermoplastic material should be applied to pavements colder than 12.8°C (55°F); and (d) the moisture in the pavement has relatively little effect on the adhesion, and thermoplastic may be applied to any surface-dry pavement.

In the past 10 years, the highway departments of this nation have taken many steps toward achieving safety for the motorist. There is a continual search for new safety devices that will save lives. Some of the major accomplishments include improvements in the geometric design of highways, better and more-standardized signing, and better highway alignments. All of these improvements have added to the safety of the driver, but they have also allowed for faster speeds. At these higher speeds, a driver must assign priorities to that which he or she will see and react to. These priorities are first, positional information; second, situational information; and third, navigational information (1). If the first priority, alignment in the traffic lane, requires all of the driver's time, then the other significant information will be ignored. For this reason, it is most important that the roadway be well defined under all conditions. Traffic engineers have realized the importance of lane lines; consequently, there is a continual maintenance program in most states to replace worn stripes. At present, in most states, lane lines on heavily traveled roadways are replaced as often as 3 times/year, and Iowa reports that the line is "frequently absent during a considerable portion of the winter period" (2). The failure of the stripe can be due to many factors, but the life of the stripe can be shortened drastically by bad application procedures. The cost and, more importantly, the personpower of reapplication becomes burdensome to the departments.

The delineation systems in use today around the country are many in number. Most of these striping systems have shortcomings that may range from poor wet-night visibility to high losses because of unprojected failures. With the limited budgets of most agencies today, these premature losses cannot be afforded. The thermoplastic stripe system is one such system. Excessive losses of thermoplastic stripe systems are particularly common in areas in which snowplows are frequently used and, in many cases, for unexplainable reasons. Thermoplastic striping, on the other hand, is a very durable material and has a service life projected to be up to 5 years. The system is also far better than most in a wet-night situation.

The price of thermoplastic striping as projected in 1972 for a 5-year effective-life cost analysis was $2.00/m ($0.61/ft) on concrete and $1.08/m ($0.33/ft) on bituminous surfaces (3). The high cost on concrete reflected its limited service life. The lower cost on bituminous surfaces, although high compared with that of an equivalent paint stripe, is competitive with other systems. The advantages of thermoplastic striping outweigh its expense as compared with conventional paint. The question then becomes, can the losses on concrete pavements be reduced and such a system be made economically competitive?

In the research reported in this paper, the failure mechanisms were investigated of the losses of thermoplastic striping in winter. Second, because a comprehensive specification for thermoplastic stripe applications is needed, requirements are suggested that should be included in a draft specification to ensure the adhesion necessary to avoid losses.

THE PROBLEM

Generally, striping, whether it be paint or thermoplastic, does well on most bituminous pavements but experiences extensive failures on concrete surfaces (and new concrete surfaces are the worst). A letter requesting information pertaining to this peculiarity was sent to highway departments in five states in an attempt to identify the source of the problem. The responses indicated that the prevalent mode of failure on bituminous pavements subjected to snowplow activity is due to shaving of the thermoplastic rather than to adhesive failure. The opposite is true on concrete pavements; lack of adhesion between the thermoplastic and the pavement is the prevalent failure mechanism. A further indication of the lack of performance of thermoplastics on concrete pavements is found in a report (4) in which this statement was made: "It has been well documented that most paints perform better on bituminous surfaces than on portland cement concrete". The problem on concrete pavements is one of adhesion and is generally not encountered on bituminous pavements. Many conjectures have been made as to why this is true, but a definitive answer has never been offered. This paper does not attempt to explain completely the phenomenon; however, it does quantify several factors that are necessary for obtaining good adhesion. Because of the general acceptance of the performance of thermoplastic striping on bituminous pavements, the typical value of the adhesion of thermoplastic to bituminous pavements was used as a quantitative standard for comparison with adhesion on concrete pavements.

THEORY OF FAILURES

Four aspects of application procedures were studied to determine their effects on the adhesion properties of thermoplastics:

1. The temperature of the molten thermoplastic material,
2. The air temperature,
3. The pavement temperature, and

Table 1. Summary of specifications.

Specification	Plastic Temperature (°C)	Air Temperature (°C)	Pavement Temperature (°C)	Moisture Condition
California	204-218			
Illinois	177-246	10		
Oklahoma	177-260 (as per manufacturer's recommendation)		4	Dry pavement
Texas			10	Dry pavement
British Standards	Manufacturer's recommendation		5	Can dry by heating
AASHTO	211 ± 7			
ITE	191-246			

Note: $t°C = (t°F - 32)/1.8$.

4. The pavement moisture content.

A literature search was conducted of the current specifications of four states [California (5), Illinois (6), Oklahoma (7), and Texas (8)] and the specifications published by the Institute of Transportation Engineers (ITE) (9), the American Association of State Highway and Transportation Officials (AASHTO) (10), and the British Standards Institution (11). The consistency of these specifications pertaining to the four aspects is summarized in Table 1. The first aspect, temperature of the molten thermoplastic material, has been ignored in most specifications, the belief being that these materials will not function properly if not heated to the right temperature. The specifications reviewed showed a maximum range from 177°C to 260°C (350°F to 500°F), i.e., that practiced in Oklahoma. A stipulation sometimes was added that the temperature should be based on the manufacturer's recommendations. The wide range might be deemed necessary by the fact that there are numerous generically different formulations in use today. Thus, the effects were explored of small temperature variations on the adhesion of the thermoplastic to determine whether an application-temperature limitation is necessary and, if so, what ranges should be used. Because of the possibility of individual temperature ranges for different materials, in these tests all parameters (including the type of material) except temperature were maintained constant.

The second application specification in use today is that of a minimum air temperature that must exist before application can begin. Many failures have been linked to applications made on cold days or early in the morning, suggesting a temperature at application that is too low. The specification search showed that only one state organization specifies minimum air temperatures [Illinois, which specifies a minimum air temperature of 10°C (50°F)]. The research in this area was initiated by the conjecture that the air temperature is not as critical to good adhesion as is the pavement temperature. A room-temperature pavement [22.8°C (73°F)] was used to simulate striping on warm pavements at times when the air may already be cool (as in the early evening). A range of air temperatures was used to determine the effects, if any, that cold air temperatures have on the adhesion of the thermoplastic material to the pavement and whether a specification of air temperature is necessary. In these tests all parameters except air temperature were kept constant.

The third step was to determine the effects of pavement temperatures on the adhesion of thermoplastic. The theory behind this type of failure is similar to that discussed above; that is, a high percentage of failures is related to cold pavements. The problem again is intensified on concrete pavements. The literature search showed that three organizations specify pavement temperatures [Oklahoma, which stipulates 4.4°C (40°F) and rising; the British Standards Institution, which specifies 5°C (41°F); and Texas, which specifies 10°C (50°F)]. The research was devised to demonstrate quantitatively a temperature at which thermoplastic should not be applied. Alleviation of unnecessary failures, whether by air-temperature or pavement-temperature specification, is of utmost importance in the conservation of monies and personpower.

The fourth aspect studied involved the effects of pavement moisture on the adhesion of thermoplastic to pavement. Much research has been conducted related to the time span necessary between the conclusion of a rainstorm and the application of paint stripes. Many agencies require a drying period of at least 48 h before paint application. On the contrary, there has been almost no research on the effects of moisture on the adhesion of thermoplastic. Early morning moisture also has been blamed as a cause of failure. The specification search showed that no agency specifies a drying period. The British specification does suggest that the pavement can be dried by flame if it is wet. If moisture has an effect on adhesion, most organizations are in need of a quantitative specification. The major difficulty lies in a method of measurement of the pavement moisture content.

TEST PROCEDURES

Because there were no practical tests available, the first step was to devise a bond-strength test to measure specifically the direct tensile strength of the adhesion of the thermoplastic to a substrate. The test was arranged so that the different adverse conditions could be measured quantitatively. This bond-strength test was the basic test of the research and was conducted on a test material and a test primer at both room temperature (22.8°C) and a freezing temperature [-17.8°C (0°F)]. The test material and the primer consisted of a commercial material and a primer extensively used in the field chosen to represent an average system common to most products in use today.

A brief description of the testing apparatus used is in order. The equipment was devised at the Texas Transportation Institute, originally to measure the tensile bond strength of concrete pavements (12). Later it was revised to accommodate the testing of the thermoplastic adhesion. The test uses the following components:

1. Portland cement concrete blocks, 8.9×19.1×39.4 cm (3.5×7.5×15.5 in), that have been sandblasted and conditioned for at least 24 h in a 22.8°C environment (Figure 1);
2. A thermoplastic patty form (Figure 2);
3. Six 5.1-cm (2-in) diameter cylinders (Figure 3);
4. The direct tensile tester (Figure 4), and
5. Epoxy cement glue or its equivalent.

Figure 1. Test concrete blocks.

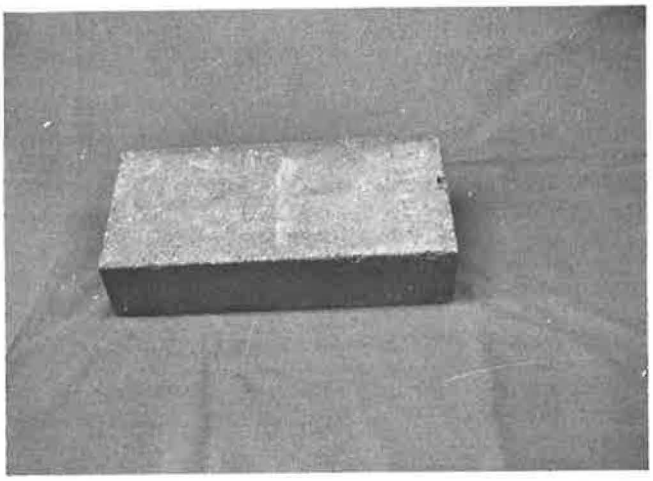

Figure 2. Thermoplastic patty form.

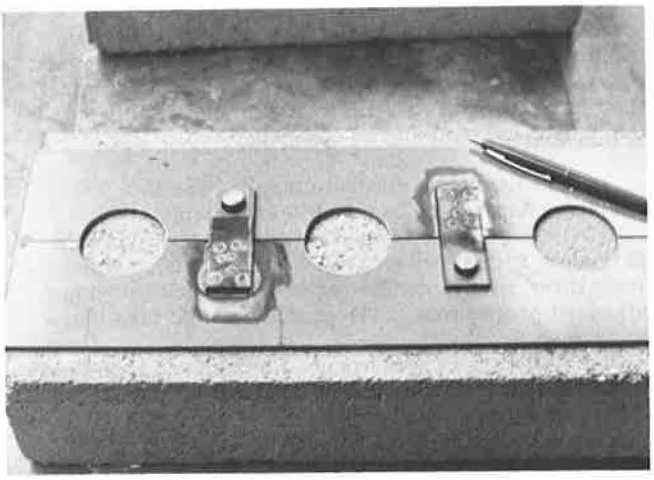

Figure 3. Aluminum cylinders.

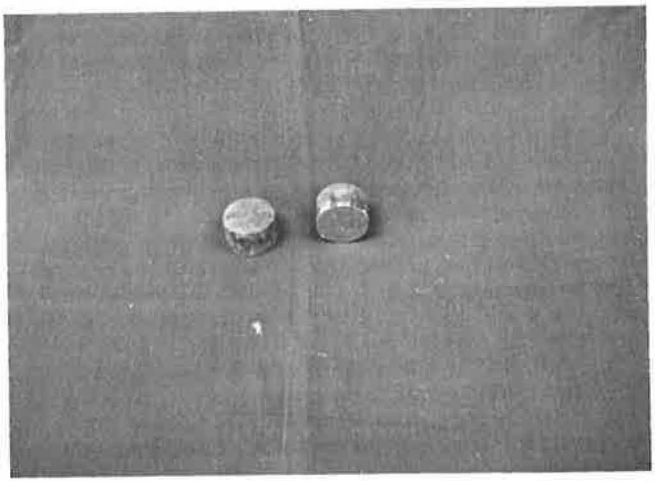

The test procedure is as follows:

1. Heat the thermoplastic material to 204°C (400°F).
2. Apply the test primer at an approximate thickness of 0.005 cm (2 mils) and allow a 10-min curing time.

Figure 4. Bond-strength test apparatus.

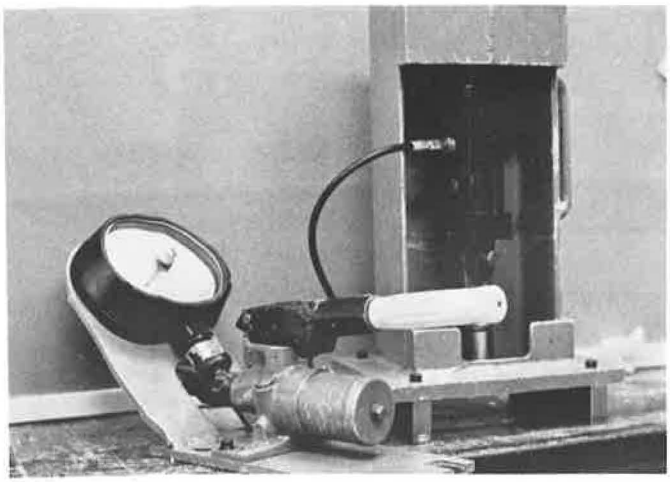

3. Remove the can of heated thermoplastic material and stir well.
4. Pour six 5.1-cm-diameter patties of the thermoplastic material into the patty form on the concrete blocks (three each on two separate blocks) and remove any excess material above the top of the form.
5. Allow to cure for 24 h.
6. Glue one of the 5.1-cm-diameter cylinders to each thermoplastic patty, taking care not to allow any epoxy to flow over the thermoplastic or removing any that does, and allow a proper curing time for the epoxy (24 h).
7. Cool one block in a -17.8°C environment for 24 h.
8. After the cooling period, test the bond strength of each patty—screw the coupler of the tensile tester into the metal cylinder and connect the coupler to the hydraulic cylinder; then apply a tensile stress to the thermoplastic at a loading rate of 890 N/min (200 lbf/min), which is equivalent to 518 kPa/min (75 lbf/in^2/min); and carefully note the pressure required to pull the material from the concrete.
9. Use the thermoplastic samples that have been subjected to normal (22.8°C) temperatures and repeat step 8.

In reporting the results, the tensile strength of the material was obtained by multiplying 0.375 (the effective area of the hydraulic cylinder) by the gauge reading obtained when the bond was broken and dividing the product by the square of the radius of the metal cylinder. The type of failure was noted as either epoxy, thermoplastic, bond, or concrete or any combination of them (see Figure 5). An epoxy failure was a failure of the epoxy to join the aluminum cylinder to the thermoplastic patty. A thermoplastic failure was a cohesive failure in the thermoplastic itself. A bond failure was an adhesive failure in the primer between the thermoplastic and the substrate. Finally, a concrete failure was the removal of a large piece of concrete.

The test produced quantitative results that were for the most part reproducible. Many factors appeared to contribute to the inconsistency of the results, and the different types of failures made the analysis difficult. The concrete and thermoplastic failure showed adhesion in excess of the recorded value, and the use of this value as is would be conservative. The epoxy failures were felt to be laboratory-procedure errors. Fortunately, no real epoxy failures were encountered in the research.

After completion of the experimentation, it appeared that the time between application of the primer to the substrate and application of the thermoplastic was a

Figure 5. Types of failures.

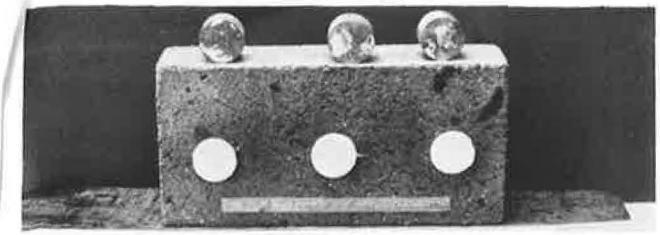

a. Epoxy Failure

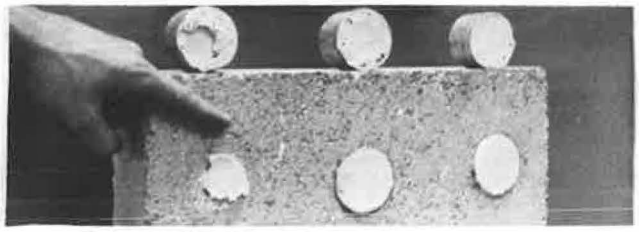

b. Thermoplastic Failure

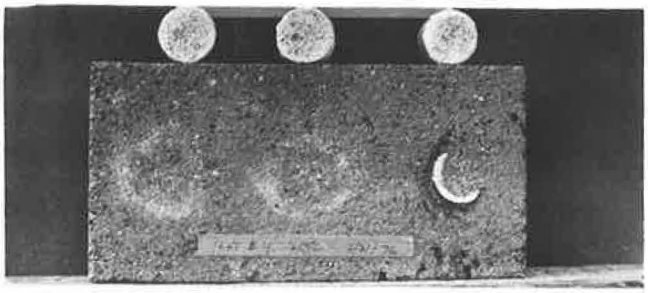

c. Bond Failure

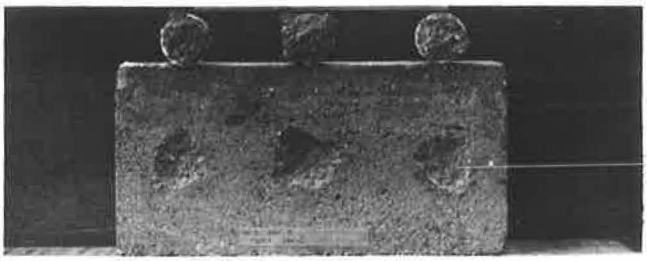

d. Concrete Failure

critical factor. Time did not permit exploration of this factor. For the test results reported, a constant time of 10 min was used; however, any variations most likely contributed to the inconsistency of the results.

The following tests are all modifications of the bond-strength test designed to investigate the various specification criteria considered. The first test determined the effect of application temperature of the thermoplastic. It was important to decide the necessity of a thermoplastic application-temperature specification. The test procedure was as follows:

1. Prepare three concrete blocks in a 22.8°C environment for a minimum of 24 h.
2. Heat sufficient thermoplastic for nine bond-strength patties to a temperature of 162.8°C (325°F) and pour three patties using the test primer and recommended curing times.
3. Heat the remaining thermoplastic to 190.6°C (375°F) and pour three more patties.
4. Heat the remaining thermoplastic to 218.3°C (425°F) and pour the remaining three patties.
5. Allow the blocks to cure 24 h and epoxy the bond-test cylinders to the patties.
6. Wait an additional 24-h period and pull each patty, recording the bond strength, mode of failure, and temperature at which the patty was poured.

The second test was designed to determine whether the air temperature has any effect on the adhesion of the material and whether this factor should be included in a specification. The test procedure was as follows:

1. Condition three blocks in a 22.8°C environment for a minimum of 2 d.
2. Heat the test material to 204°C and apply the test primer to each block.
3. Remove the three blocks and place one in a -17.8°C environment and two in a 0°C (32°F) environment. Pour bond-strength patties immediately on each block.
4. Allow 1-h curing time and remove all blocks to a 22.8°C environment.
5. Test all patties for bond strength after a minimum curing period of 24 h.

A substitute for the air-temperature specification would be to specify a minimum pavement temperature. The following procedure was developed to determine the effects of pavement temperature on the adhesion of thermoplastic material to concrete.

1. Condition two concrete blocks, one in a 0°C environment and one in a 12.8°C environment.
2. Heat the thermoplastic material and apply the primer to each block and allow the set curing time. Pour three bond-strength patties per block following standard procedures. The pouring should take place in each environment.
3. Allow the blocks to cure for 24 h and then epoxy the bond-test cylinders to the patties.
4. Allow the epoxy to cure and then test each patty for bond strength (include the values of bond strength at 22.8°C found in the first test for reporting purposes).

Finally, a test was devised to determine whether a high moisture content of the concrete at the time of thermoplastic placement has an adverse effect on the bond of the thermoplastic to the concrete. The test procedure was as follows:

1. Place two concrete blocks in each of three different relative humidity (RH) environments (0, 58, and 95 percent RH). Record the block number and the RH of the environment in which it is placed. Stack the blocks with small wooden separator strips to permit full air circulation around them. Leave in the environment a minimum of 5 d.
2. Heat sufficient thermoplastic to 204°C for 18 bond-strength test patties.
3. Remove the concrete blocks from the RH environment. Wipe each lightly with a paper towel.
4. Wait 10 min, and then apply the primer and thermoplastic in accordance with the bond-strength test instructions.
5. After the thermoplastic has set (a minimum of 2 h), epoxy an aluminum test cylinder to each thermoplastic patty.
6. Place each block in the RH environment from which it came for an additional 24 h (to allow the epoxy to fully cure).
7. Remove one concrete block from each environment and place it in a -17.8°C environment.

8. After a minimum of 24 h, test and record the bond strength of each patty.

These procedures were the basis of the results reported below. It is realized that the tests have fallacies, but it is believed that the results reflect the general trends. From the results, quantitative solutions were obtained that can be used as specifications to ensure good thermoplastic adhesion to concrete pavements.

TEST FINDINGS

The initial objective of this research was to determine an acceptable value for the bond strength. The AASHTO and the California specifications recommend a minimum value of 1.24 MPa (180 lbf/in^2) whereas the ITE specification uses a minimum value of 1.03 MPa (150 lbf/in^2). As discussed above, many agencies report that the adhesion to bituminous pavements is sufficient but that adhesive losses are prevalent on concrete pavements. The first test procedure described above (bond strength) was conducted on the test thermoplastic and primer on both a concrete pavement and a bituminous pavement. The average bond strength for the samples tested at 22.8°C on the concrete pavement was 1.54 MPa (222 lbf/in^2) (see below) (1 MPa = 145 lbf/in^2).

Figure 6. Effect of thermoplastic application temperature on adhesion.

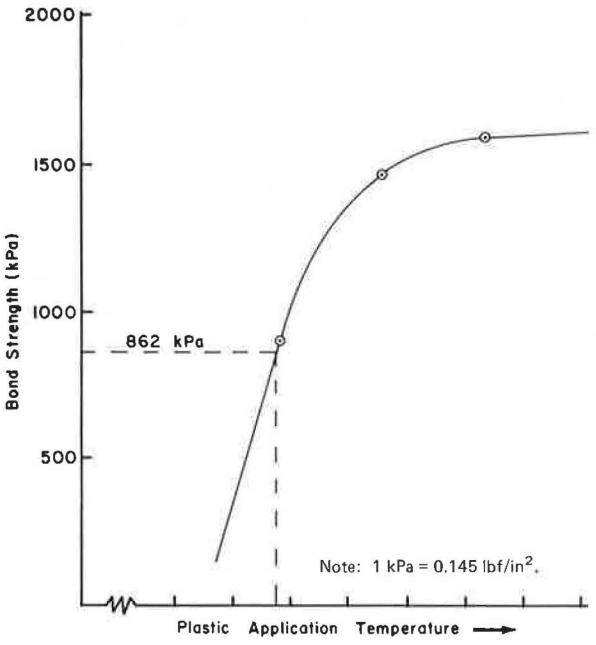

Figure 7. Effect of air temperature on adhesion.

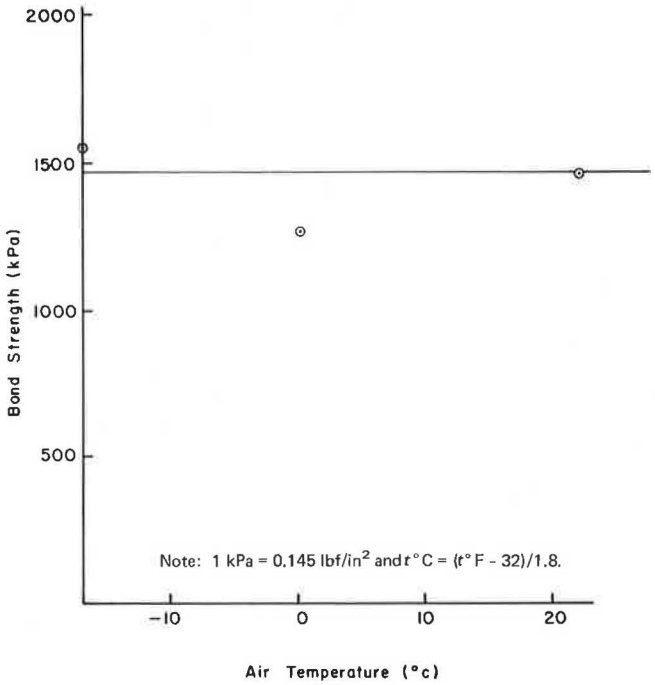

Condition	Bond Strength (MPa)	Type of Failure
23°C (73°F)	1.52	Bond and concrete
	1.60	Bond and concrete
	1.50	Bond and concrete
-18°C (0°F)	1.42	Concrete
	1.66	Concrete
	1.19	Concrete
After five freeze-thaw cycles	0.283	Bond
	0.283	Bond
	0.103	Epoxy and bond

The bond strengths of the patties bonded to the bituminous surfaces reflected the strength of the substrate; all failures were failures of the pavements. A modification of the bond-strength test, called the freeze-thaw test, was conducted on the patties bonded to both concrete and bituminous pavements. A freeze-thaw cycle consisted of 8 h in a -23.3°C (-10°F) environment and 18 h in a 77.8°C (100°F) environment. The samples were subjected to five cycles of freeze-thaw. On completion of the cycles, the bond strengths were measured. The bond strength of the samples on the concrete pavement after the subjection to freeze-thaw cycles was only 221 kPa (32 lbf/in^2); the failures were mostly of the bond. Therefore, subjection to freeze-thaw cycles was identified as a critical factor in adhesive failures. The fact that, in most cases, thermoplastic placed on bituminous pavements performed well resulted in the testing of the bituminous substrate. After 5 cycles of freeze-thaw, the results were relatively consistent with previous bond-strength tests (see below).

Condition	Bond Strength (MPa)	Type of Failure
After five freeze-thaw cycles	0.931	Bituminous
	0.800	Bituminous
	0.772	Bituminous

An average bond strength of 834 kPa (121 lbf/in^2) was found; these failures were failures of the substrate. This reflected the fact that freeze-thaw cycles do not cause deterioration of the adhesion on bituminous pavements. Therefore, under the most critical condition, an adhesion greater than 834 kPa should be sufficient for good field service. Consequently, it is recommended that a value of 862 kPa (125 lbf/in^2) be used as a minimum specification criteria. This value was used to determine the minimum requirements reported here.

The second test was performed to determine the effect of the thermoplastic application temperature on the bond strengths. As can be seen from Figure 6, the curve shows a sharp increase in bond strength with only slight temperature changes. The minimum value for 862 kPa is approximately 189°C (373°F). The curve shows no upper limit. The top limiting factors would be the temperature at which the thermoplastic could

still be extruded or sprayed and the temperature at which the components would not break down. The curve does show a leveling off between 216°C and 232°C (420°F and 450°F). The test demonstrates that adhesion can be enhanced greatly by proper application temperatures. Furthermore, a designated range should be included in a specification according to the desired adhesion. A set range for all materials is not feasible. Therefore, a range should be set by using the test procedure described, and field compliance should be insisted upon.

The third test determined the effect of air temperatures on the adhesion of the thermoplastic. Figure 7 shows that, although there is slight inconsistency, air temperatures have almost no effect on the adhesion.

Figure 8. Effect of pavement temperature on adhesion.

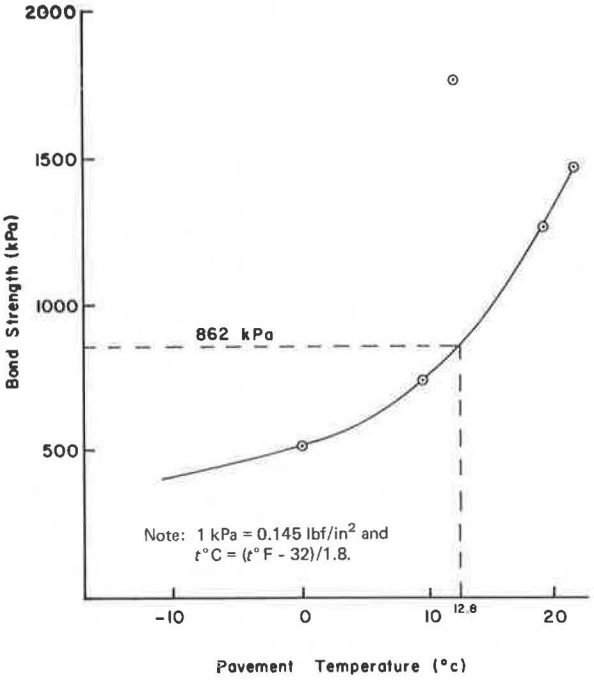

Figure 9. Effect of pavement moisture on adhesion.

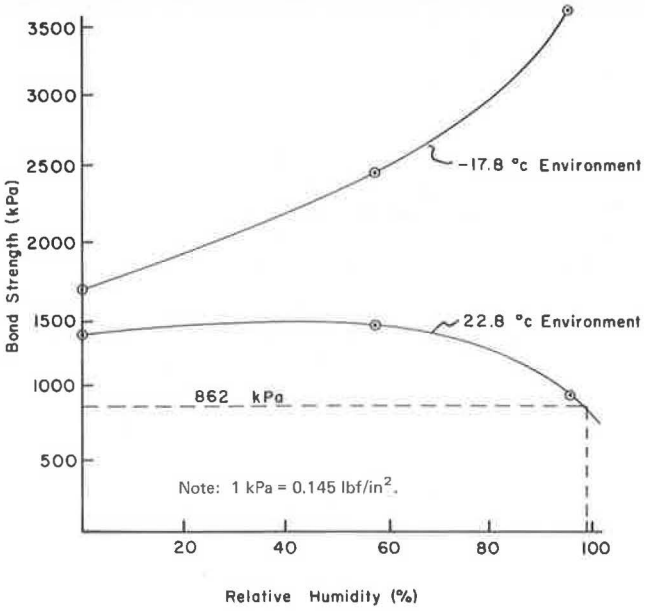

The minimum value of 862 kPa is well below even the lowest value found. Consequently, it is believed that an air-temperature specification is unwarranted and could even be detrimental to the adhesion if relied on. The air temperature can be above the minimum when the pavement temperature is still very low (early morning), which would result in poor adhesion.

The fourth test demonstrated the necessity for a pavement-temperature specification to replace the air-temperature specification. Figure 8 shows a definite increase in the bond strengths of thermoplastics applied at pavement temperatures greater than 7.2°C (45°F). Values obtained at temperatures of 12.8°C (55°F) were consistently greater than 1379 kPa (200 lbf/in²), but values at temperatures greater than 15.6°C (60°F) were lower. This phenomenon was unexplainable. Consequently, the curve was drawn through the minimum points to obtain a conservative estimate of the minimum temperature effects. For a minimum bond strength of 862 kPa, a value of 12.8°C (55°F) was obtained. Thermoplastic should not be applied to pavements at temperatures less than 12.8°C and, as can be seen, the warmer the pavement, the greater the adhesion. When possible, warmer pavements should be sought; however, for specification purposes, a minimum value of 12.8°C is recommended.

Finally, the effects of pavement moisture on adhesion were tested. The test was run in both a 22.8°C environment and a -17.8°C environment. As seen below and in Figure 9, the minimum bond strength for the cold environment is 1662 kPa (241 lbf/in²), which is well above the 862 kPa minimum.

Condition	Relative Humidity (%)	Bond Strength (MPa)	Type of Failure
23°C (73°F)	0	1.32	Thermoplastic
		1.34	Concrete and bond
		1.37	Concrete and thermoplastic
	58	1.46	Bond
		1.14	Bond
		1.71	Bond
	95	0.883	Bond
		0.772	Bond
		1.01	Bond
-18°C (0°F)	0	1.63	Concrete
		1.45	Concrete
		1.92	Concrete and bond
	58	2.22	Thermoplastic
		2.77	Concrete
		2.43	Thermoplastic
	95	3.62	Thermoplastic
		3.44	Thermoplastic
		3.62	Thermoplastic

The moisture in the block tended to increase the bond strength under freezing conditions but, on thawing, the bond strength is reduced. The second curve demonstrates that there is a reduction in adhesion with an increase in the relative humidity at 22.8°C. The lowest value, 889 kPa (129 lbf/in²), occurs at a relative humidity of 95 percent and is thus still above the acceptable minimum of 862 kPa. It is recommended that thermoplastic not be applied to a wet surface.

CONCLUSIONS

This research has investigated the effects of four important specification criteria on the adhesion of thermoplastic materials to concrete pavements. The graphs generated from the data illustrate the various temperatures and conditions necessary to obtain maximum adhesion. Also, minimum criteria are set that should

be included in a specification for application of thermoplastic materials.

When conducted on a bituminous surface after five freeze-thaw cycles (the critical situation that is succeeding in the field), the basic bond-strength test resulted in a substrate strength of 834 kPa. From this, a value of 862 kPa was determined as the minimum bond strength that will ensure an effective life.

Secondly, a thermoplastic application temperature range was deemed important and it was determined that the range should be small. For the test material and primer, the minimum temperature was determined to be 189°C and the desirable range for maximum adhesion to be 216°C to 232°C. It is recommended that a range be included in a specification and that the range should be determined by the test method described above for the material being used. The test is simple and requires very little time. As the curves show, if the material is applied at too low a temperature, the adhesion is very poor. Therefore, a range should be set and complied with in the field.

The air temperature was determined to be irrelevant to adhesion of the thermoplastic to the pavement. For this reason, a specification should not include an air-temperature criterion but should substitute a pavement-temperature criterion.

The pavement temperature was probably the most important aspect studied. It was found that pavement temperatures are quite critical to good adhesion. At the minimum bond strength, a pavement temperature of 12.8°C was reported. This value is recommended as a minimum pavement-temperature specification. When possible, thermoplastic material should be applied to warmer pavements because this enhances the adhesion.

Finally, it was found that only under wet conditions does pavement moisture affect the adhesion. Only at 98 percent RH does the bond strength drop below the minimum acceptable value. Therefore, it is suggested that a specification should state that the pavement should be dry to the satisfaction of the inspecting engineer.

The use of thermoplastic striping "has practically doubled since 1965" (3). The system has many advantages relating to the safety of the driver and, if the early failures can be avoided, it will become a more important tool for the transportation engineer. It is believed that these specification recommendations are a step forward in reducing the losses of thermoplastic striping systems on concrete pavements. The curves presented here are a basis for determining the adhesion that can be expected under various conditions, and the test procedures provide an excellent means of obtaining quantitative data.

ACKNOWLEDGMENT

This paper was prepared as a result of a Federal Highway Administration research project. The opinions, findings, and conclusions are mine and not necessarily those of the Federal Highway Administration.

REFERENCES

1. G. J. Alexander and H. Lunenfeld. Satisfying Motorists Need for Information. Traffic Engineering, Vol. 43, No. 1, Oct. 1972, p. 46.
2. Thermoplastic Pavement Markings. Highway Division, Iowa Department of Transportation, July 1975, p. 1.
3. Roadway Delineation Systems. NCHRP, Rept. 130, 1972, p. 118.
4. Pavement Traffic Marking Materials and Application Affecting Serviceability. NCHRP, Synthesis of Highway Practice 17, 1973, p. 5.
5. White Thermoplastic Traffic Lane. California Department of Transportation, State Specification 701-80-31, Jan. 1970, p. 2.
6. Standard Specifications for Traffic Control Items. Illinois Department of Transportation, Aug. 1973, p. 34.
7. Standard Specifications for Highway Construction. Oklahoma Department of Transportation, Section 855.04, 1976.
8. Thermoplastic Pavement Markings. Texas State Department of Highways and Public Transportation, Special Specification Item 7249, Feb. 1975, p. 4.
9. A Model Performance Specification for the Purchase of Thermoplastic Pavement Marking Materials. ITE, Traffic Engineering, March 1972, p. 29.
10. Standard Specification for White and Yellow Thermoplastic Traffic Lanes. AASHTO, M249-74, p. 635.
11. British Standards Specification. Hot Applied Thermoplastic Road Marking Materials. BS 3262, 1976, p. 5.
12. R. Poehl, G. Swift, and W. M. Moore. An Investigation of Concrete Quality Evaluation Methods. Texas Transportation Institute, Texas A&M Univ., College Station, Res. Rept. 2-18-68-130-10, Nov. 1972, p. 10.

Publication of this paper sponsored by Committee on Coatings, Signing, and Marking Materials.

Acceptance Sampling of Structural Paints

David A. Law and Gerald L. Anania, New York State Department of Transportation

An investigation of acceptance sampling procedures for structural paints is described. The general paint manufacturing process was briefly reviewed, and historical data on frequency of rejections under specifications formerly in use in New York State were analyzed, resulting in some

changes in those for viscosity. New York State Materials Method 6 and Federal Test Method Standard 141a (Method 1021), which cover paint acceptance testing, are compared. Current sampling plans are discussed and analyzed, and a suggested revision to the container sampling scheme is presented.

Some results are described of a project that was established to analyze various materials and develop statistically sound acceptance criteria for them. Structural paint, the subject of this paper, was the second product to be analyzed.

PAINT MANUFACTURING PROCESS

Figure 1 schematically shows a general production process for manufacturing paints. This process can be modified in several ways, such as by combining the paste and grinding tanks, by using more than one blending tank, or by combining the blending and pouring tanks. For the purposes of this study, however, we will refer to the general production process, rather than a modified one, because the portion of greatest interest to us is the pouring tank.

The general production process begins at the paste tank, where the pigment and vehicle are mixed to the proper consistency for grinding. After the paste is formed, it is placed in the grinding tank, where it is ground in a mill until it reaches the proper fineness. This is determined by running a fineness-of-grind test. From the grinding tank, the paste is transferred to a blending tank, where the remainder of the ingredients are mixed into the paint. Finally, the paint is transferred to the pouring tank, where it is pumped through a strainer into the final package for shipment.

SPECIFICATIONS

Specifications are limitations placed on products to make them consistent with engineering requirements. Buyers use appropriate acceptance sampling plans to ensure, with known risks, that the products they are purchasing are within specification limits. It must be emphasized that acceptance sampling is used to determine a course of action (accept or reject) and not to control quality (1).

Because specification limits can affect acceptance-sampling techniques, specifications should be reviewed periodically to see that they are consistent with the engineering requirements for the product. The paint specifications used in New York State evolved over the years based on performance data. Britton (2) used performance data accumulated by the state, by the National Lead Company, and in Highway Research Board publications to set specifications that would result in a 10- to 12-year life for structural paints. The rationale for specifications applicable to other field paints is not well documented, but presumably they were based on performance data. (The specifications discussed here are specifically those published by New York State on January 2, 1962, and their addenda until the completely revised edition of January 3, 1973.)

COMPLIANCE AND SPECIFICATIONS CHANGES

Data accumulated in the course of the routine acceptance testing of paints in 1970 and 1971 are summarized in Table 1, which was prepared to determine the degree of compliance with specification limits. It can be seen that, of 394 paint lots tested during the 2-year period, 207 (52.5 percent) did not meet specification requirements. However, only 30 lots were actually rejected; the other 177 were accepted for use on the basis of "substantial compliance."

The high percentage of "substantial compliance" decisions prompted a reevaluation of the specification limits. The specification limits, degree of compliance, and breakdown of failures were reviewed. It was decided that the specification limits should be kept the same, despite the large percentage of lots that were outside these limits. The only exception was that viscosity limits could be broadened without detrimental effects on paint performance. The data indicated that the viscosity limits presented problems for most paints. It was also decided that, after a revised viscosity specification became effective, acceptance by "substantial compliance" would be discontinued.

After it was decided that the specification limits for viscosity could be broadened, data on this property were statistically summarized (see Table 2). This table shows that, for structural paints, the standard deviations for viscosity obtained by combining data from all producers ranged from 3.4 to 4.3 Stormer-Krebs units. [The Stormer-Krebs unit is an index of paint viscosity derived from a chart for classifying consistency. It is a tabulation by the drive weight (in grams) against the time (in seconds) for 100 revolutions of a paddle; thus, if 500 g caused the paddle to make 100 revolutions in 30 s, the material being tested would have a consistency of 112

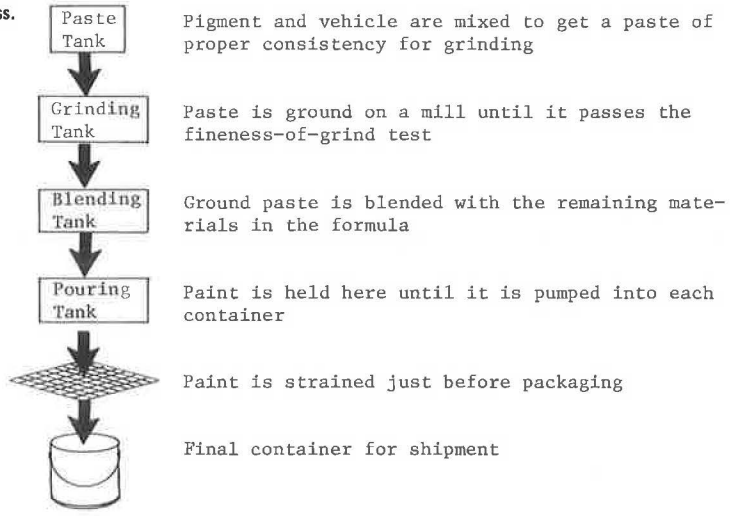

Figure 1. General paint production process.

Stormer-Krebs units.] From these standard deviations—understanding that the standard deviation for any individual producer should be smaller—the specifications for structural-paint viscosity were revised to allow a range of 20 Stormer-Krebs units. Similarly, the viscosity limits for textured concrete paint were changed to allow a range of 40 Stormer-Krebs units, as indicated in Table 3. The viscosity limits for white curb paint were changed to allow a range of 20 Stormer-Krebs units. Some changes were also made in color specifications, but these were rather arbitrary, subject to change from time to time, and will not be addressed further here because they are not directly related to performance and durability.

As mentioned above, after the specifications were changed as shown in Table 3, acceptance by "substantial

Table 1. Rates of rejection and noncompliance with specifications: 1970-1971.

Specification Item No.	Paint	Total No. of Lots	Lots Rejected		Lots Accepted Under "Substantial Compliance"		Lots Not Complying To Specifications	
			N	Percentage of Total	N	Percentage of Total	N	Percentage of Total
M18B	Maroon primer	3	1	33.3	0	0.0	1	33.3
M18CA	Dull orange primer	131	3	2.3	46	35.1	49	37.4
M18D	Black	2	0	0.0	1	50.0	1	50.0
M18E	Stain-resistant white	26	2	7.7	20	76.9	22	84.6
M18G, GA, GY	Gray	60	0	0.0	34	56.7	34	56.7
M18GR	Fast-drying white guiderail	15	1	6.7	7	46.7	8	53.3
M18GZ	Light gray	4	2	50.0	2	50.0	4	100.0
M18HA	Gray-green	2	0	0.0	0	0.0	0	0.0
M18J	Aluminum (types 1 and 2)	20	5	25.0	8	40.0	13	65.0
M18K	Zinc chromate primer	6	0	0.0	4	66.7	4	66.7
M18M	White curb	15	3	20.0	7	46.7	10	66.7
M18SH	Sage green	77	6	7.8	35	45.5	41	53.2
M18TA	Textured concrete gray finish	33	7	21.2	13	39.4	20	60.6

Table 2. Means and standard deviations for viscosity: 1970-1971.

Statistical Index	Manufacturer 1	2	3	4	5	6	7	All Manufacturers Combined
Structural paints								
Dull orange primer								
N	21		20	15	11	20	17	128
Mean	79.5		74.6	80.1	76.1	76.4	74.8	78.0
SD	3.8		2.1	2.3	1.9	3.3	4.8	4.2
Stain-resistant white								
N								26
Mean								88
SD								3.7
Gray								
N		11	15				26	60
Mean		75.7	77.4				73.3	74.7
SD		2.4	4.4				2.2	3.4
Fast-drying white guiderail								
N							15	15
Mean							77.5	77.5
SD							3.4	3.4
Sage green								
N		17	15				27	72
Mean		77.3	74.0				78.7	76.6
SD		4.8	3.8				3.2	4.1
Other field paints								
White curb								
N								13
Mean								84.5
SD								6.0
Textured concrete gray finish								
N							19	33
Mean							127.0	125.0
SD							8.5	8.3

Table 3. Specification changes.

Paint	Viscosity Range (Stormer-Krebs units)		Tristimulus Values				Trilinear Coordinates					
			Old				Old			New		
	Old	New	x	y	z	New (y only)	x	y	z	x	y	Other
Dull orange primer	74-85	69-89										None
Stain-resistant white	80-90	75-95										Total carbonate = 2.04+
Gray	72-82	67-87				9.0-10.0	0.374	0.415	0.211	0.300-0.335	0.320-0.355	None
Fast-drying white guiderail	70-78	65-85										None
White curb	70-85	68-88										None
Sage green	70-80	65-85	16.17	19.64	13.69	14.4-24.8	0.327	0.397		0.278-0.376	0.334-0.460	None

compliance" was dropped in favor of strict enforcement. All producers doing business with New York State were notified of this change by letter. Since the changes went into effect in October 1972, data have been collected that show dramatic improvement in compliance (see below).

Paint	Total No. of Lots	No. of Lots Rejected	Percentage of Lots Rejected
Dull orange primer	104	12	8.6
Stain-resistant white	24	8	33.3
Gray	80	10	12.5
Fast-drying white guiderail	54	8	14.3
Sage green	87	7	12.4
All combined	349	45	12.9

To cite one example, there was 52.5 percent noncompliance before October 1972 and 12.9 percent thereafter. This improvement could not be wholly attributed to the specification change, but is more likely due to elimination of "substantial compliance." In fact, looking back, elimination of all noncompliance due to viscosity would only reduce noncompliance by 18 percent (rather than the 39.6 percent actually experienced). After elimination of "substantial compliance," manufacturers have probably watched their processes more closely because they know that no specification limits will be waived.

CURRENT ACCEPTANCE PLANS

Background

In designing acceptance sampling procedures, one usually must study the production process. From such a study, information is obtained concerning sampling location and a rational lot. The latter should consist of production units that have low variability and are produced under the same conditions. The location of sampling should be where there is a common element from process to process, and the most logical one for paint as a finished product should be as it leaves the pouring tank. However, it is not always possible to sample at this location; sometimes it is physically impossible or too dangerous, and at other times inspection personnel cannot be present during the pouring operation. Thus, two different sampling procedures have been developed—one for paint sampled at the pouring tank and a second for paint sampled from containers. The procedures to be followed for both cases are specified in New York State Materials Method 6 (NYSMM 6), issued in February 1970. When sampling from pouring tanks, this method requires that the plant inspector draw two 0.95-L (1-qt) samples directly from the (pouring) tank pouring spout, one after approximately one-third and the other after approximately two-thirds of the pour is completed.

For sampling canned paints, the procedure requires that the inspector examine the labeling of each container to ensure that all paint is from the same batch and that all was mixed at the same time in the same pouring tank. Then, the inspector is required to sample a number of containers at random after the contents of each have been thoroughly mixed. The number of containers to be sampled is determined by the lot size as follows:

Lot Size (total containers from same pouring tank)	Sample Size (containers to be sampled)
1 to 15	3
16 to 25	4
26 to 90	6
91 to 150	8

Acceptance is judged on the basis of a uniformity test and a chemical analysis as follows. In the case of sampling from the pouring tank, the two 0.95-L (1-qt) samples are tested for fineness of grind, unit weight, and viscosity. The results of these measurements for each sample are compared to determine uniformity. Uniformity tests are performed first because the full chemical analysis of paint is very time-consuming and expensive. If a paint should fail the uniformity criteria, then it is rejected without performing the full chemical analysis.

The two samples are said to be uniform if they vary by no more than 1.0 unit for fineness of grind, 0.04 kg/L (0.3 lb/gal) for unit weight, and 3.0 Stormer-Krebs units for viscosity. If the paint has been judged uniform, then a complete chemical analysis is performed on one of the samples. If the properties checked in the chemical analysis are within the specified limits, the paint is accepted for use; otherwise, it is rejected.

Similarly, the paint samples recovered from containers are screened by testing each for fineness of grind, unit weight, and viscosity. If no two samples differ by more than the tolerances stated for sampling from the pouring tank, then the lot is judged uniform and one sample is used for a chemical analysis. The lot is then accepted if the results of the chemical analysis are within the specification limits. If the samples fail the uniformity test, then the lot is rejected without doing the chemical analysis.

Efficiency of the Plans

In determining the efficiency of acceptance plans, the risks desired by the consumer and the risks determined for the actual plan are compared. The consumer's risks are formulated from design and performance requirements as well as the consequences of a failure. Theoretically, risks are determined and then the sample size is computed to operate within such risks. Traditionally, sample sizes have been chosen without consideration of risks and, in most cases, without knowing the risks. Paint acceptance-sampling plans are no exception. Development of these techniques without regard to statistical theory or sampling methodology makes it very difficult to determine the risks associated with them. By using approximations of the risks based on statistical theory, the risks are shown by means of operating-characteristic (OC) curves. These curves give probabilities (Pa) of accepting lots of varying quality levels. The OC curves that we will consider are shown in Figure 2 for various sample sizes; they are based on the ratio (λ) of the standard deviation of the lot to the desired standard deviation, rather than on average quality levels [as developed by Duncan (1, p. 289)].

Sampling Plan for Pouring Tanks

As described above, two 0.95-L (1-qt) samples are taken from the pouring tank at specific times during the pour. Tolerance levels were established for unit weight, fineness of grind, and viscosity. The range of readings for each of these criteria, from the two samples, is compared with its respective specified tolerance, and it is assumed that if the range of the two samples does not exceed the specified tolerance, then the lot meets the criteria for variability. Unfortunately, there is always a risk that, even if the range from samples falls within the tolerance limit, the lot might not be uniform if a better estimate could be established. Assuming that the lot passes the initial criteria, then one sample is tested for all remaining physical and chemical properties.

The acceptance plan has been broken down into two

Figure 2. Operating-characteristic curves.

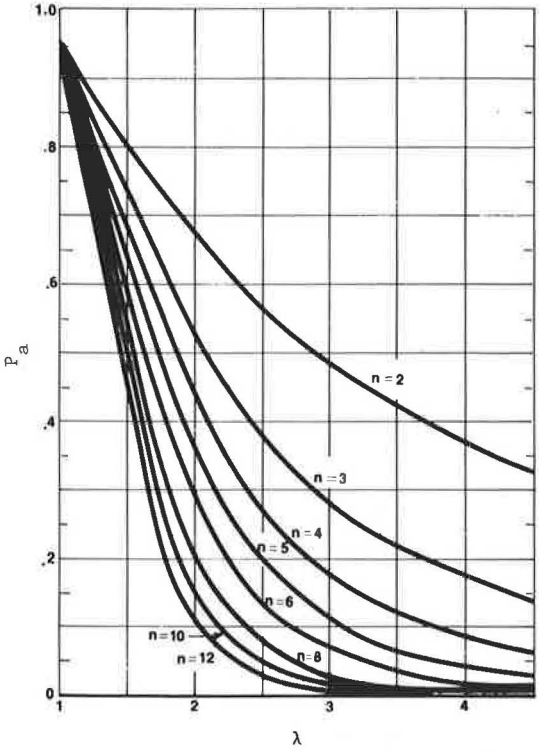

Figure 3. Sampling locations: New York State Materials Method 6 and Federal Test Method Standard 141a (Method 1012).

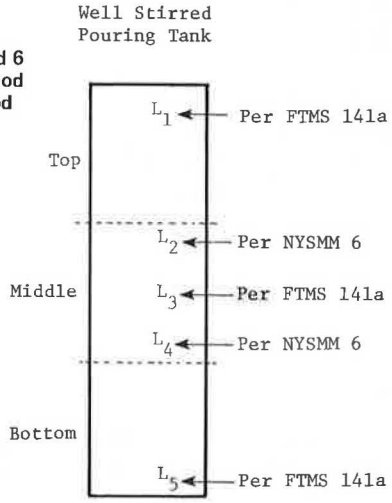

schemes. The first—uniformity testing—consists of the range of two measurements of each of the three properties used in determining uniformity. This is illustrated by the OC curve for n = 2 in Figure 2. This curve is somewhat weak; for example, if the lot standard deviation is three times the desired standard deviation, there is about a 48 percent chance of acceptance. The second scheme—chemical analysis—is performed on a single sample, provided the uniformity test was acceptable. This single-sample testing assumes that, if the uniformity criteria are met, then the single sample used for chemical analysis is representative of the production unit. The chemical analysis determines whether the ingredients are correctly proportioned. The analysis is performed without benefit of known testing error and assumes minimal sampling error (based on passing the uniformity test).

Sampling Plan for Containers

Similarly, the procedure for container sampling and testing consists of first, a uniformity, and second, a chemical analysis. The uniformity test consists of comparing the viscosity range, fineness of grind, and unit weight to the same tolerances used for pouring-tank sampling. Because the sample size for container sampling varies (from three to eight, depending on lot size), the risks associated with acceptance of paints based on this scheme vary also. As the OC curves shown in Figure 2 for n = 2 through n = 12 show, the smaller the sample size, the higher the risk associated with this scheme. This is true because the variance depends on sample size rather than on lot size. However, because the current acceptance tolerances remain the same as the sample size increases, this in effect assumes a smaller desirable standard deviation with increased sample size. This means that the larger the sample size, the more stringent the acceptance criterion really is. Thus, as sample size increases, the present uniformity tests are somewhat more stringent than are the curves shown in Figure 2. If the paint passes this uniformity criterion, then it is accepted or rejected based on one chemical analysis under the same assumptions and conditions as those of the pouring-tank sampling scheme.

Analysis of Sampling Procedures

The current sampling procedure for pouring tanks (Figure 3) takes two samples from the middle portion of the tank. By contrast, the Federal Test Method Standard 141a (method 1021) (FTMS 141a) suggests the following procedure (also shown in Figure 3).

> With large containers such as tanks or tank cars, three separate 1-qt [0.95-L] samples shall be taken, one from the top, one from the bottom, and one from an intermediate point, by means of a sampling tube, and shall be forwarded to the laboratory without mixing to permit a determination of uniformity of product as well as compliance with the specification requirements.

The federal standard does not provide any criterion for determining whether the range of the samples is too large. If we wish to use this standard, we need information on sampling-location bias, testing error, and sampling error. No historical data were available concerning these variations. Thus, two experiments were designed to provide the desired information at different degrees of accuracy. The first design required 300 complete paint tests and provided the best estimates of desired variances; it considered both New York State Materials Method 6 and Federal Standard 141a in its sampling design. This experiment should have provided the information needed to decide between the two methods and to design an adequate acceptance procedure around the sampling scheme. The second design required 138 samples and considered only Federal Standard 141a. Unfortunately, the sample sizes in both experiments were judged to be too large. New York State has been analyzing about 150 paint samples/year for the paint types considered here. Conducting either experiment would thus double or triple the work load of the testing laboratory. Because there was not enough time, money, or personpower available for such an effort, another alternative was carried out by the testing laboratory.

A smaller pilot experiment (see Figure 4) was developed to give an idea of the magnitudes of the sampling error and the within-tank variability. To obtain the data within the constraints of the laboratory, no replicates were taken, and testing error thus could not be sepa-

Figure 4. Pilot experiment.

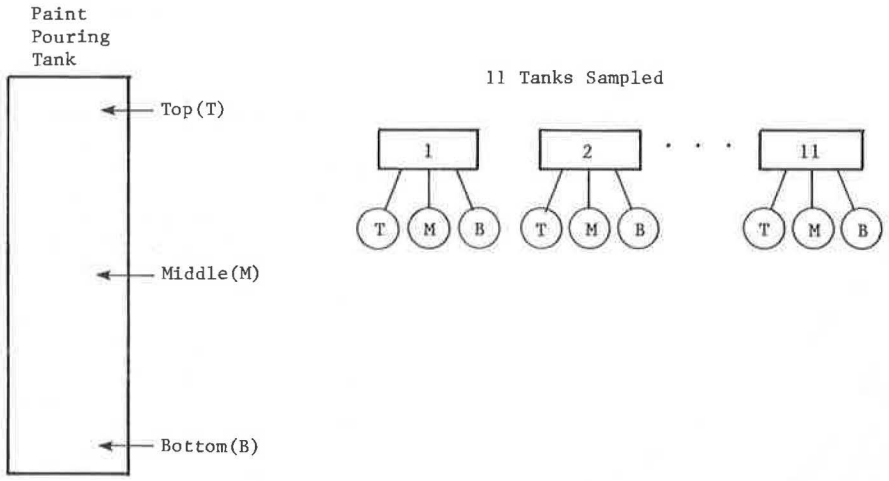

Table 4. Results of t-test to determine existence of significant differences among sampling locations.

Property	Σx^2	$\bar{x}$	$\bar{x}^2$	$(SD)^2$	SD	t
Bottom versus middle						
Pigment	0.48	0.000	0.0000	0.044	0.209	0.000
Solids	5.30	0.018	0.0003	0.481	0.694	0.082
Phthalic anhydride	0.05	-0.009	0.0001	0.004	0.067	0.426
Basic lead silico chromate	1.24	-0.091	0.0082	0.104	0.323	0.889
Viscosity	11.0	0.273	0.0744	0.926	0.960	0.898
Fineness	0.75	0.045	0.0021	0.066	0.257	0.559
Unit weight, kg/L	0.003	0.009	0.0001	0.0001	0.011	2.770
Middle versus top						
Pigment	1.18	0.054	0.0030	0.104	0.323	0.529
Solids	3.95	-0.100	0.0100	0.349	0.591	0.535
Phthalic anhydride	0.02	0.000	0.0000	0.002	0.043	0.000
Basic lead silico chromate	1.84	-0.018	0.0000	0.167	0.409	0.141
Viscosity	27.0	-0.636	0.4050	2.049	1.430	1.407
Fineness	4.00	-0.182	0.0330	0.331	0.575	1.000
Unit weight, kg/L	0.01	0.000	0.0000	0.001	0.024	0.000
Bottom versus top						
Pigment	0.56	0.054	0.0030	0.047	0.226	0.756
Solids	3.01	0.009	0.0001	0.274	0.523	0.054
Phthalic anhydride	0.02	0.018	0.0003	0.002	0.039	1.470
Basic lead silico chromate	0.66	-0.109	0.0119	0.048	0.219	1.570
Viscosity	8.00	-0.182	0.0331	0.694	0.833	0.690
Fineness	3.75	-0.045	0.0021	0.339	0.582	0.247
Unit weight, kg/L	0.003	0.008	0.0001	0.000	0.015	1.788

Note: 1 kg/L = 8.35 lb/gal.

rated from sampling error; however, if the total error were low, then both testing and sampling errors would be low. If the results of this experiment were found inconclusive or large errors and large within-tank variability were found, it would be advisable to perform the experiment outlined in Figure 3 as part of the routine testing program.

The eleven samples collected in the experiment were of three paint types, from several manufacturers. Seven properties common to most paints were selected for the actual analysis. The data were analyzed by determining differences within each sample according to the three locations tested. The differences were calculated as follows:

1. Bottom sample minus middle sample,
2. Bottom sample minus top sample, and
3. Middle sample minus top sample.

Thus, for example: 66.1 - 66.4 = -0.3.

Sample variances of the differences and the average of the differences were calculated for all seven properties at the three comparison levels. Student's t-test was used to determine whether a significant difference existed between sampling locations. The following equation was used:

$$t = [|\bar{X} - \bar{x}|\,(n-1)^{1/2}]/SD \qquad (1)$$

where

$\bar{x}$ = average of the differences for each property,
SD = standard deviation of the differences used to calculate $\bar{x}$, and
$\bar{X}$ = population mean difference to which the sample average $\bar{x}$ is compared (1).

In this experiment, $\bar{X} = 0$ because we would expect that a well-mixed paint with no significant bias due to sampling location should have a zero difference between each comparison of sampling locations.

Test results are given in Table 4. The data show no statistically significant difference at the 0.05 significance level between combinations of sampling locations, except the unit weights for the bottom versus the middle sample. Examination of the means for all properties shows that all of them approach zero, implying again that no significant bias exists due to sampling locations. These data agree with the historical data used to set the uniformity limits discussed above. Both sets of data indicate no significant bias due to sampling location, and the majority of the variations among samples can be attributed to sampling and testing errors. From these

results, it does not appear to be advantageous to change from the state to the federal test method.

SUGGESTED REVISION TO SAMPLING PLAN

When designing an acceptance sampling plan, we try to achieve the following objectives:

1. To accept products that meet the desired specifications,
2. To set the risks involved in sampling and accepting to the requirements of the consumer and still be fair to the producer, and
3. To keep the number of samples taken and the costs involved to a minimum.

Designing a plan that meets all three objectives is often impossible. Usually one or more objectives must be modified to produce a workable plan. All of these factors are considered in developing an acceptance plan for paints (1, 3, 4, 5). Paint can be considered a bulk material and could be tested as such. Bulk sampling can be broken into two major categories—segmented material and material moving in a stream. Each can be further broken down into isolated lots moving in a series. Segmented material is subjected to stratification, and stream material to segregation (4).

Data from the uniformity testing showed no significant variation in the tanks, and thus stratification in containers filled from properly mixed tanks seems unlikely. Tank sampling can be modeled as one of a series moving in a stream, and container sampling can be modeled as distinctly segmented lots in a series. Unfortunately, most of the work done on bulk sampling to date has been in prediction of the mean quality of the lot. Determination of the mean quality of the lot and its confidence limits is based on knowledge of (a) the variabilities associated with the particular material, (b) the variance between segments in a lot, (c) the variance within segments, (d) the reduction variance (reducing the total sample to a usable size for the actual testing), (e) the sampling variance, (f) the analytical variance, and (g) the segregation variance if it exists (4). The tables given above in this paper present several of these variables but not all. Additional experiments would be necessary to determine the remaining variables. The problem, however, is that this analysis should be run for each producer, each type of paint, and all properties and occasionally all analyses should be rerun to ensure that none of the variances has changed significantly. Each analysis would require a large number of calculations. This indicates that such a variables plan for acceptance, based on the mean quality of the lot, would be very time-consuming and expensive and probably not justified based on the criticality of a failure. The risks taken in accepting paints can far exceed those for the strength of steel, reinforcing bars, or concrete used in the structure to be painted. If a variables sampling plan were constructed and used, the result would be that a separate plan would be needed for each property of each type of paint. In the case of tank sampling, had either of the two designed experiments been carried out, it would have been possible to assess sampling and testing variations and to develop a sampling plan that had fewer assumptions. Because the experiment actually performed did not lend itself to such detail, the following was deduced. As discussed above, from the experiment comparing the FTMS 141a and NYSMM6, no reason was found to change to the federal test method. If we assume that the two samples required for tank sampling adequately determine whether the material is uniform—i.e., thoroughly mixed—then it would seem reasonable to assume that a single chemical analysis such as is now performed would be adequate to characterize whether the paint meets the desired specifications. This is based on the assumptions that the bulk sample, in the form of a tank or vat of paint, can be considered a production unit and that the consequences of accepting paint that might fail are not critical enough to outweigh the increased costs of performing more than one chemical analysis. These assumptions were considered reasonable because an inspector is present at the plant to make certain that the paint is thoroughly mixed and properly prepared in the process from which he or she is about to sample. An approximate OC curve for the two-sample uniformity test from tank sampling is the n = 2 curve shown in Figure 2.

In the case of container sampling, the assumptions were somewhat different. It was assumed that an inspector was not present when the containers were filled from the pouring tank and that it was important to determine that the paint in the lot of containers was from the same production unit, as required by the specifications. As noted above, sample sizes from containers vary according to the number of containers in the lot, and the uniformity test ranges (viscosity, fineness of grind, and unit weight) are required to meet the same tolerance applied to the two samples taken when sampling from pouring tanks. From statistical theory and acceptance sampling methodology, it is obvious that this scheme does not apply equal risks to the various production lot sizes. This type of plan has been used historically in many fields and seems rational because the sample size increases with lot size, but in fact the acceptance criteria change for each group of lot sizes. For any given lot, the larger the sample size, the larger the expected range should be. From established tables, the allowable range for two samples can be adjusted to maintain the same confidence level for increased sample sizes. The following table permits comparison of allowable ranges based on the uniformity tolerances for two samples and the assumption of an 0.05 significance level:

	Acceptance Tolerance for Sample Size				
Test	Of 2	Of 3	Of 4	Of 6	Of 8
Viscosity, Stormer-Krebs units	3.0	3.58	3.93	4.36	4.65
Unit weight, kg/L	0.4	0.04	0.05	0.05	0.05
Fineness of grind, units	1.0	1.19	1.31	1.45	1.55

These values were found by using the equation $\sigma = R/W$, where σ is known and W is determined by using the sample size and special tables and solving for the new allowable range (1). From this comparison, it can be seen that, by applying the same tolerances used for two samples, the larger the sample size, the tighter the standards of acceptance become.

If we were to apply the appropriate tolerances to each sample size, then the OC curves for such sampling plans would approach those shown in Figure 2. It can be seen that the probability of acceptance of a material that has a standard deviation three times as large as that desired does not fall below 10 percent until a sample size of eight is reached. Because this ought to be only a minimum criterion for a noncritical material such as paint, it was decided that a new sampling scheme for containers was in order. A suggested scheme would be to sample all containers if the lot consists of eight or fewer and eight if the lot consists of more than eight. This sample would undergo the uniformity testing and be judged against the appropriate tolerances for the sample size. If the paint from the containers passes the uniformity

criteria, then it should be assumed that all were containers filled from the same well-mixed vat of paint and, for the reasons discussed above in pouring-tank sampling, one chemical analysis on one sample should suffice. Also, it is worthwhile to note that, for sample sizes of 10 and 12 in Figure 2, the greater protection afforded by these sample sizes over that chosen (eight) does not justify the increased testing efforts that would be involved. Furthermore, because of methods of determining probabilities (which we will not discuss here) for small lot sizes, the OC curves shown in Figure 2 would be somewhat conservative and probably represent the worst case.

CONCLUSIONS

1. It was determined from historical data that the limits for viscosity of paint could be broadened.
2. The practice of accepting paints on the basis of "substantial compliance" with the specifications was eliminated, and this was believed to aid in improving the overall quality of paints accepted by causing producers to pay closer attention to their manufacturing processes.
3. No advantage was found for replacing NYSMM6 by FTMS 141a (method 1021).
4. It was determined that, if the uniformity criteria are met, then it is practical to assume that a paint lot can be considered as one bulk unit for further chemical analysis.
5. A new sampling scheme is suggested for container sampling.

ACKNOWLEDGMENTS

This paper was prepared in cooperation with the U.S. Department of Transportation, Federal Highway Administration.

REFERENCES

1. A. J. Duncan. Quality Control and Industrial Statistics. Richard D. Irwin, Homewood, IL, 3rd Ed., 1965.
2. H. B. Britton. An Engineering Approach to Improved Protection of Structural Steel. HRB, Highway Research Record 140, 1966, pp. 23-38.
3. E. L. Grant. Statistical Quality Control. McGraw-Hill, New York, 3rd Ed., 1964.
4. J. M. Juran and others. Quality Control Handbook. McGraw-Hill, New York, 3rd Ed., 1974.
5. J. B. DiCocco. Quality Assurance for Portland Cement Concrete. Federal Highway Administration, Rept. FHWA-RD-73-77, Sept. 1973.

Publication of this paper sponsored by Committee on Coatings, Signing, and Marking Materials.

Accelerated Performance Testing of Bridge Paints for Seacoast Environments

W. R. Tooke, Jr., Tooke Engineering Associates, Atlanta

The design and operation are described of an accelerated-corrosion-environment chamber for evaluation of metal protective paints. The findings are discussed of experiments designed to test the reproducibility of the results obtained in the chamber and are correlated with the limited available data from an exterior weathering test fence at a tidal estuary in Brunswick, Georgia. The fundamental premise underlying the design of the chamber is that the primary stresses that account for paint-system failures on structural steel in seacoast environments are caused by continuing cycles of wetting and drying and heating and cooling in the presence of the corrosion-stimulating chloride ion. The major conclusions are that the chamber exhibits high precision of test results within runs and an exceptionally close similarity in a greatly accelerated test to the modes of panel failure observed in the field. The prospects for close laboratory-field correlation appear very good but, for general use, this correlation will require control system techniques that have been proposed but not yet validated by comprehensive experimental studies.

Research on accelerated-weathering devices spans a period of one-half century. During the 1920s, Nelson and co-workers (1, 2, 3, 4) developed artificial weathering machines and investigated various exposure cycles. An interesting illustrated review of much of this early work has been given by Gardner (5). Standard methods for operating weathering equipment (6) and preparing and evaluating test panels (7) were developed and published by the American Society for Testing and Materials (ASTM) during the 1930s.

Notwithstanding the intensive research over an extended period of time, difficulties in obtaining similar results from different machines and in correlating these results with field experience have continued to create problems (8). The multiplicity of factors involved in accelerated weathering and corrosion tests was discussed at length in 1963 by Valentine (9) and by Talen (10) (particularly, the aging process). Clearly, the problem of defining and measuring some important fundamental properties and variables had not been specifically addressed, and no evidence was seen of any effort to formulate a comprehensive physical theory of the performance of anticorrosive paints. Thus, in 1967, Burns and Bradley (11) referred to laboratory-field correlation research as follows: "This correlation has never been achieved despite the efforts of many laboratories over a period of many years." Later, however, in referring to the work of Gay (12), they observe that "The significant

variables in accelerated weathering of paints have been studied, and information has been obtained that should lead to improvements in durability testing procedures for paints."

This is almost certainly the most important problem in the range of paint technical problems.

The above observations are mostly relevant to the problem of accelerated weathering in its broad aspects. When interest is more specifically directed to the evaluation of coatings for use in a humid salt environment (i.e., a seacoast), then much more encouraging results were reported nearly 40 years ago. In 1932, Gardner described a test that involved overnight immersion of painted panels in seawater and daytime exposure at 45° south (13). Six weeks of exposure on this test was found to simulate about 1 year of normal exposure on structures. Later, Wray automated the test to provide cycles of 5-min immersion and 25-min sunlight in air and reported that results were obtained in a few weeks that were equivalent to 1 or more years at the seacoast (14). In 1961, in an extensively documented and comprehensive study involving 16 primers, Rischbieth and Bussell (15) found that a salt droplet test (British Standards 1391-1952) was superior to humidity or salt fog tests in rating the primers in agreement with exterior weathering tests. This study also showed the large magnitude of variations in exposure results among exterior weathering sites that would necessarily confound simple direct-correlation efforts.

The literature on accelerated weathering is very large indeed. In a survey that covered the period 1955-1967, 228 papers were listed under the subject heading "coating exposure tests" (16). Thus, if unifying concepts can be developed, a huge store of data is available for experimental determination of parameters in the relevant equations.

Figure 1. Chamber and controls.

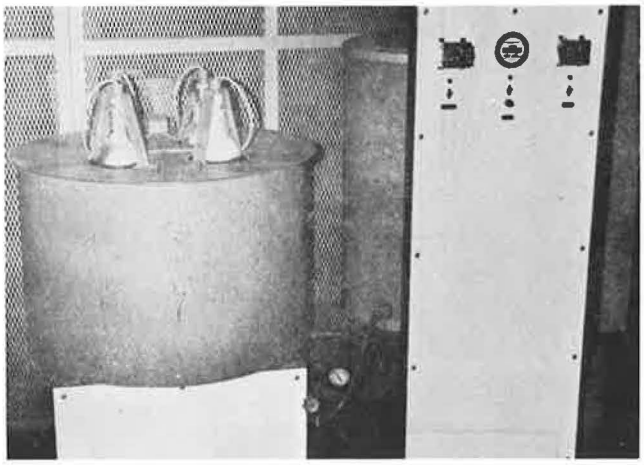

Figure 2. Interior view of chamber.

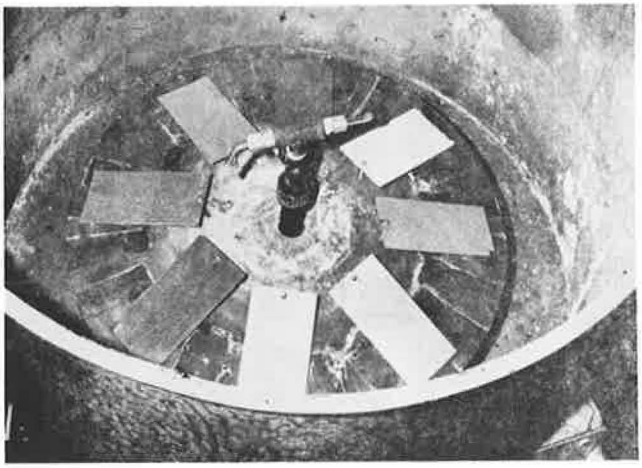

ENVIRONMENTAL SIMULATION CONSIDERATIONS

Conventional weatherometer studies were included as standard test procedures within the project in which this environmental test chamber study was pursued. Consideration was not given to the possibility of modifying the weatherometer into an environmental test chamber primarily because it was committed to conventional operation. Moreover, it was suspected that the elaborate carbon arc of the weatherometer was not necessary for the accelerated testing of moderately aggressive environments. Presumably, the chemical and physical stresses to be imparted to the test films in the chamber should exert their destructive effects before the radiation could cause significant damage. In addition, a flexible design that could readily accommodate various liquid or gaseous corrodents and provide rapid heating-cooling and wetting-drying cycles dictated a custom design for the apparatus. Although the primary immediate use for the apparatus was in simulating the humid salt seacoast environment, a capability of simulating various special chemical and cyclical environments was considered to be a desirable secondary design objective.

CHAMBER DESIGN

General Description

The environmental chamber apparatus has two main sections—the chamber enclosure and the control and servicing equipment (see Figure 1). The chamber is equipped with a rotating specimen table, four overhead ultraviolet (UV) lamps, two wetting-solution nozzles, and a drain (see Figure 2). The table rotates at a rate of 4 revolutions/min. Eight panels are mounted in a circular pattern on the table, sloping at a 30° angle toward the outer edge (see Figure 3). The rotation of the table provides a completely uniform positioning of the panels with respect to both light and wetting solutions.

The four 275-W UV lamps are mounted in the chamber cover. When in operating position, they are 36 cm (14 in) above the panels.

The two wetting-solution nozzles are located on a central pipe and are aimed so that one stream of solution hits the panels 6.4 mm (0.25 in) from the top and the other hits halfway down the panels. Both of the streams strike the panels at compound angles. This provides a uniform wetting over the entire surface of the panels. The nozzles are made of 6-mm (0.23-in) flint glass tubes with the end drawn and fire polished until only a small hole [approximately 0.3-mm (0.012-in) diameter] remains (see Figure 3) (because this equipment was designed and built to U.S. customary units, SI units are not shown on Figure 3). This nozzle design was adopted after metal and plastic nozzles were found to develop problems of corrosion and plugging. The glass nozzles operate for long periods of time without plugging and are easily cleaned if plugging does occur. Another advantage of these nozzles is that, because they direct a thin stream of solution directly onto the panels rather than produce a general spray of solution, there is less incrustation of

the lamps with salt. The expended wetting solution leaves the chamber through the drain.

Service and Control Systems

The ancillary equipment consists of a 114-L (30-gal) solution holding tank, the electrical system, the piping system, the solution pump, and the table rotation motor. A pump bypass line equipped with a valve and pressure gauge is used to control the pressure at the nozzles. A solenoid valve, which is connected in the electrical circuit of the pump, was installed in the line from the holding tank to prevent leakage at the nozzles (caused by the pressure head in the tank) when the pump is not operating (see Figure 4).

The wetting cycle and the UV light cycle are controlled by independent timers. This provides two unsynchronized cycles: (a) a wet-dry cycle in which a solution [normally synthetic seawater conforming to ASTM D1144-52 (revised 1965) (section 4)] is periodically sprayed on the panels and (b) a light-dark (heating-cooling) cycle in which the panels are periodically subject to UV radiation and heat gradients. An elapsed-time meter is connected

Figure 3. Rotating specimen table and nozzle assembly.

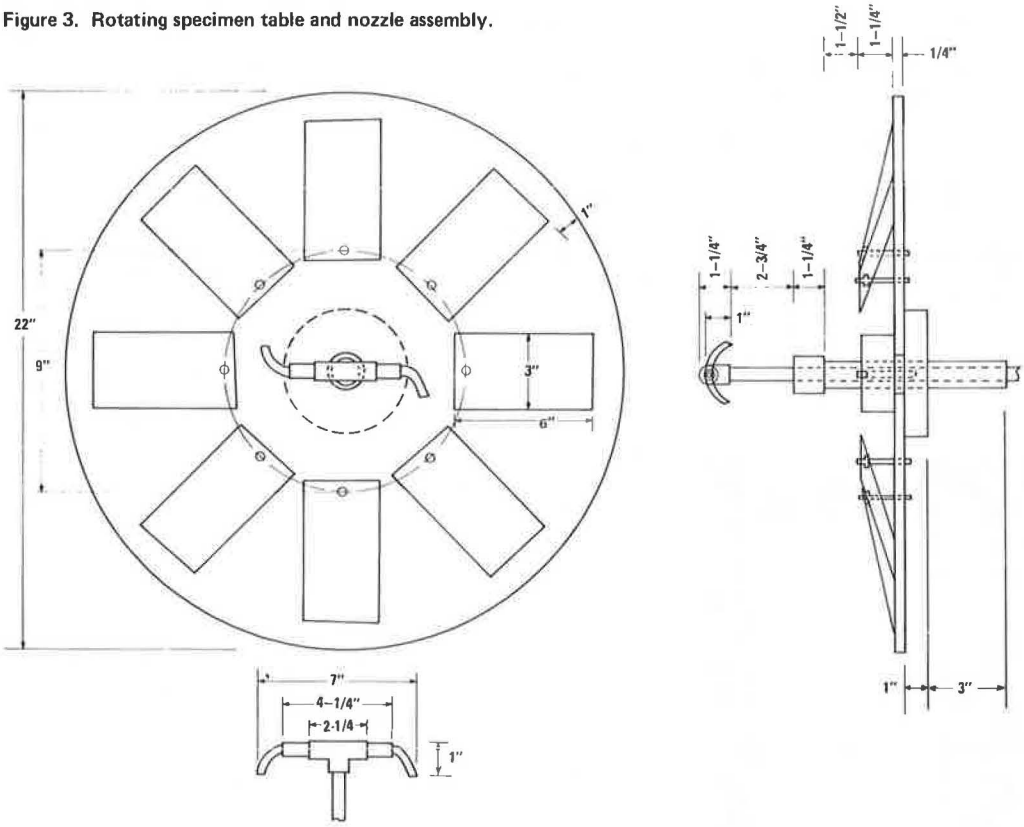

Figure 4. Piping system.

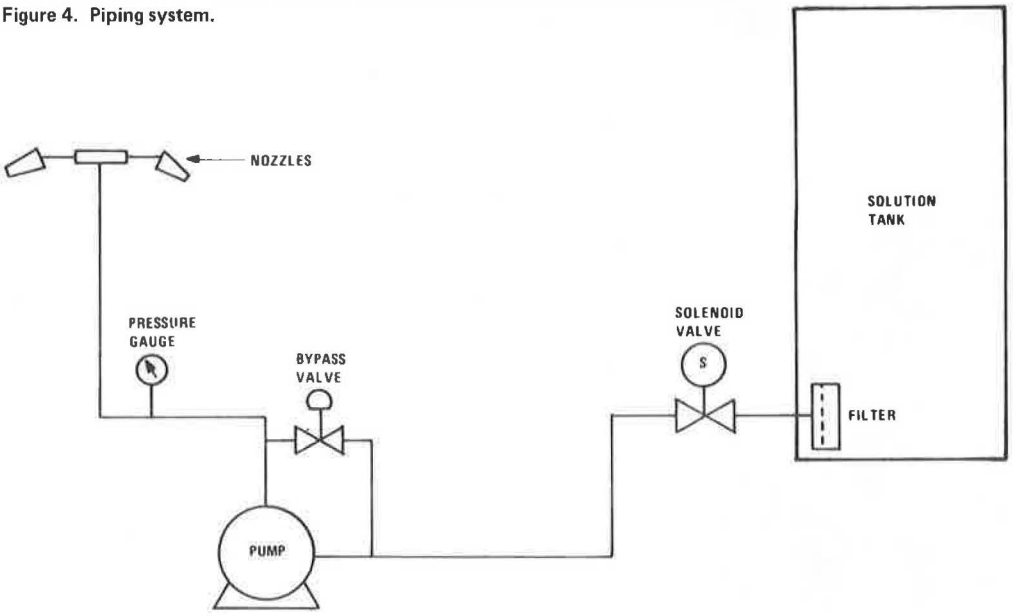

Figure 5. Electrical system.

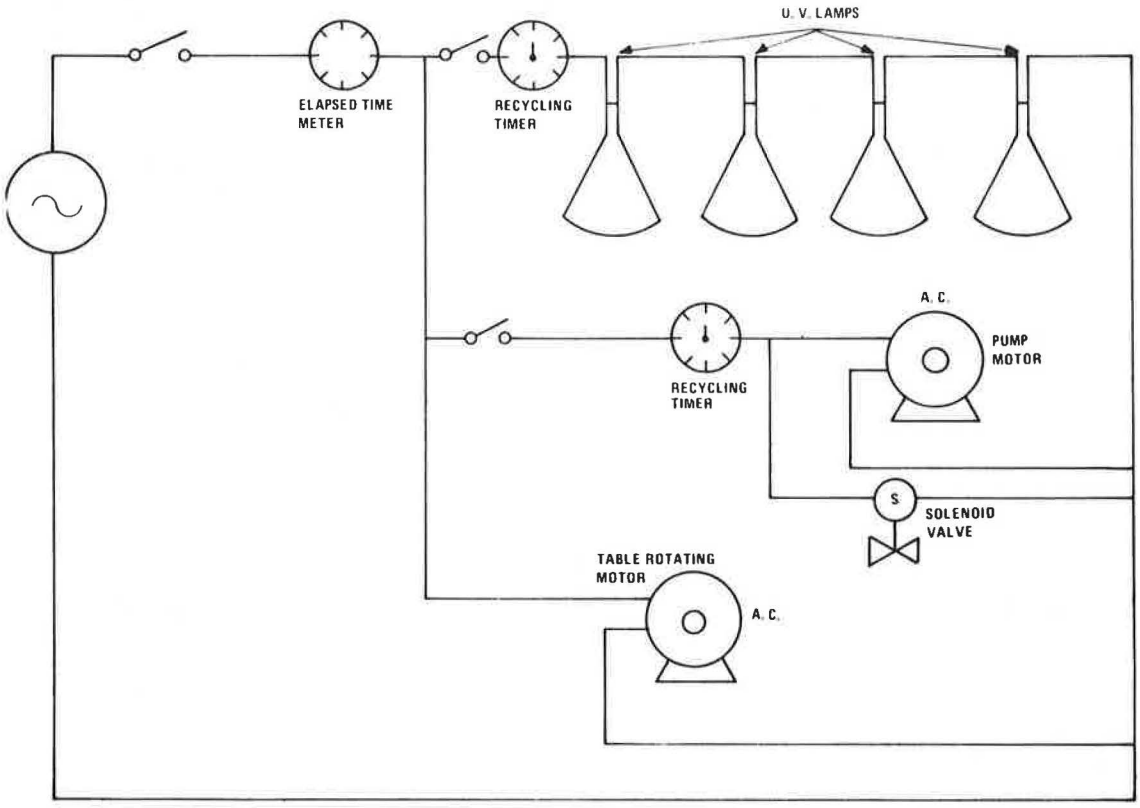

to the main power line to indicate the number of hours of operation (see Figure 5).

OPERATING CONDITIONS AND TEST PROCEDURES

The conditions and procedures used were selected with the particular objective of attaining an accelerated simulation of a seacoast environment.

Operating Conditions

The standard operating conditions for the environmental chamber are as follows:

Condition	Procedure
UV light (heat)	40 min on and 40 min off
Wetting solution	Synthetic seawater conforming to ASTM 1141-52 (1965) section 4
Wetting cycle	30 s on every 15 min
Wetting rate	65-75 ml of solution/cycle

Panels and Preparation

The standard panels for use in the environmental chamber are 7.6×15.2-cm (3×6-in) cold-rolled, 0.812-mm (20-gauge) thick, SAE 1020 steel panels meeting the specifications of ASTM D609-61. The test panels are prepared as specified in ASTM D609-61 method A, procedure 2 and sandblasted to white metal as specified in Steel Structure Painting Council standard procedure 5-63. The panel number is stamped in the upper left-hand corner, and the panels are painted both front and back with the paint system and by the application method specified (usually brushing). The coated panels are then conditioned by a 24-h oven heat-aging period at 80°C (176°F). After conditioning, the panels are scribed with a special scribing tool. The scribe is made from the upper corner to the lower center on both left and right. Film thickness is measured with a paint thickness gauge. The panels are then ready to be placed in the environmental chamber.

Inspection and Grading

The panels are inspected and graded at intervals of approximately 100 h or as appropriate to the specific study.

The period of time required for testing depends on the resistance of the paint system to degradation and the objectives of the specific test. For structural steel paint systems, failure is considered to have occurred when repainting is required (as judged by an ASTM grade of rusting-5 in the scribe or integrity-9 on the planes). This condition will be reached by most structural steel systems within 600 h in the environmental chamber.

Data Reduction

A computer program was developed that abstracts an integrity (integrity corresponds to the lowest ASTM type rating among the attributes rusting, blistering, cracking, flaking, and erosion) grade from both the scribe and the planes observations and performs a least-squares fit of the data to give separate degradation equations. The program computes a planes service life [SL_p (integrity-9)] and a scribe service life [SL_s (integrity-5)]. These are the main characterizing performance parameters from the environmental test. Examples of the data plots are shown in Figure 6. Note that SL_s is computed from a simple log-decay equation, appropriate for panels predamaged by scribing, whereas SL_p is computed from a growth-decay equation that provides for a necessary induction period before undamaged surfaces begin to deteriorate.

PRECISION STUDIES

Systems

The paint systems selected for this study included the Georgia specification green bridge-paint system (Pb), a standard system of chromate oil-alkyd primer with a gray alkyd finish (Cr), a zinc-rich system of organic zinc primer and aluminum phenolic finish (Zn), and three one-coat primer-only systems.

Experimental Plan

The complete study involved three experimental runs for 750 h each of 8 panels/run—a total of 24 panels. Each run included duplicates of the three full systems (6 panels) and two single-replicate primer panels. The primer panels were scheduled so that a different paint was exposed together for each run, and each primer received two runs.

Figure 6. Computation of service life from experimental data.

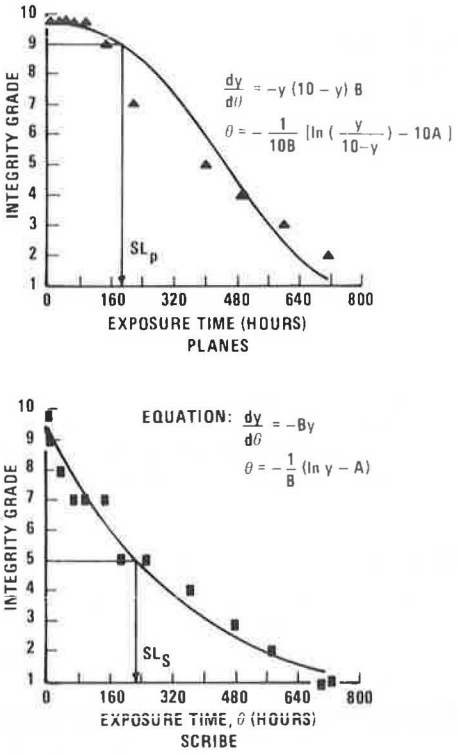

Figure 7. Service-life plots.

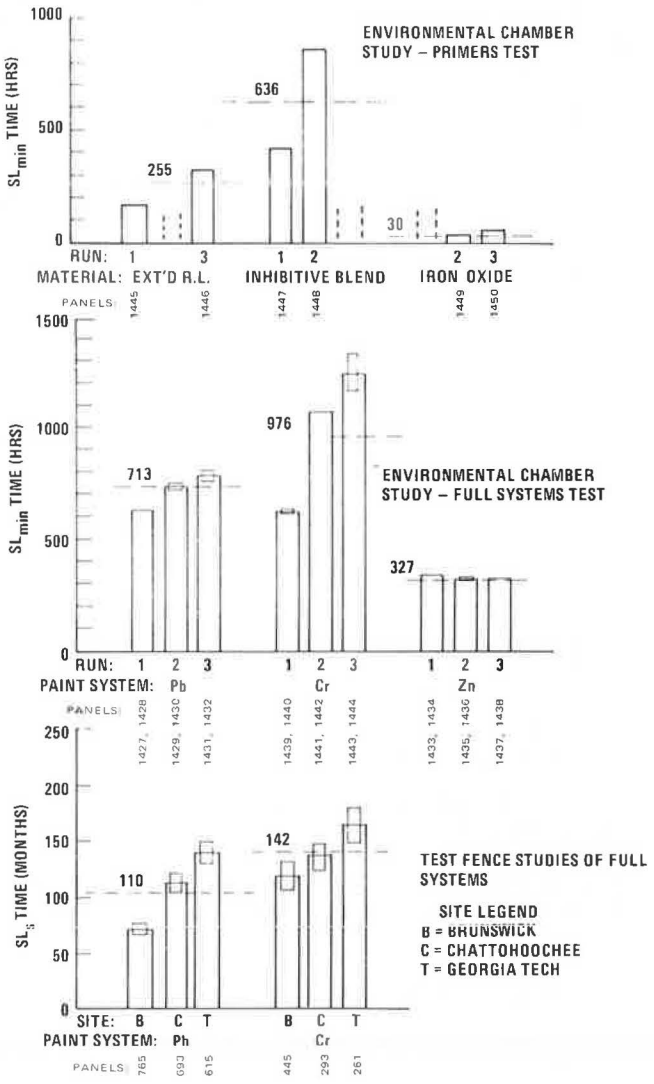

Table 1. Confidence limits for test results.

Type of System	Statistical Index	Computed Service-Life Difference[a] (h)					
		Pb	Cr	Zn	Extended Red Lead	Inhibitive Blend	Iron Oxide
Full	Detectability of system differences[b] [if, in common runs of a pair of joint (simultaneous) experiments[c], the results[d] of two paint systems are compared and the mean difference exceeds the tabulated value, then the systems are significantly different in performance]	20	125	1.5			
	Repeatability of experiments[e] (if, in separate runs of a pair of experiments, the results of two paint systems are compared and the mean difference exceeds the tabulated value, then the systems are significantly different in performance)	191	833	34			
Primers only	Detectability of system differences[b] [if the coefficient of variation of each of these primers is assumed to be similar to that of the chromate full system (Cr) and the experiment consists of two runs in single replicate (one panel), when the mean difference in results between two systems in common runs of joint experiments exceeds the tabulated value, then the systems are significantly different in performance]				56	141	8
	Repeatability of experiments[e] (if, when the coefficient-of-variation assumption and the separate-runs procedure are used, the mean difference in results between the system exceeds the tabulated value, then the systems are significantly different in performance)				266	664	41

[a] Based on 95 percent confidence limits.
[b] From Equation 3a.
[c] An experiment here refers to three runs of one system.
[d] Results are the average service life of duplicate panels.
[e] From Equation 3b.

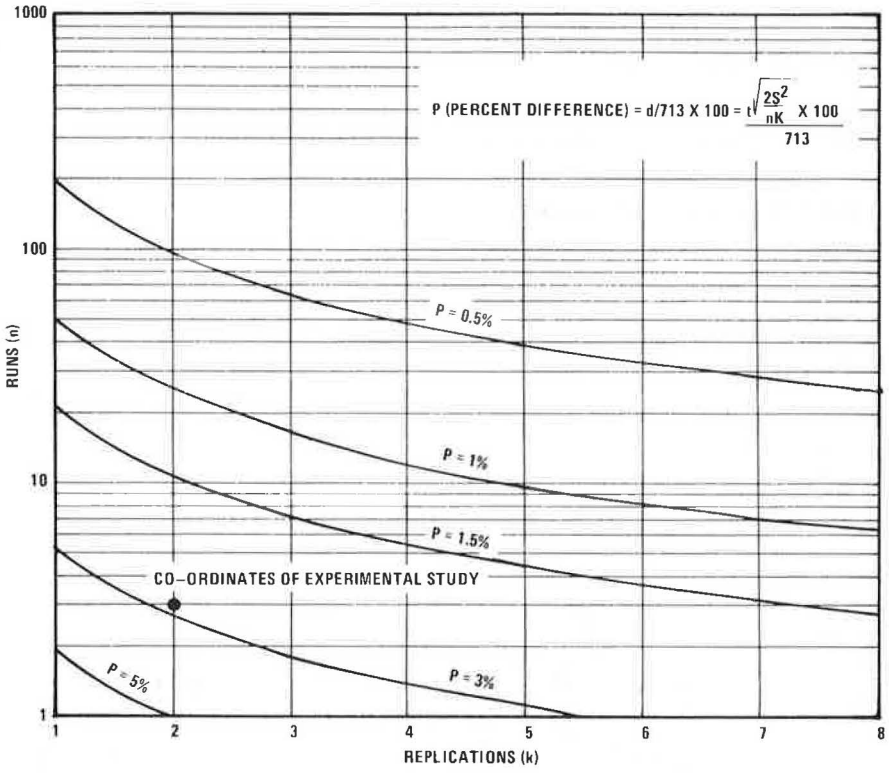

Figure 8. Experimental sensitivity as function of runs and replications: red lead paint systems.

Table 2. Confidence limits for synthesized test-fence data.

Statistical Index	Computed Service-Life Difference[a] (months) Pb	Cr	Zn
Detectability of system differences[b] [if, in common runs of a pair of joint (simultaneous) experiments[c], the results[d] of two paint systems are compared and the mean difference exceeds the tabulated value, then the systems are significantly different in performance]	19	33	-
Repeatability of experiments[e] (if, in separate runs of a pair of experiments, the results of two paint systems are compared and the mean difference exceeds the tabulated value, then the systems are significantly different in performance)	89	63	-

[a] Based on 95 percent confidence limits.
[b] From Equation 3a.
[c] An experiment here refers to three runs of one system.
[d] Results are the average service life of duplicate runs.
[e] From Equation 3b.

Test Results

Reduced service-life data (SL_p and SL_e) were computed and are shown in Figure 7. A statistical analysis of the data from the full-systems tests leads to some useful quantitative generalizations. The variances for replicates (S_R^2) and the variances for runs (S_ϵ^2) were computed by using Equations 1 and 2 and are shown below:

$$S_R^2 = nk \Sigma [(X_{rR} - \bar{X}_R)^2/(k - 1)n] \quad (1)$$

$$S_E^2 = n \Sigma [(\bar{X}_R - \bar{\bar{X}})^2/(n - 1)] \quad (2)$$

where

r = replication,
R = run,
k = replications per run, and
n = number of runs per system.

Source of Variation	df	Full System, S^2 Pb	Cr	Zn
Duplicates within runs	3	124	4 654	0.67
Among run means	2	5405	103 040	171

Values for the detectability of system differences were computed from the statistic

$$d = t \times (2S_R^2/nk)^{1/2} \quad (3a)$$

and values for the repeatability of experiments were computed from the statistic

$$d = t \times (2S_E^2/n)^{1/2} \quad (3b)$$

Some derived 95 percent confidence limits for these are given in Table 1.

Discussion of Precision Studies

The data given in Figure 7 and the confidence limits given in Table 1 clearly show that the environmental chamber is capable of discriminating significant performance differences among the primers and full systems tested. For example, for two lead-type paints run simultaneously in the environmental chamber in duplicate, a difference of only 20 h in their observed service lives justifies a conclusion that the paints are really different.

The relationship between runs and replications for tests of the lead-type paint system (Pb) is plotted in Figure 8, in which the significant difference is expressed as a percentage of the mean service life. The sensitivity of the discrimination exhibited by the equipment used in this study was judged to be well advanced into the area of practical use. One notes, however, from Table 1, that the repeatability of experiments shows large values for significant differences. This means that the run-to-run variability is large and thus the machine-to-machine and machine-to-field correlation must be subject to the same large variation. Additional research to uncover

the source of this variability would be of value.

CORRELATION STUDIES

The purpose of these experiments was to compare the exposure results obtained in the environmental chamber with test-fence data from a marine atmospheric environment (Brunswick, Georgia) that the chamber is intended to simulate.

Figure 9. Single-coat primers: laboratory versus field.

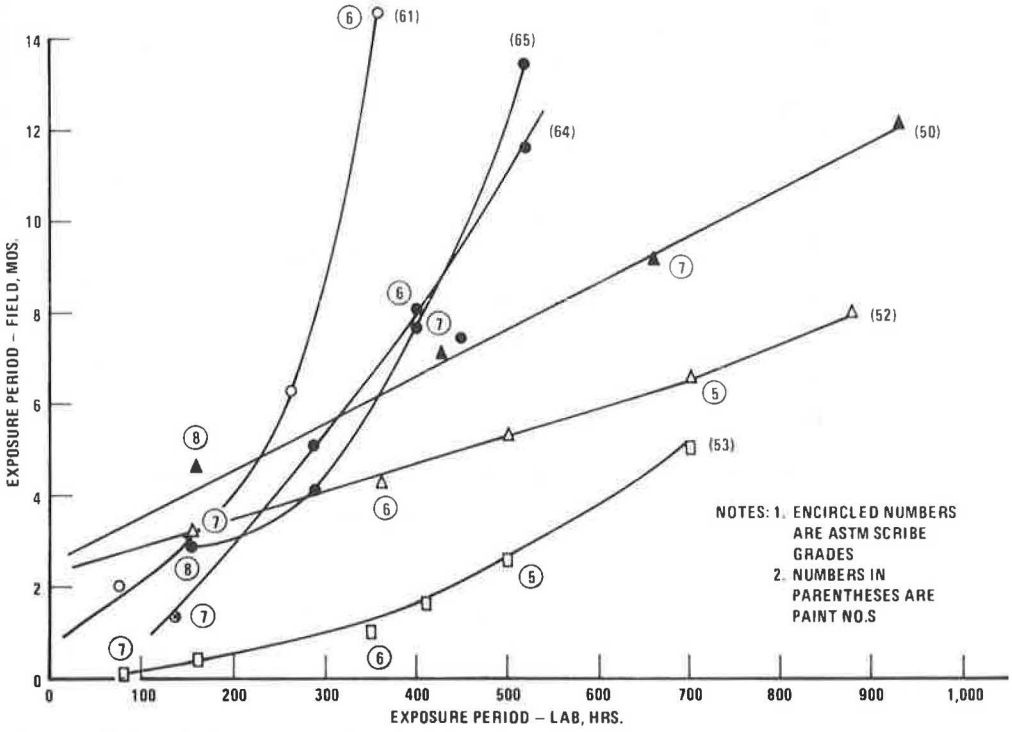

Figure 10. Full systems: laboratory versus field.

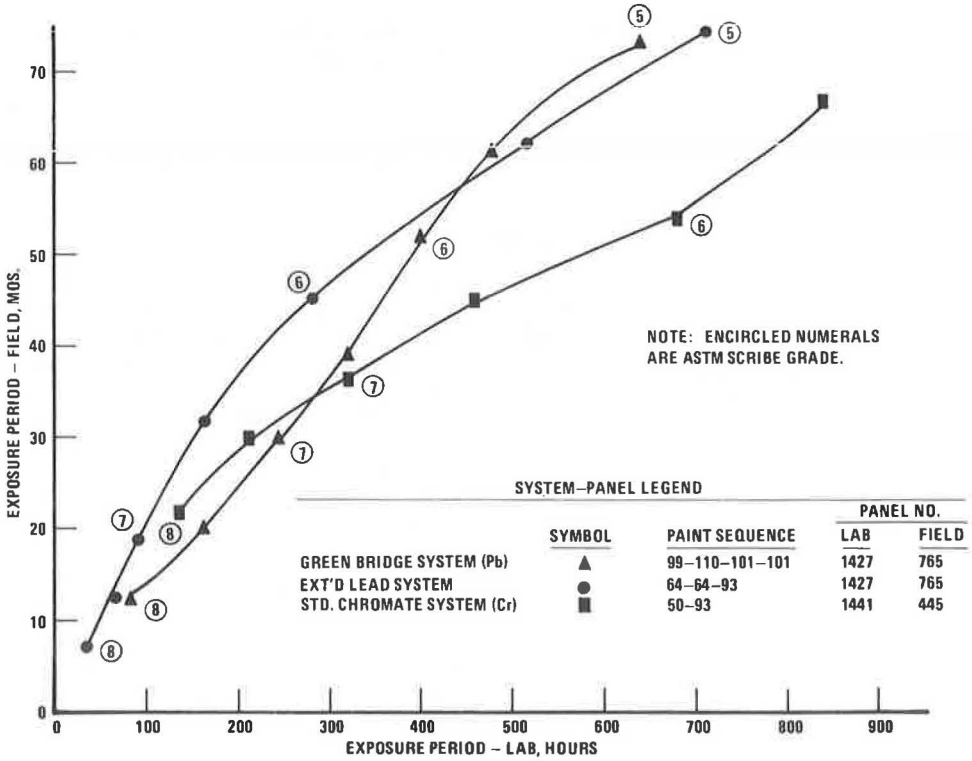

Figure 11. Correlation of two paint systems in environmental chamber.

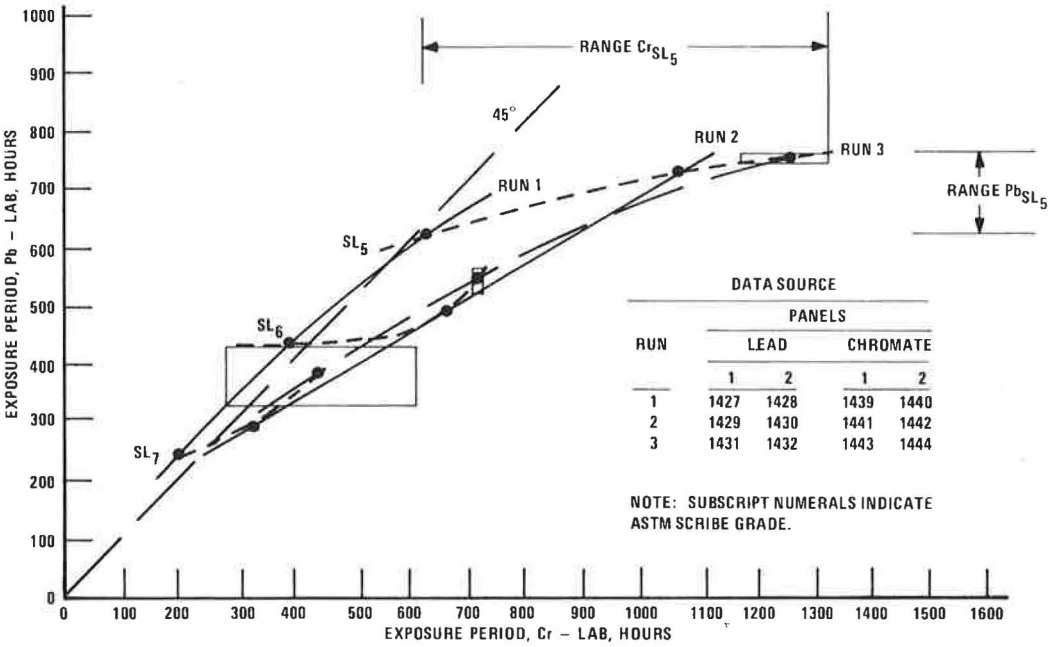

Systems

This study includes all experiments of the precision study and a number of other runs for which corresponding laboratory-field data were available.

Experimental Plan

The correlation experiments were not designed to have the analytical rigor of the precision study but were expected to reveal much about the character of both the laboratory and the field exposure. The general procedure was to plot equal-integrity observations of corresponding single panels (laboratory and field) on time coordinates (hours and months) throughout the exposure periods. To abstract equal-integrity times from the exposure data, it was least-squares fitted to exponential decay curves. Plots were prepared for scribe and planes observations from panel pairs.

Test Results

All of the correlation plots are taken from single-panel data. The laboratory-field lines were traced on a continuous basis to reflect faithfully the correlation with two continuous curves that had been previously fitted to observed performance data. Further smoothing of a resultant curve would be a questionable procedure, despite the suggestion of unusual complexity in some of the correlations.

Finally, the matter of accuracy and precision of correlation was addressed. Available relevant basic data are given in Figure 7 and derived data in the form of confidence limits for laboratory and field data are given in Tables 1 and 2 respectively.

The number of test systems that had exact laboratory-field correspondence was not large; therefore, field tests involving several types of panels and test conditions were assembled to supplement the findings.

Figure 9 shows the laboratory-field correlation of single coat primers (blasted panels in the laboratory and mill-scaled panels in the field).

Figure 10 shows the correlation of laboratory-field systems of closest correspondence—full systems on blasted panels in the laboratory and similar systems on blasted panels exposed 45° south in the field.

Figures 11 and 12 show the Pb versus Cr systems in laboratory and field respectively.

Discussion of Correlation Studies

It would have been unrealistic to have expected that distinctively different paint systems and test conditions (surface preparation and vertical exposure) would all exhibit identical correlation curves. Families of curves as shown in Figure 9 are a reasonable result of diverse conditions. The observed diversity is augmented by the fact that all of the plots presented are for individual pairs of panels rather than for averages. The data shown in Figure 10 are the best available basis for any generalization that is to be drawn. As an approximation, based on a linear least-squares correlation, the mean slope is about 32.5 months/275 h = 0.118 months/h. This corresponds to a rate acceleration of 0.118 months/h × 24 h/d × 30 d/month = 85 field (Brunswick) h/laboratory h.

An effort to read particular interpretations into the individual curves of Figure 10 is probably not justified because of the limited statistical basis. Undoubtedly, however, some systems are nonlinear for the test conditions selected. Conceivably, these results could be linearized by rendering the laboratory test less aggressive (thereby extending the test period). But this may not be the procedure of choice, because an important feature of laboratory tests is the reduction of testing time to a minimum. A better procedure might be to develop standard performance curves for known reference (control) systems in both laboratory and field and use these controls to convert raw observations to standard laboratory results. Standard field results would also embody the advantage of substantially reducing run-to-run variability (which is a major source of experimental error). The efficiency of this general idea has been demonstrated by Mitton and Church (18) in their concept of an "average year of Florida weather."

A detailed development of this subject is beyond the scope of this report, but attention is directed to a dem-

Figure 12. Correlation of two paint systems on test fence.

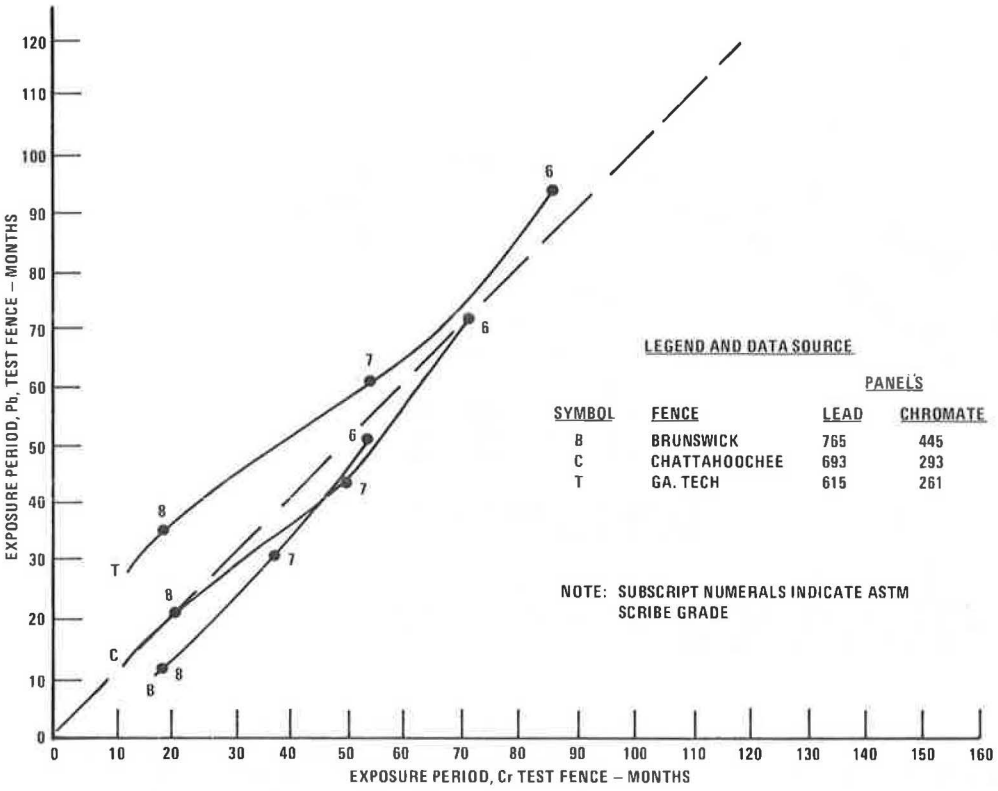

Figure 13. Joint (laboratory-field) 95 percent confidence limits for maximum differences expected under stated conditions: green lead paint system.

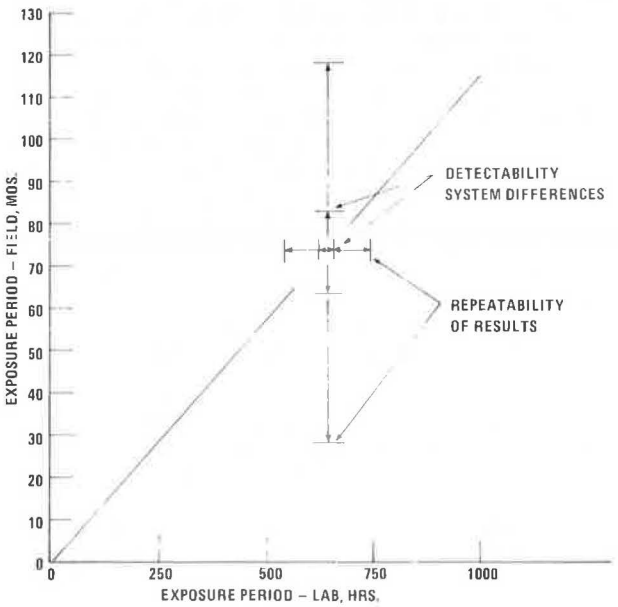

onstrated fact that weather variability (year to year as well as day to day) is a significant variable in exterior paint system tests, just as run-to-run variability is significant in the environmental chamber. A reduction in the variability of the latter by improved mechanical controls could be helpful, but this would not alter the variability of the former (exterior) in any way.

It is possible to derive 95 percent confidence limits at the service-life value (as illustrated in Figure 13 for the green-leaded paint system) for both laboratory and field data. The confidence limits for the field results represent only a conservative estimate, as discussed above. The limits are based on the definitions stated in Tables 1 and 2 wherein the ranges shown represent the maximum difference between two experiments. The outer limits may be regarded as accuracy (between-run) limits, which are applicable in the absence of standardization. The inner or precision (within-run) limits are those that would obtain if standardization eliminated run-to-run variation. Clearly, standardization procedures must become routine if a satisfactory basis for paint-system design is to be achieved.

CONCLUSIONS

An environmental chamber of fairly simple construction, as assembled for this project, displayed a useful capability for accelerated simulation of the effects of corrosion on painted panels of a seacoast test-fence environment as observed at Brunswick, Georgia. More specific conclusions follow:

1. The observed average panel-degradation rates of several representative test systems were approximately 85 times the test-fence rate. (This is an order-of-magnitude figure and not intended for performance estimation.)
2. The reproducibility or precision within runs of the environmental chamber experiment was quite good; the procedure was capable of distinguishing, at 95 percent confidence limits, within-run differences as small as 7.3 percent of the mean service life [average of Pb and Cr system means = $100 \times [(20/713) + (125/976)]/2 = 7.3$ percent]. Thus, operating conditions for all specimen

positions within the chamber may be regarded as essentially identical.

3. The repeatability or accuracy of results between runs appeared to require the use of control systems to reduce the variability. With an effective control technique, the run-to-run variation could approach the within-runs limits.

4. The correlation with the Brunswick 45° south seacoast test-fence results was generally good, but sufficient distinct differences in correlation curves were observed among different paint systems to make the use of control systems advantageous for the detection and computation of nonlinear correlations.

ACKNOWLEDGMENTS

My associate, David R. Hurst, was actively involved in all phases of the work reported in this paper and contributed significantly to both conception and implementation. Lewis Young patiently led us through the intricacies of the design and analysis of experiments that use statistical methods. At the time the work was conducted (1971-1973), we were employed at the Georgia Institute of Technology Engineering Experiment Station. The work here reported was sponsored by the Georgia Department of Transportation in cooperation with the Federal Highway Administration. The contents of this paper reflect my views only and do not necessarily reflect the views or policies of the Georgia Department of Transportation or the Federal Highway Administration.

REFERENCES

1. H. A. Nelson. Accelerated Weathering of Paints on Wood and Metal Surfaces. Proc., ASTM, Vol. 22, Pt. 2, 1922.
2. H. A. Nelson and F. C. Schmutz. Further Study of Accelerated Weathering: Effect of Variation in Exposure-Cycle Combinations on Common Types of Varnishes. Proc., ASTM, Vol. 24, Pt. 2, 1924.
3. H. A. Nelson and F. C. Schmutz. Accelerated Weathering: A Consideration of Some Fundamentals Governing Its Application. Industrial and Engineering Chemistry, Vol. 18, 1926, p. 1222.
4. H. A. Nelson, F. C. Schmutz, and D. L. Gamble. Accelerated Weathering: Further Development of Apparatus and Exposure Cycles. Proc., ASTM, Vol. 26, Pt. 2, 1926.
5. H. A. Gardner and G. G. Sward. Physical and Chemical Examination of Paints, Varnishes, Lacquers, and Colors. ASTM, 11th Ed., Jan. 1950, pp. 239-257.
6. ASTM E 42-64: Operating Light- and Water-Exposure Apparatus (Carbon-Arc Type) for Artificial Weathering Test. ASTM, Standards, Pt. 30, May 1965, pp. 262-269.
7. ASTM D 822-60: Operating Light- and Water-Exposure Apparatus (Carbon-Arc Type) for Testing Paint, Varnish, Lacquer, and Related Products. ASTM, Standards, Pt. 21, Jan. 1965, pp. 161-163.
8. Evaluation of Various Weatherometers for Determining the Service Life of Organic Coating. Cleveland-Dayton-Indianapolis-Cincinnati Society for Paint Technology Official Digest, Vol. 34, No. 454, 1191, 1962.
9. L. Valentine. Limitations of Paint Testing. Journal of the Oil and Color Chemists Association, Sept. 1963, pp. 674-717.
10. H. W. Talen. The Requirements for the Prediction of Paint Performance. Journal of the Oil and Color Chemists Association, Nov. 1963, pp. 940-975.
11. R. M. Burns and W. W. Bradley. Organic Coatings Performance and Evaluation, Protective Coatings for Metals. American Chemical Society, Monograph 163, 3rd Ed.; Reinhold, New York, 1967, p. 499.
12. P. J. Gay. Accelerated Weathering of Paint and Varnish Films. Journal of the Oil and Color Chemists Association, Vol. 34, No. 368, 1951, pp. 43-77.
13. H. A. Gardner. Rapid Exposure Tests on Finishes. Industrial and Engineering Chemistry, Analytical Ed., Vol. 4, 1932, pp. 94-97.
14. R. I. Wray. Painting Magnesium Alloys. Industrial and Engineering Chemistry, Vol. 33, 1941, p. 932.
15. J. R. Rischbieth and K. R. Bussell. The Evaluation of Priming Paints by Corrosion Tests. Journal of the Oil and Color Chemists Association, Vol. 44, 1961, pp. 367-376.
16. J. D. Keane. Protective Coatings for Highway Steel: Literature Survey. NCHRP, Rept. 74A, 1969.
17. A Study of Highway Corrosion Problems and Metal-Protective Coatings Systems. Engineering Experiment Station, Georgia Institute of Technology, Atlanta, July 1, 1971.
18. P. B. Mitton and R. L. Church. Measuring and Minimizing the Variability in Evaluating Outdoor Exposure Results. Journal of Paint Technology, Vol. 39, No. 514, Nov. 1967.

Publication of this paper sponsored by Committee on Coatings, Signing, and Marking Materials.

Measurement of Polarized Potentials in Concrete Bridge Decks

H. J. Fromm, Research and Development Division, Ontario Ministry of Transportation and Communications, Downsview

An investigation was conducted to determine the best method of measuring the polarized potential of the reinforcing steel in a cathodically protected bridge deck. The use of carbon rods and copper-copper sulfate and zinc-zinc sulfate half-cells as probes was studied in laboratory slabs and bridge decks. The carbon probes were found to be more accurate and reliable; the half-cells produced variable results. The coke layer was found to act as a half-cell and its voltage had to be taken into account when measuring the polarized potentials in the deck.

The application of cathodic protection to concrete bridge decks to mitigate the corrosion of the reinforcing steel has been shown to be successful by the work of Stratfull (1, 2) and of Fromm and Wilson (3, 4). This type of application, however, requires careful control of the potential to which the reinforcing steel is lowered with reference to the copper-copper sulfate ($Cu-CuSO_4$) half-cell. For pipelines, the steel is protected if the potential is maintained at less than -0.85 V (5). For reinforcing steel in concrete, the potential must not be lower than -1.1 V. It has been claimed by Scott and Hausmann (6, 7) that potentials lower than -1.1 V can cause disbonding of the steel. It is thus necessary to be able to measure and control accurately the potentials induced on the reinforcing steel.

Stratfull (2) has measured these potentials by placing a $Cu-CuSO_4$ half-cell on the nonconducting asphalt concrete surfacing and soaking the surfacing with a detergent solution to obtain conduction. Fromm (3, 4) has made use of the unused anodes in the conductive layer or placed special carbon probes in the conductive layer to sense the potential, which was then measured at the junction box. Others have tried to sense the potential in a deck by using half-cells cast in the upper surface of the concrete, but the results were confusing and could not be interpreted.

The purpose of this investigation was to test the method of using carbon probes and to further investigate the use of half-cells as probes and controls for the rectifier.

SURFACE MEASUREMENT OF POTENTIAL

Three types of probes have been used by the Ontario Ministry of Transportation and Communications to measure the potentials in bridge decks. On the first two bridges tested (3, 4), high-silicon-content cast-iron anodes were used to sense the potentials. Each anode was connected to the junction box by a separate wire so that each area could be measured separately. On the next two bridges (3, 4), carbon rods set in the coke layer were used to measure the potentials. Since that time, square graphite rods, 50×50×150 mm (2×2×6 in) long, have been used to measure the potentials. These graphite probes were embedded in the deck with only the surface of the probe in contact with the coke. In all cases, the potentials were measured at the junction box to which the probes were connected by separate wires.

The potential measurements made by using the anodes and the carbon probes described above are reported as being similar to those obtained by using a $Cu-CuSO_4$ half-cell. Typical data are given in Table 1 (the sign given before the voltage is that conventionally used in corrosion measurements and refers to the saturated $Cu-CuSO_4$ half-cell). This table shows the measurements made on bridge 9, the first bridge to be protected. The anodes were spaced along the length of the deck, 3.66 m (12 ft) apart. Next to each anode, a hole 63 mm (2.5 in) in diameter was cored through the surfacing to bare the concrete deck, and a $Cu-CuSO_4$ half-cell was placed on the concrete in each of the holes. The difference between the mean anode voltage and the mean $Cu-CuSO_4$ half-cell voltage for the power-on columns is 0.16 V and that for the power-off columns is also 0.16 V. This identical difference suggests that some other factor (such as a voltage contribution due to the coke) may be involved.

Table 1. Comparison of voltage measurement methods: bridge 9.

	Anode Potential (V)		$Cu-CuSO_4$ Half-Cell Potential (V)	
Anode No.	Power On	Power Off	Power On	Power Off
1	-0.68	-0.67	-0.56	-0.56
4	-0.70	-0.70	-0.52	-0.52
6	-0.72	-0.71	-0.57	-0.56
9	-0.76	-0.75	-0.60	-0.59
11	-0.78	-0.77	-0.58	-0.58
14	-0.80	-0.79	-0.64	-0.63
16	-0.83	-0.82	-0.67	-0.65
19	-0.87	-0.85	-0.72	-0.69
21	-0.93	-0.86	-0.82	-0.73
Avg	-0.79	-0.77	-0.63	-0.61

DETERMINATION OF COKE POTENTIAL

Coke similar to that used for the conductive mix on bridge 9 was obtained, placed in a glass beaker, and moistened with 1N hydrochloric acid. A platinum connector was immersed in the coke. A $Cu-CuSO_4$ half-cell was then pressed onto the coke, and the voltage between the coke and the $Cu-CuSO_4$ cell was measured by using a 100-MΩ impedance voltmeter. This procedure was repeated using a zinc-zinc sulfate ($Zn-ZnSO_4$) half-cell and finally using a saturated calomel electrode. The results obtained are given below:

Electrolytic Cell	Potential (V)
Coke-H^+ ‖ Cu^+-$CuSO_4$	0.31
Coke-H^+ ‖ Zn^+-$ZnSO_4$	1.43
Coke-H^+ ‖ Saturated calomel	0.44

The half-cell potentials for the above half-cells referenced to the standard hydrogen electrode (8) are given below:

Half-Cell	Potential (V)
Cu^+-$CuSO_4$	+0.3402
Zn^+-$ZnSO_4$	−0.7628
Saturated calomel	+0.2415

Thus, the half-cell potential of the Coke-H^+ was

According to	Potential (V)
$Cu-CuSO_4$ half-cell	+0.65
$Zn-ZnSO_4$ half-cell	+0.67
Calomel electrode	+0.68
Mean	+0.67

If 1N sodium chloride solution is substituted for the 1N acid, the results are almost identical.

If only tap water is used to moisten the coke, the average carbon potential obtained by using the same techniques is 0.44 V.

This carbon potential thus explains the higher potentials obtained when the anodes are buried in the coke compared with those obtained by using the $Cu-CuSO_4$ half-cell on the concrete deck. The results shown in Table 1 suggest an average carbon potential of +0.50 V. This value is reasonable because the readings were taken during the summer when most of the winter salt would have been flushed out of the coke layer.

When the $Cu-CuSO_4$ half-cell was placed in contact with the top of the coke layer on the bridge deck to read the polarization of the deck, a somewhat higher potential was obtained. Higher, that is, than if the cell had been placed directly on the concrete deck surface. This potential varied between 0.10 and 0.16 V and was due to the contribution of the coke layer.

Figure 1. Arrangement of half-cells and carbon probes on rebar: test specimen 1.

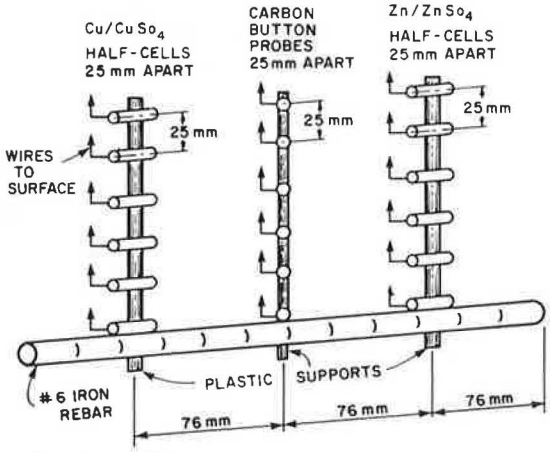

Note: 1 mm = 0.04 in.

MEASUREMENT OF BRIDGE-DECK POTENTIALS BY USING HALF-CELLS

Half-cells for measuring rebar potentials were buried below the surface of the concrete in four bridge decks. Two types of cells were used—Zn-$ZnSO_4$ and Cu-$CuSO_4$. The potential readings obtained by using these half-cells were difficult to interpret and did not correlate with the potentials sensed in the coke layer by electrodes or by carbon probes.

Examples from two bridge decks that illustrate this problem are given below.

	Potential (V)		
Bridge	Carbon Probe in Coke	Cu-$CuSO_4$ in Deck	Zn-$ZnSO_4$ in Deck
Medway Creek	-1.15	-0.86	+0.62
Paint Lake (1)	-0.95	-0.46	+0.45
Paint Lake (2)	-0.95	-0.36	+0.51

To more fully understand the meaning of the voltage readings and the variation of the readings, some concrete specimens containing half-cells and carbon probes were cast in the laboratory.

Test Specimen 1

Test specimen 1 was a block of concrete 300×300×184 mm (12×12×7.25 in) high that had a no. 6 rebar cast into it 25 mm (1 in) above the bottom. A series of Cu-$CuSO_4$ half-cells, a series of Zn-$ZnSO_4$ half-cells, and a series of carbon button probes (slices of a dry-cell carbon electrode) were arranged on plastic supports rising vertically from the bar to the top of the block. This arrangement is shown in Figure 1.

Before the block was cast, the rebar was covered with a thin coating of grout, which was allowed to dry. The first cell of each of the three series was placed in contact with the grout (thus being set very close to the rebar). The remaining five cells in each series were arranged above this bottom cell, 25 mm apart. The top cell in each series was just below the top surface of the block. The carbon-probe series was positioned between the Cu-$CuSO_4$ and the Zn-$ZnSO_4$ half-cells. Each series was separated from the adjoining one by 76 mm (3 in) on centers and each was 76 mm in from the sides of the block. The top of the block was covered with coke breeze and power was applied to the block by connecting the coke to the positive terminal of a rectifier and the rebar to the negative terminal.

The cells in each series were numbered consecutively, no. 1 being closest to the rebar and no. 6 being at the top of the block.

After the block had cured, a 1.5-V DC potential was applied between the coke covering the block and the rebar. After a few days, some of the cells and carbon probes were found to be giving potential readings different from the others. The power was turned off, and the block was allowed to discharge until there was no further change in cell readings. (Before the block was made, all half-cells had been tested and found to produce acceptable half-cell voltages).

When the potential readings were taken at equilibrium between the rebar and the half-cells and carbon probes, it was found that the no. 1 carbon probe had shorted to the rebar and was therefore useless, and that one carbon probe, one Cu-$CuSO_4$ half-cell, and two Zn-$ZnSO_4$ half-cells were producing different readings. Correction factors for these were computed so that their readings could be used with the others.

Because all cells had been tested before use, it is thought that the differences may have been due to small local differences in composition of the concrete. This does point out, however, that caution must be exercised when relying on half-cells to control the potential in a bridge deck and that backup cells should be installed.

After the half-cells in the block had been calibrated, a 1.0-V DC potential was applied to the block. The build-up of polarized voltage in the block was monitored daily by taking potential readings between each half-cell lead and the rebar and a Cu-$CuSO_4$ half-cell reading between the surface coke and the rebar. The readings were taken with the applied DC current turned off. On the sixteenth day, the applied voltage was increased to 1.5 V and maintained at this level to the end of the test. The results obtained are shown in Figure 2.

The specimen potential measured by a Cu-$CuSO_4$ half-cell on the surface coke is shown in the lower curve of Figure 2. The next curve shows the average potential indicated by the six internal Cu-$CuSO_4$ half-cells. The middle curve is the mean potential of the carbon probes and the top curve is the mean potential of the Zn-$ZnSO_4$ half-cells.

The first portion of these curves shows the equilibrium potential as indicated by the four methods of measurement. The specimen had previously been polarized and then the current was removed and it was allowed to settle to the condition as shown. On the seventh day, a 1.0-V potential was applied. At first, the polarization overshot the new equilibrium value by about 0.1 V. Equilibrium was achieved on the twelfth day and was held until the sixteenth day. The applied voltage was then increased to 1.5 V and, here again, there was a small overshoot before equilibrium was achieved. In the case of the polarized potential indicated by the Zn-$ZnSO_4$ half-cells, there was a continued slow decrease in value.

The polarization indicated by the Cu-$CuSO_4$ half-cell on the surface of the coke was lower than that indicated by the upper Cu-$CuSO_4$ half-cells in the block. This was due to the half-cell effect of the coke layer.

The mean voltages for the half-cells and probes at equilibrium are given in Table 2, and the results are shown in Figures 3, 4, and 5.

Figure 3 shows the potential gradient that existed within the block when power was applied at both 1 and 1.5 V as indicated by the Cu-$CuSO_4$ half-cells. A definite potential gradient existed within the block, decreasing as the rebar was approached. The polarized potential measured by the Cu-$CuSO_4$ cells throughout the block was the same because no current was being ap-

Figure 2. Change of polarized voltage in test specimen with time.

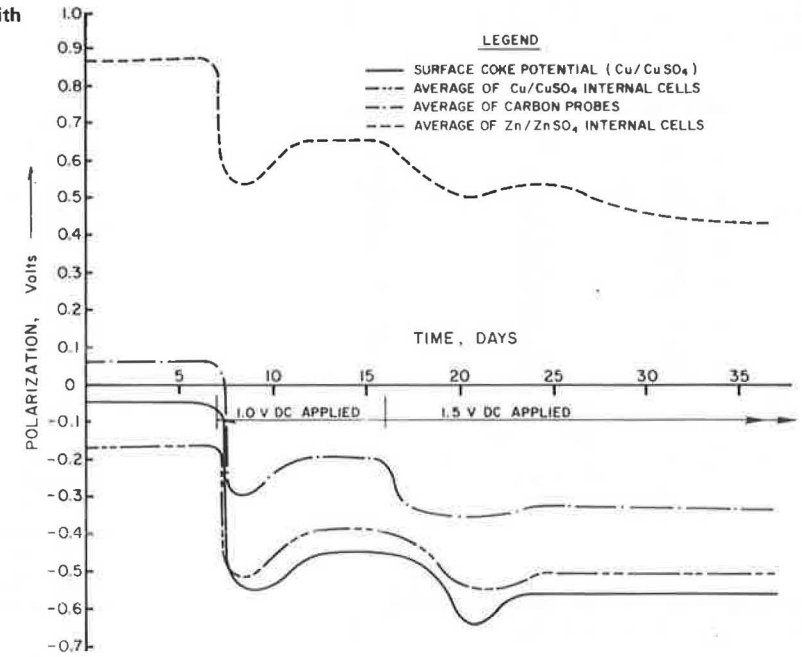

Table 2. Mean polarized potentials in test specimen 1.

Type of Cell	Cell No.[a]	Applied Potential (V) 1.0 V Power On	1.0 V Power Off	1.5 V Power On	1.5 V Power Off
Cu-$CuSO_4$	1	-0.42	-0.40	-0.58	-0.52
	2	-0.51	-0.43	-0.78	-0.57
	3[b]	-0.51	-0.40	-0.81	-0.53
	4	-0.55	-0.42	-0.90	-0.55
	5	-0.56	-0.40	-0.96	-0.55
	6	-0.56	-0.38	-1.00	-0.52
Zn-$ZnSO_4$	1[b]	+0.76	+0.78	+0.50	+0.56
	2	+0.57	+0.66	+0.29	+0.52
	3[b]	+0.55	+0.68	-[c]	-[c]
	4	+0.54	+0.68	+0.19	+0.56
	5	+0.57	+0.73	+0.19	+0.60
	6	+0.58	+0.74	+0.16	+0.90
Carbon probe	1[d]				
	2[b]	-0.37	-0.19	-0.79	-0.32
	3	-0.34	-0.18	-0.76	-0.34
	4	-0.34	-0.23	-0.72	-0.35
	5	-0.35	-0.23	-0.68	-0.36
	6	-0.35	-0.25	-0.66	-0.40

[a] No. 1 cells located at the rebar and no. 6 cells located at the top of the specimen.
[b] Values adjusted as per calibration.
[c] Half-cell failed.
[d] Probe shorted to rebar.

Figure 3. Applied and polarized potential gradients: Cu-$CuSO_4$ half-cells.

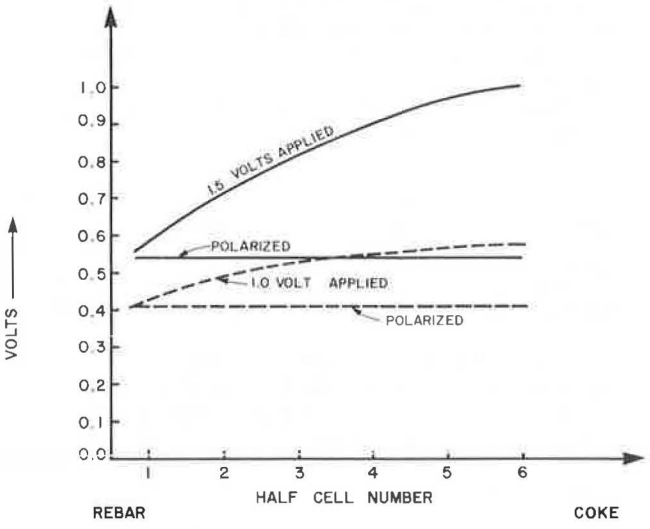

plied and no current was being drawn. The polarized potential is shown here as the meter reading and not with the sign reversed as is customary in corrosion measurements. This was done to better illustrate the potential gradient that existed when a positive voltage was applied to the surface. Figure 4 shows the same effect as indicated by the Zn-$ZnSO_4$ half-cells.

The carbon probes (Figure 5) behaved in a way that could not be explained. When power was applied at 1.0 V, they showed no gradient, and at 1.5 V, they showed a reverse gradient. They did, however, indicate the polarization level as expected.

The potential gradients shown in Figures 3 and 4 indicate that, as the amount of cover of concrete over the rebars increases, higher applied potentials will be necessary to attain the desired polarization voltage.

Relationship Between Voltages Indicated by Different Half-Cells

It is common practice to determine the polarized potential on pipelines and bridge decks by using the Cu-$CuSO_4$ half-cell. The maximum and minimum limits placed on the polarized potential for bridge decks have always been stated as volts negative to this half-cell. When other cells are used to sense the polarized potential in the deck, it is necessary to change the values thus obtained to values in terms of the Cu-$CuSO_4$ cell. It is also normal practice to connect the measuring half-cell to the positive terminal of the voltmeter and to report the voltage as positive or negative with regard to this alignment.

The relationship between the Cu-$CuSO_4$ voltage and the other half-cell voltages is the following:

$$V_{Cu(R)} - V_{X(R)} = V_{Cu(M)} - V_{X(M)} \quad (1)$$

where

$V_{Cu(R)}$ = Cu-$CuSO_4$ equilibrium reduction potential (+0.34 V),
$V_{X(R)}$ = equilibrium reduction potential of half-cell in question,
$V_{Cu(M)}$ = polarized potential of the slab as measured by the Cu-$CuSO_4$ half-cell, and
$V_{X(M)}$ = polarized potential of the slab as measured by the half-cell in question.

Equation 1 can be rearranged as follows:

$$[V_{Cu(R)} - V_{X(R)}] + V_{X(M)} = V_{Cu(M)} \quad (2)$$

which gives the voltage that a Cu-$CuSO_4$ half-cell would read if used in place of the half-cell in question.

This method was tested on the polarized-potential results obtained from test specimen 1; the procedure is illustrated below.

	Applied Potential (V)	
Item	1.00	1.50
1. Cu-$CuSO_4$ cell	0.41	0.54
2. Zn-$ZnSO_4$ cell	−0.69	−0.57
3. Carbon probe	0.22	0.35
Item 1 - item 3	0.19	0.19
Item 1 - item 2	1.10	1.11
Item 2 - item 3	−0.91	−0.92

Figure 4. Applied and polarized potential gradients: Zn-$ZnSO_4$ half-cells.

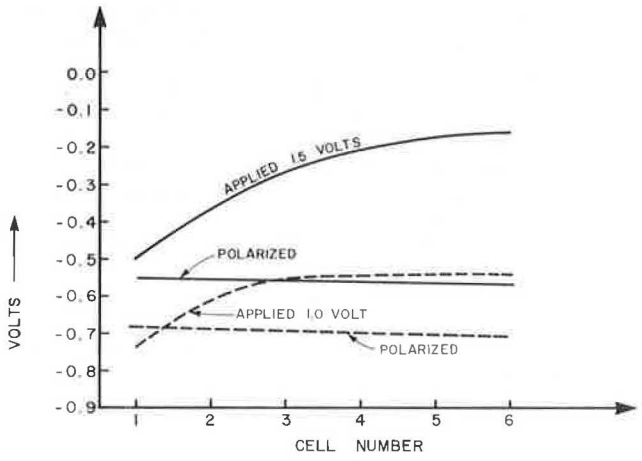

Figure 5. Applied and polarized potential gradients: carbon probes.

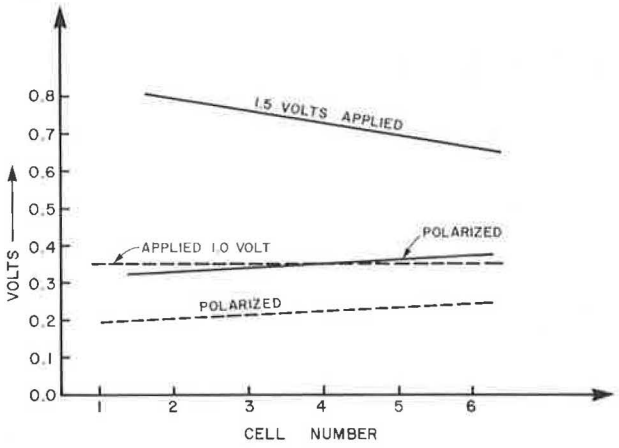

(The signs used do not follow the usual corrosion convention for signs. Here the polarized potential is shown as +0.41 for the Cu-$CuSO_4$ half-cell. This is the value as read on the meter. These values were used to be consistent with the standard half-cell-reduction potential values.) By using the half-cell potentials, we have

$$V_{Cu(R)} - V_{Zn(R)} = 0.34 + 0.76 = 1.10\,V \quad (1a)$$

and the Zn-$ZnSO_4$ half-cell reading of -0.69 V can be converted to the equivalent Cu-$CuSO_4$ half-cell reading by using Equation 2.

$$1.10\,V + (-0.69) = 0.41\,V \quad (2a)$$

This is the same value as that measured by the Cu-$CuSO_4$ half-cell (see table above). Similarly, the Zn-$ZnSO_4$ half-cell value of -0.57 V is equivalent to 0.53 V for the corresponding Cu-$CuSO_4$ half-cell, which agreed with the measured value of 0.54 V within experimental error.

If a value shown in the table above for the Zn-$ZnSO_4$ is subtracted from the corresponding value for the Cu-$CuSO_4$ cell, the result should be the potential of the combined electrolytic cell. These results (i.e., item 2 - item 1) are the same as the theoretical results for the Cu-Zn cell cell couple, i.e., 1.10 V. Similarly, the differences between items 1 and 3 and between items 2 and 3 of the table above can be used to estimate the potential of the carbon half-cell. The half-cell potential calculates to be 0.15 V. The result is considerably lower than the value reported in the first part of this paper for carbon in a solution of ions of unit activity. In the reinforced concrete slab, the carbon probe is surrounded by concrete that contains a saturated solution of calcium hydroxide (which is a weak electrolyte). This could account for the much lower potential.

The procedure shown above can be used to convert the potential shown by any half-cell, such as the Ag-AgCl half-cell, to a value in terms of the Cu-$CuSO_4$ half-cell. After the calculation is made, the sign for the equivalent Cu-$CuSO_4$ half-cell must be reversed to conform to the conventional notation.

Cu-$CuSO_4$ and Zn-$ZnSO_4$ half-cells were placed in four bridge decks in slits cut in the deck and covered so that they were about 25 mm below the surface. For the most part, these cells produced readings that did not agree with those given by voltage probes distributed throughout the coke layer. Similar half-cells were used to control the potential-controlled rectifiers used on these bridges. The rectifiers were adjusted to produce the desired voltage as sensed in the coke layer by the probes. The actual readings of the half-cells were disregarded. The curves shown in Figure 2 and the data given in Table 2 confirm the validity of this approach. The data for only one test specimen are reported here. Several other specimens have been made and tested in the laboratory; the results have been the similar.

DISCUSSION OF RESULTS

The results of this investigation have shown that an acceptable way to monitor the potential in a cathodically protected bridge deck is to use voltage probes in the coke layer. This investigation has also shown that the coke and electrolyte act as a half-cell and that its potential must be taken into account when evaluating results. Experience has shown that the voltage sensed in the coke is 0.1 to 0.16 V higher than that sensed by a Cu-$CuSO_4$ half-cell on the concrete deck surface. Therefore, the minimum and maximum limits for the degree of polarization required to give protection to the bridge deck steel

must be changed accordingly. It was found (3) that corrosion did not begin to occur in a bridge deck until the polarized voltage had dropped to -0.55 V, which shows that the recommended -0.85-V minimum (5) has a considerable margin of safety built into it. As a result, the minimum and maximum polarized voltages sensed by carbon probes in the coke layer are recommended as -0.80 and -1.25 V. These values still contain a safety factor.

Half-cells buried in concrete are subject to failure or erratic behavior. This was shown in test specimen 1 in which the failure rate was quite high. Similarly, in bridge decks, these cells showed variable results. The reason for this behavior is not known.

Some results have been obtained from the bridges treated with cathodic protection that suggest that half-cells located close to rebars tend to give higher readings than those located farther away from the bars. This result may appear to contradict that obtained in the laboratory test specimen in which there was no potential gradient when, with no current being applied, the polarized potential was measured by several half-cells located at different distances from the bar. This may be explained by the fact that the laboratory specimen was electrically isolated and had no connection to ground, so that the polarized voltage could not leak off. In the case of a bridge deck, this is not the case. There is always some connection through the concrete and rebars to ground, so that the voltage can leak off, slowly or rapidly, and this will give rise to a potential gradient in the deck. This effect could also be the cause of lower polarized potentials that have been measured on the undersides of bridge decks.

The use of a carbon probe in the coke and in contact with the deck tends to average the potential and removes the effect of the distance from a rebar. This averaging effect is not found when a half-cell is buried in the concrete; this cell reads only the potential at that point. Thus, the carbon probe in the coke is the preferred way to determine the polarized potential.

The amount of power required to protect a bridge deck will vary with the amount of cover over the rebars and the electrical leakage from the deck. Higher amounts of cover will require a higher applied voltage.

CONCLUSIONS

1. Carbon probes located in the coke layer and in contact with the deck provide a good method of measuring the polarized potential on the reinforcing steel.
2. The moist coke layer acts as a half-cell and its voltage must be taken into account when measuring the polarized potential of deck rebars.
3. The recommended range of polarized potential to provide protection to the reinforcing steel is -0.80 to -1.25 V, when read by carbon probes located in the coke layer and in contact with the concrete deck.
4. Half-cells buried in the deck and used as voltage probes produce variable results and should be used cautiously.
5. Various types of half-cells can be used to control the potential-controlled rectifiers on bridges. Here the rectifier must be set, not on the theoretical value of the half-cell, but to the calibration that will provide the desired potential on the deck steel.

REFERENCES

1. R. F. Stratfull. Inhibiting the Corrosion of Steel in a Reinforced Concrete Bridge. Corrosion, Vol. 15, No. 6, 1959, p. 331.
2. R. F. Stratfull. Experimental Cathodic Protection of a Bridge Deck. TRB, Transportation Research Record 500, 1974, pp. 1-50.
3. H. J. Fromm and G. P. Wilson. Cathodic Protection of Bridge Decks: Study of Three Ontario Bridges. TRB, Transportation Research Record 604, 1976, pp. 38-47.
4. H. J. Fromm. Cathodic Protection of Rebar in Concrete Bridge Decks. Materials Performance, Vol. 16, Nov. 1977, pp. 21-28.
5. Control of External Corrosion on Underground Piping Systems. National Association of Corrosion Engineers, Standard RP-01-69.
6. D. A. Hausmann. Criteria for Cathodic Protection of Steel in Concrete Structures. Materials Protection, Vol. 8. No. 10, 1969, p. 23.
7. G. N. Scott. Corrosion-Protection Properties of Portland Cement. American Water Works Association Journal, Vol. 57, No. 8, 1965.
8. Handbook of Chemistry and Physics. Chemical Rubber Company, 48th Ed., 1968.

Publication of this paper sponsored by General Materials Section and Committee on Corrosion.

Methods of Determining Corrosion Susceptibility of Steel in Concrete

A. M. Rosenberg and J. M. Gaidis, W. R. Grace and Company, Columbia, Maryland

Several test methods were used to study the effectiveness of calcium nitrite as a corrosion inhibitor in concrete. Measurements of open-circuit potential and of polarization in concrete were found to be useful, provided the steel area studied was completely covered by concrete. Tests in which limewater was used as a substitute for concrete yielded similar results. Induced electrolysis was found to be misleading because of other reactions that occurred. Tests on large slabs [1.8x0.6x0.15 m (6x2 x0.5 ft)] that were salted daily showed that calcium nitrite reduced the corrosion susceptibility more than fourfold.

Corrosion is an electrochemical phenomenon (1). An oxide coating does not form on iron in a dry atmosphere.

Corrosion continues because the iron oxide film is not thermodynamically stable in the presence of metallic iron and moisture (2). The result is the formation of the more soluble ferrous ion, which can move away, thus exposing more iron surface to corrosion.

In concrete, where the pH of the medium is approximately 12.5, iron in the ferric state is the most stable form (3). This makes concrete one of the best rust-preventive coatings. A thin film of iron oxide acts as the cathodic part of the reinforcing bar where oxygen is reduced

$$\tfrac{1}{2}O_2 + H_2O + 2e^- \rightarrow 2OH^- \quad (1)$$

Iron goes into solution at the anode but, in concrete, it rapidly goes to the highest oxidation state as

$$Fe \rightarrow 2e^- + Fe^{++} \quad (2)$$

$$Fe^{++} + 2OH^- \rightarrow Fe(OH)_2 \quad (3)$$

and, by subsequent oxidation,

$$Fe(OH)_2 \rightarrow Fe(OH)_3 \quad (3a)$$

Unfortunately, this simple protection scheme offered by concrete breaks down in the presence of chloride ions. Chloride ions can penetrate the passive film on iron in concrete and carry ferrous ions away from the anodic areas as transient complexes, thus preventing polarization of the anode. In this way, considerable corrosion can take place.

$$Fe^{++} + Cl^- \rightarrow [\text{FeCl complex}]^+ \quad (4)$$

$$[\text{FeCl complex}]^+ + 2OH^- \rightarrow Fe(OH)_2 \quad (5)$$

and, by subsequent oxidation,

$$Fe(OH)_2 \rightarrow Fe(OH)_3 \quad (5a)$$

In earlier work (4), we used calcium nitrite as an admixture in concrete to prevent corrosion of iron and found that it reacts with ferrous ions as follows:

$$2Fe^{++} + 2OH^- + 2NO_2^- \rightarrow 2NO + Fe_2O_3 + H_2O \quad (6)$$

In this way, a tight protective film is produced around the iron to prevent chloride penetration and further corrosion.

To show the effects of any protective system in concrete is not simple, because the corrosion process that actually disrupts the concrete takes place over many years. Corrosion depends not only on the chloride ion concentration but also on the water content, the availability of oxygen, and the concrete itself.

Most rapid methods test only one aspect of the process. In our development of a corrosion-inhibiting admixture, we used a number of test methods previously reported in the literature.

Our testing program was divided into five different studies:

1. Measurements of the open-circuit potential of steel in concrete placed in chloride solutions,
2. Measurements of the polarization of steel in concrete placed in chloride solutions,
3. Measurements of the induced electrolysis of concrete in chloride solutions,
4. Electrical measurements of steel in limewater, and
5. Accelerated bridge-deck-corrosion tests involving daily ponding with 3 percent sodium chloride solution.

TESTING PROGRAM

Open-Circuit Potential

A valuable tool for assessing whether corrosion is progressing in concrete is the measurement of the spontaneous potential of the iron versus a standard electrode (5, 6). Tafel has shown that the change in measured potential (η) is proportional to the current density (i) (7)

$$\eta = \beta \log i + K \quad (7)$$

where β and K are constants. Thus, a large change in potential is approximately proportional to a large increase in current or rate of corrosion.

The open-circuit potential (E) is actually composed of several factors (see Equation 8).

$$E_{\text{open-circuit}} = E^\circ_{O_2} - E^\circ_{Fe} - (RT/2F) \log \{[Fe^{++}] [OH^-]^2/P_{O_2}\} + \eta \quad (8)$$

where

R = gas constant,
T = temperature, and
F = Faraday's constant.

Although there are concentration changes as corrosion progresses, the major change in potential is due to η. Also, in Equation 8, the transfer coefficients of the anodic and cathodic reactions, which indicate the fraction of the additional electric field added by the activation polarization and are used to decrease the chemical activation energy of the electrode reactions, have been neglected.

The specimens were 7×7×22 cm (2.8×2.8×8.8 in) and were made from ASTM C185 mortar in 0.95-L (1-qt) waxed cardboard containers and had no. 4 rebars embedded. The specimens were cured 1 week at 24°C (75°F) and 100 percent relative humidity, and then half were immersed in saturated sodium chloride solution and the other half were dried to constant weight [4 d at 50°C (122°F) and 0 percent relative humidity] before immersion to a depth of approximately 11 cm (4.4 in). The potentials of these specimens were followed for more than 1000 h, when it became clear that all specimens, even the inhibited ones, were exhibiting active potentials. At first, this was ascribed to the accelerated nature of the test, but careful examination suggested that the rust on the protruding section of rebar might be in electrical contact with the damp concrete. Breaking several specimens apart showed that, on the whole, the uninhibited specimens and those that contained 0.5 percent $Ca(NO_2)_2$ (based on cement) had rust spots well within the concrete, but those that contained 2 percent $Ca(NO_2)_2$ as well as some of those that contained 1 percent $Ca(NO_2)_2$ were corroded only at the steel-concrete-air interface. When the specimens were sandblasted to remove a cone about 1 cm (0.4 in) deep and this was filled with epoxy, the potentials decreased up to 200 mV for those specimens that had the larger quantities of inhibitor.

Polarization

When an external negative potential is impressed on iron beyond the normal corrosion levels, an insulating film forms over the surface and the corrosion rate decreases. Thus, by impressing a potential across steel embedded in concrete, we can study the relationship

Figure 1. Polarization diagram.

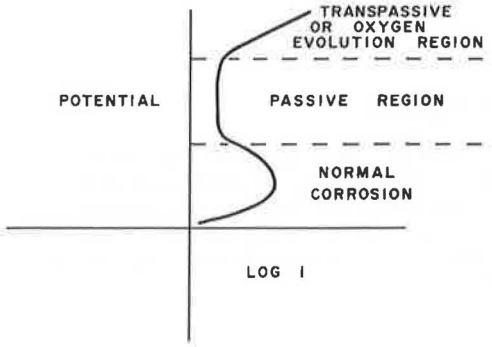

Figure 2. Polarization of steel in concrete.

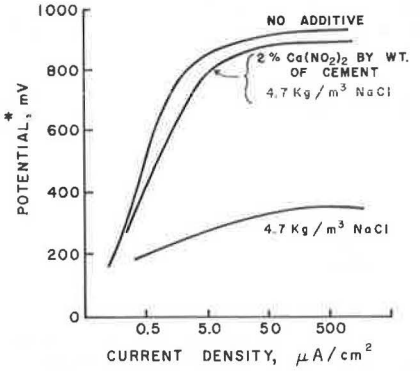

Note: 1 $\mu A/cm^2$ = 6.5 $\mu A/in^2$ and 1 kg/m^3 = 1.69 lb/yd^3.

between potential and corrosion rate (see Figure 1).

Mortar (prepared according to the recipe of ASTM C185 but using concrete sand) was cast into 10.2× 20.3-cm (4×8-in) molds around no. 4 reinforcing bars that had been sandblasted. After curing for 7 d, the specimens were subjected to impressed anodic currents of 0.05 to 200 mA over the whole iron area [approximately 20 cm^2 (3 in^2)], and the change from the open-circuit potential was measured. Figure 2 shows the potential versus current density curves for specimens tested in saturated NaCl solution immediately after moist curing for 1 week and for specimens containing 4.7 kg/m^3 (8 lb/yd^3) of NaCl and tested in saturated NaCl solution after 1 week of moist curing.

Induced Electrolysis

Because corrosion is an electrochemical phenomenon that leads to the destruction of concrete over a period of many years, it seems logical to speed up the process by externally increasing the voltage to increase the rate, which would enable the whole process to be studied in several months.

Thus, specimens similar to those used for the polarization studies were cured 28 d, then soaked in 5 percent NaCl solution for 28 d, and subjected to 10 V of impressed potential in saturated NaCl solution.

Limewater as a Substitute for Concrete

Although a solution of limewater can never duplicate the environment inside concrete (which changes over the years), it does show the corrosion susceptibility of steel at a pH of 12.5. And indeed, the slope of a plot of voltage versus current is the same in limewater and in concrete (8).

Table 1. Concrete properties of bridge decks.

$Ca(NO_2)_2$ (percent by weight of cement)	Water-to-Cement Ratio	Slump (cm)	Air (percent)	Compressive Strength (MPa)		
				3 d	7 d	28 d
Series 1						
0		11.1	5.5	19.96	24.0	31.0
1		12.1	6.4	21.6	25.4	35.0
2		10.2	4.8	25.1	28.3	39.2
3		10.8	4.9	28.3	33.9	43.8
Series 2						
0	0.57	12.1	4.5	15.1	19.2	24.8
1	0.57	7.6	5.8	16.6	20.4	26.4
2	0.56	8.25	4.6	21.6	25.5	31.1
Series 3						
0		15.2	2.0	18.5	24.4	32.4
1	0.61	13.3	1.9	18.7	26.4	33.8
2	0.62	15.2	2.8	19.7	29.1	36.3
Series 4						
0	0.53	14.0	5.8	21.3	28.9	35.3
2	0.55	14.0	5.2	24.4	33.7	43.1
Series 5						
0	0.57	10.2	4.8			
1	0.58	9.5	5.2			
2	0.59	12.7	4.8			

Note: 1 cm = 0.4 in and 1 MPa = 145 lbf/in^2.

Thus, no. 3 reinforcing bars were totally immersed in aqueous solutions containing various amounts of NaCl and $Ca(NO_2)_2$ and containing excess calcium hydroxide. The bars were removed after 1 h for determination of open-circuit potential and polarization.

Accelerated Bridge-Deck-Corrosion Tests

Probably the closest way to approximate the actual corrosion process is to construct bridge decks and salt them daily. This procedure was pioneered by the Federal Highway Administration (9) and the California Department of Transportation. This is a highly exaggerated test because the salting is daily, the steel is 5.1 cm (2 in) on centers, and the concrete cover is only 2.5 cm (1 in) thick. Thus, five series of concrete decks were constructed. Each deck was 1.8×0.6×0.15 m (6× 2×0.5 ft). Each series contained decks that had 0, 1, and 2 percent $Ca(NO_2)_2$ by weight of the cement. The series are described below:

1. Ready-mix concrete that contained an air-entraining agent,
2. Small-batch concrete that contained an air-entraining agent,
3. Small-batch concrete that did not contain an air-entraining agent,
4. Small-batch concrete that contained an air-entraining agent and a water-reducing agent [decks only at 0 and 2 percent $Ca(NO_2)_2$], and
5. Small-batch concrete that contained an air-entraining agent (repeat of series 2).

All slabs were formulated along the design of the Federal Highway Administration, cast, cured, fitted with dams, and then treated with 3 percent NaCl solution daily. The undersides of the decks were fitted with skirts (essentially upside-down dams) to prevent runoff NaCl solution from traveling around to the bottom of the deck and causing corrosion there. Plastic feet on the chairs used to support the rebars also helped to keep the bottoms free of corrosion and spalling. Two rebar mats were used; the upper one consisted of no. 5 rebars on 5.1-cm (2-in) centers. A connection to the rebars was taped and then potted in silicone caulking

Figure 3. Open-circuit potentials of reinforcing steel in mortar.

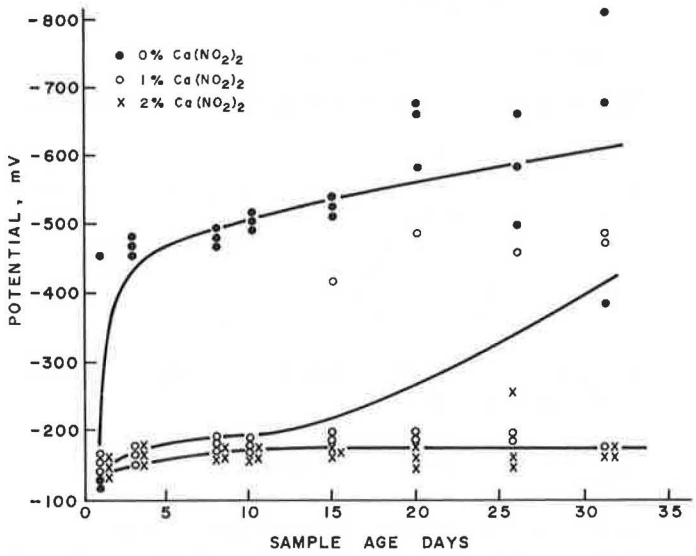

Figure 4. Induced electrolysis.

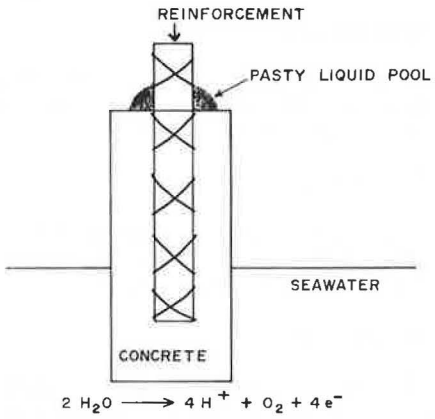

Figure 5. Voltage distribution : experimental bridge deck.

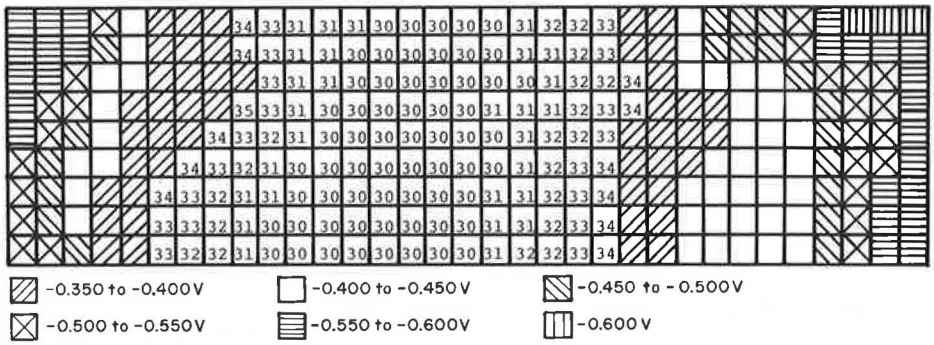

Notes: Values x 10 are negative potentials versus the Cu-$CuSO_4$ electrode.
Series 3: no additive and length of test = 23 weeks.

compound. The concrete properties of the decks are given in Table 1.

Open-Circuit Potential Measurements

Before making the open-circuit measurements on the decks, the salt solution was swept off and the decks were flushed with clean water and sponge dried. After 15 min to 1 h, depending on wind and temperature conditions, the decks had dried to the point where the concrete was still damp, but the sheen of water was gone. A commercial copper-copper sulfate reference electrode was connected through an autoranging digital voltmeter to the rebar mat by means of the wire attached before the concrete was poured. A sponge, approximately 3×3×3 cm (1.2×1.2×1.2 in), soaked in 3 percent NaCl solution was attached to the porous cap of the reference cell, and the potentials were measured on each deck. The decks were mapped by dividing them into a 9 by 33 grid of 5.1×5.1-cm squares.

X-Ray Measurements

Ten 35.6×52.6-cm (14×17-in) x-ray pictures were taken of selected concrete slabs. The irradiation source was 3.7 TBq (100 curies) of iridium-192 in a 2.5×2.5-mm (0.1×0.1-in) cylinder. The energies of the gamma rays were 0.50 and 7.5 aJ (310 and 470 keV). The x-ray pictures show the positions of the rebars, tie wires, furniture, and voids.

Sonic Testing

Sonic testing was attempted by using ultrasonic-pulse-velocity test equipment. Although it appeared that gross abnormalities could be recognized easily, the method was premature for the degree of concrete deterioration we have encountered to date.

Chloride Analysis

After 6 months of daily salting, a 76×23-cm (30×9-in) portion of one deck (the blank of series 2) was sawed off and brought inside for further examination. Holes were drilled in 1.2- and 2.2-cm (0.5- and 0.87-in) depth increments by using a carbide bit and, after extraction, the concrete dust was analyzed by Volhard titration. Then, the top 2.5 cm of concrete was removed by hammer and chisel. Areas of corrosion were noted by discolorations in the concrete and on the steel.

Corrosometer Probes

Corrosometer probes were hung below the rebars and insulated from them at a mean depth of 5.1 cm. Readings were taken weekly.

RESULTS

Open-Circuit Potential

Figure 3 shows the open-circuit potentials we obtained after we corrected for the corrosion taking place on the steel outside the concrete.

Polarization

Figure 2 compares the polarization results we obtained when $Ca(NO_2)_2$ was used in the mortar with the results obtained when it was not used.

Induced Electrolysis

All of the samples, whether or not they contained $Ca(NO_2)_2$, ruptured after about 1 week of electrolysis at 10 V. The rupture was in most cases preceded by a green pasty liquid that rose to the top of the concrete, as shown in Figure 4.

Limewater as a Substitute for Concrete

The results we obtained in limewater are shown below.

$Ca(NO_2)_2$ (%)	Potential (mV)			
	No NaCl	0.3 Percent NaCl	1.0 Percent NaCl	3.0 Percent NaCl
0	210	380	418	545
0.3	219	204	217	315
1.0	205	194	212	245
3.0	210	206	233	253

Here it can be seen that $Ca(NO_2)_2$ maintains the potential in the passive region.

Accelerated Bridge-Deck-Corrosion Tests

In Figure 5, the type of data that was collected from our five series of decks is shown. Previously, we had established the relationship shown in Figure 6 between the potential and the instantaneous corrosion rate.

Thus, we have chosen to show our results on these series of decks in terms of the corrosion rate, the summary of which is shown in Figure 7. These data were collected after about 6 months of daily salting, which is comparable to more than 7 years of salting on the roads in Kansas (9). The data collected 1 month later showed a very slight increase in overall corrosion. The lower temperatures in the winter will probably retard corrosion.

The data collected on a regular basis from each deck were analyzed by computer. Our goal was to use these data to predict a useful lifetime. The data were reduced from 297 data points for each deck to 33. The first analysis is shown in Figures 8 and 9.

This method of data compilation shows that the domains of the concretes that do not have an admixed corrosion inhibitor overlap, although there is some variability from series to series. However, among the domains of the decks that contain 2 percent $Ca(NO_2)_2$, there are two distinct groups and, when we compare the strength data for these decks (given in Table 1) with these results, it appears that $Ca(NO_2)_2$ is more effective with higher strength concrete. When series 2 and 5 are

Figure 6. Linear polarization.

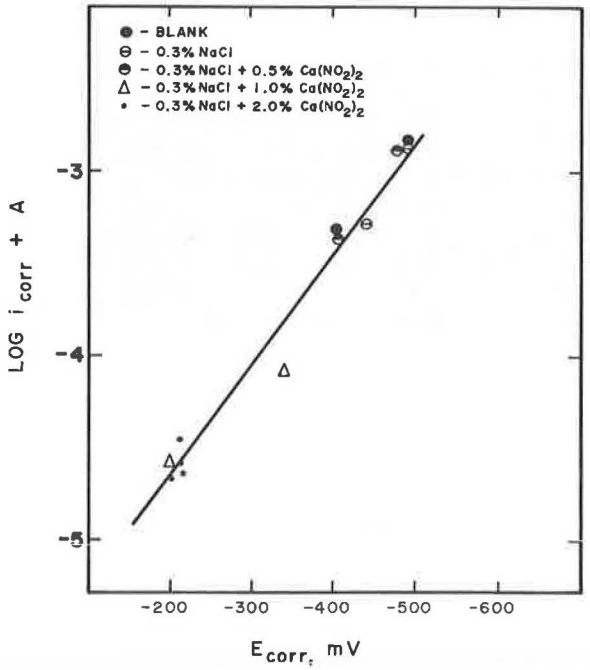

Figure 7. Average rate of corrosion as determined by potential distribution in experimental bridge decks.

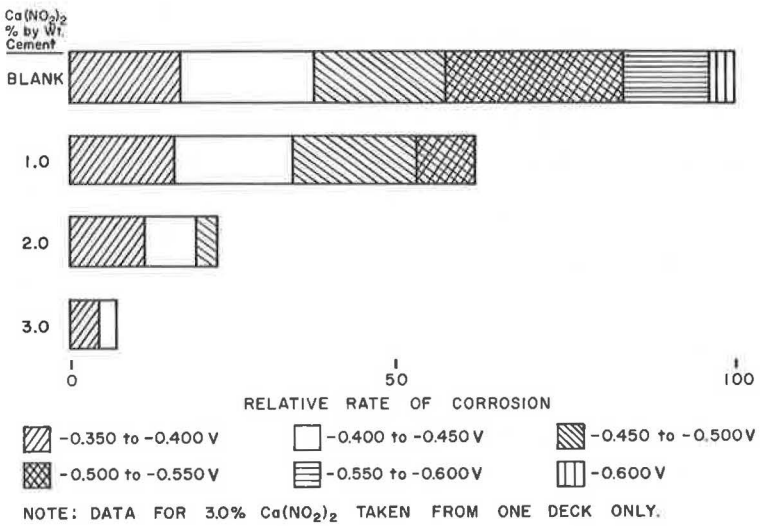

Figure 8. First data analysis : concrete containing 0 percent $Ca(NO_2)_2$.

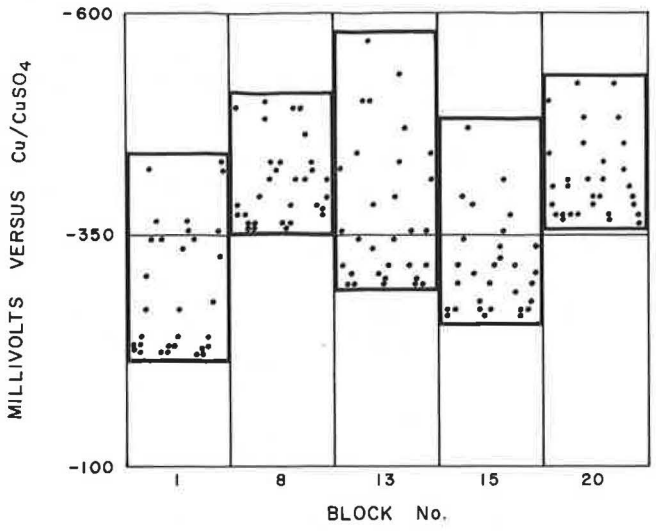

Figure 9. First data analysis : concrete containing 2 percent $Ca(NO_2)_2$.

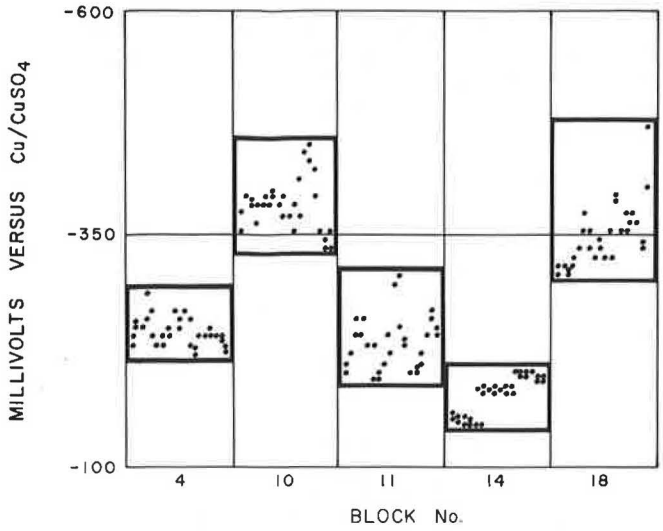

Figure 10. Normalized rate of corrosion obtained by using data from high-strength series (1, 3, and 4) only.

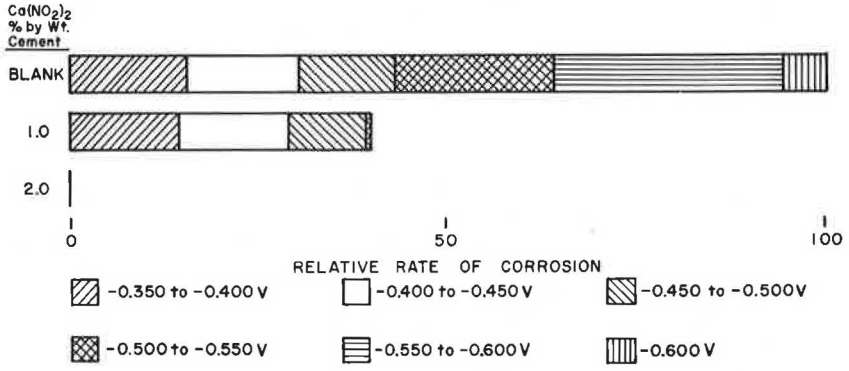

eliminated, the summary of the data becomes as shown in Figure 10.

At present, we are planning to construct more decks to confirm this finding. We determined that the chloride ion concentration was 5.9 kg/m^3 (10 lb/yd^3) at the depth of the steel and that the corroded area was in the immediate vicinity of the highest potential reading obtained. This is in agreement with our previous findings (8).

The x-rays of the decks were not clear enough to be related to the corrosion. The same seems to be true of the sonic testing also. There was not enough of a difference in the small areas examined to warrant further investigation. The corrosometer probes in the concrete have not shown significant changes.

DISCUSSION OF RESULTS

The open-circuit potential that was measured in concrete can be considered to be composed of several contributions (see Equation 8).

The standard potentials do not change. The potential contribution due to the change in concentration of ferrous and hydroxide ions is relatively small. The large change noted in this study is due to the corrosion-process contribution (see Equation 7). Although it is presumed that, once started, the corrosion process continues, there were no data found in this study to relate actual life times of concrete structures to electrical measurements of samples. Stratfull has found that there is a relationship between high potential readings and eventual cracking of the concrete (11). Andrade (12) found, in prestressed concrete that contained 2 percent calcium chloride by mass of cement, that the nitrite inhibitor was still effective after 5.5 years of testing.

Polarization curves show that a passive film will form on iron in concrete. It appears from Figure 3 that a protective coating on steel in concrete can form only when chloride is not present or when both chloride and calcium nitrite are present.

Although corrosion is an electrochemical phenomenon, speeding up the process by induced electrolysis is not recommended because, as the potential is increased, the reactions in concrete change. Rather than the corrosion reaction shown in Equation 2, water is electrolyzed

$$2H_2O \rightarrow 4H^+ + O_2 + 4e^- \quad (9)$$

and hydrogen ions are produced. Hartt and Turner (13) found that, when they put samples under constant current or a high potential, the pH measurements of the solutions that oozed to the top ranged from less than 0 to an upper limit of 4. Not only will the H^+ and O_2 produced damage the iron in the concrete and at the top of the sample, but also the acid will destroy the concrete itself.

Testing in limewater has proved valuable because the results correlate well with those found in concrete. In the accelerated bridge-deck-corrosion testing, there appears to be a correlation between the strength of the concrete and the effectiveness of calcium nitrite. When only concrete that has a 28-d compressive strength of more than 34.5 MPa (5000 lbf/in^2) is con-

sidered, the inhibitor-containing concrete is free of corrosion. This is not too unusual because strong concrete will aid the formation of a tight passive film on the steel. In weaker concrete, where some signs of corrosion are apparent even when $Ca(NO_2)_2$ is present, inhibited concrete still shows less corrosion than the unprotected concrete.

CONCLUSIONS

Accelerated tests for determining the corrosion susceptibility of iron in concrete, such as

1. Open-circuit-potential measurements in concrete,
2. Polarization measurements in concrete, and
3. Similar electrical measurements in limewater,

show that $Ca(NO_2)_2$ offers effective corrosion protection.

Induced electrolysis of concrete is not a reliable technique for studying a corrosion inhibitor when electrolysis of water takes place.

Large deck tests confirm the effectiveness of $Ca(NO_2)_2$ as a corrosion inhibitor in concrete after 6 months of daily salting. Because this is an accelerated-test procedure, the use of $Ca(NO_2)_2$ as an inhibitor should lead to many years of corrosion-free concrete.

REFERENCES

1. H. H. Uhlig. Corrosion and Corrosion Control. Wiley, New York, 1971, p. 1.
2. D. Gilroy and J. E. O. Mayne. British Corrosion Journal, Vol. 1, Nov. 1965, pp. 102-106.
3. W. M. Latimer. Oxidation Potentials. Prentice-Hall, New York, 2nd Ed., 1952, p. 228.
4. A. M. Rosenberg, J. M. Gaidis, T. G. Kossivas, and R. W. Previte. ASTM, Special Technical Publication 629, 1977, pp. 89-99.
5. K. C. Clear. Rebar Corrosion in Concrete: Effect of Special Treatments. ACI, Publication SP-49, 1975, pp. 71-82.
6. R. F. Stratfull, W. J. Jurkovich, and D. L. Spellman. Corrosion Testing of Bridge Decks. Paper presented at the 54th Annual Meeting, TRB, 1975; California Transportation Laboratory, Res. Rept. CA-DOT-TL-5116-12-75-03, 1975.
7. H. H. Uhlig. Corrosion and Corrosion Control. Wiley, New York, 1971, p. 45.
8. J. T. Lundquist, Jr., A. M. Rosenbert, and J. M. Gaidis. A Corrosion Inhibitor Formulated With Calcium Nitrite for Chloride-Containing Concrete: II—Improved Electrochemical Test Procedure. Paper presented at National Association of Corrosion Engineers Meeting, San Francisco, 1977.
9. K. C. Clear and R. E. Hay. Time-to-Corrosion of Reinforcing Steel in Concrete Slabs. Federal Highway Administration, Rept. RD-73-32, April 1973.
10. B. F. McCollom. Design and Construction of Conventional Bridge Decks That Are More Resistant to Spalling. TRB, Transportation Research Record 604, 1976, pp. 1-5.
11. R. F. Spellman. Half-Cell Potentials and the Corrosion of Steel in Concrete. California Department of Public Works, Division of Highways, Res. Rept. CA-HY-MR-5116-7-72-42, Nov. 1972.
12. C. Andrade. The Inhibitive Action of Different Quantities of $NaNO_2$. Cuadernos de Investagacion, Instituto Edwardo Tourroja de la Construction y del Cemento, Madrid, No. 30, 1974, p. 15.
13. D. H. Turner. Cracking of Concrete Due to Corrosion of Various Embedded Metals. College of Engineering, Florida Atlantic University, Boca Raton, thesis, 1976.

Publication of this paper sponsored by Committee on Corrosion.

Measurement of Cement Content by Using Nuclear Backscatter-and-Absorption Gauge

Terry M. Mitchell, Office of Research, Federal Highway Administration

The delays inherent in current methods for the quality control of portland cement concrete allow large volumes to be placed before problems are discovered. This paper discusses an instrument and a test method for obtaining early quality information: The device is a nuclear backscatter-and-absorption gauge that measures the cement content of plastic concrete. The paper includes a description of the device, a summary of two laboratory evaluation studies, and a discussion of the data obtained by using the gauge on five highway construction projects. Laboratory evaluations established the accuracy of the gauge, its field worthiness and dependence on aggregate composition, and its lack of dependence on concrete density, temperature, and other batching variables. The results showed accuracies of ±13 kg/m³ (±22 lb/yd³) for most siliceous aggregate mixes and ±18 kg/m³ (±31 lb/yd³) for calcareous aggregate mixes. In most cases, nuclear-gauge determinations on the field sites agreed with calculated cement factors established from batch tickets. Discrepancies encountered on two of the field projects are discussed. The major limitations of the gauge are the necessity for recalibration whenever the aggregate source or the ratio of coarse to fine aggregates is changed and its reduced accuracy for calcareous and certain siliceous aggregates.

The need for early-age composition measurements on portland cement concrete is becoming more and more evident. Reliance on compressive-strength tests made 7 or 28 d after placement can allow large quantities of pavement or structural concrete to be placed before defects are discovered. Accelerated strength tests, which

give results after 24 or 48 h, reduce the delays before problems become known, but even these shorter delays may be very costly. Gravimetric control also has shortcomings; it leaves the quality of the final concrete subject to scale errors, to accidental substitution of incorrect materials (e.g., fly ash for cement), and to other batching and mixing problems.

A rapid field test for the cement content of plastic concrete would allow an earlier assessment of the eventual quality of the materials. Several methods (1, 2, 3, 4) have been developed recently for cement-content measurements. One, a nuclear backscatter-and-absorption gauge, is the subject of this paper. The paper includes (a) a description of the device, (b) a summary of the results of laboratory evaluations, and (c) a discussion of some of the data obtained by using the gauge at construction sites.

Figure 1. Configuration of probe and concrete sample.

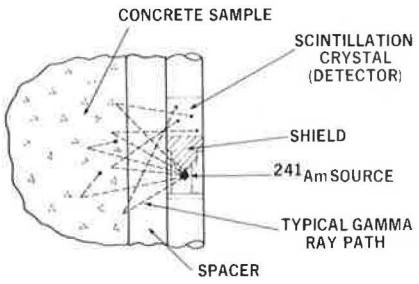

Figure 2. Cement-content gauge: polymer-impregnated concrete test standard, sample holder and probe, and analyzer.

Figure 3. Schematic of sample holder and probe.

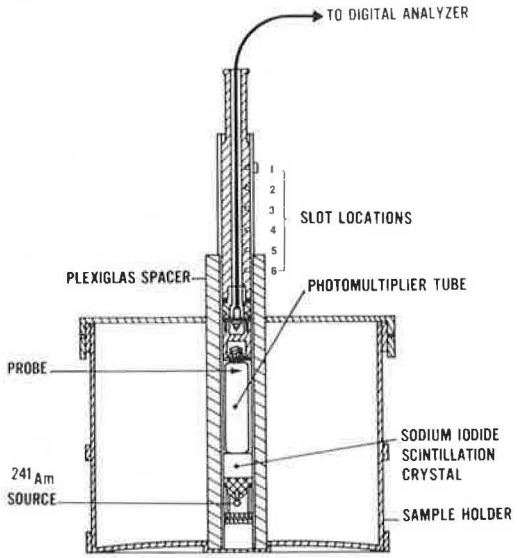

DESCRIPTION OF DEVICE

The principles underlying the operation of the cement-content gauge are similar to those involved in the widely used nuclear gauges for measuring the density of soils and bituminous pavements. However, the cement-content gauge uses a much lower energy source than does the density gauge and, hence, the chemically sensitive, photoelectric absorption process is the dominant attenuating mechanism for the gamma rays.

Figure 1 shows a cement-content gauge probe immersed in a concrete sample. The probe contains a 14-mCi low-energy (60-keV) gamma-ray source (americium-241) and a radiation detector [a 25-mm (1-in) diameter by 25-mm-long sodium iodide scintillation crystal and a photomultiplier tube]. The detector is shielded on the direct line from the source, so that the only path by which the gamma rays can reach the detector is through the sample. The figure shows typical gamma-ray paths; the gamma rays are both scattered and absorbed by a concrete sample. The amount of absorption depends strongly on the chemical composition of the sample, particularly on the quantities of high-atomic-number (high-Z) elements present. Calcium is generally among the highest Z elements present in significant quantities in concrete; it also occurs in fairly constant amounts in portland cements of various types and sources. Thus, as the proportion of cement in concrete is increased, the number of gamma rays absorbed in the concrete is also increased and the fraction of the original gamma rays that will reach the detector is correspondingly reduced.

Figure 2 shows the components that make up the most recent model of the gauge. These include a polymer-impregnated concrete (PIC) test standard, the probe sitting in a sample holder, and an analyzer. The PIC standard is used to periodically determine a standard count, so that a count-ratio procedure can be used to compensate for changes in the electronics with time and temperature. For testing, the analyzer is connected to the probe by a length of coaxial cable; it is a portable single-channel analyzer whose main function is to count the pulses that arrive from the probe. It also provides the high voltage necessary to operate the photomultipier tube. The probe and sample holder are shown schematically in Figure 3. The sample holder is a slightly modified 0.03-m^3 (1-ft^3) unit-weight bucket.

One cement-content determination takes less than 15 min to complete, including the time required to fill the sample holder before the test and to empty and clean it afterwards. After establishing the standard count by using the PIC standard, the sample holder is filled with the fresh concrete sample according to the standard procedure for filling unit-weight buckets (AASHTO T121). A sequence of six 20-s counts is then made by placing the probe at the vertical slot locations 25 mm apart in the sample.

The operator calculates the ratio of the observed sample count (the average of the six readings) to the standard count and reads the corresponding cement content from a previously established calibration curve such as that shown in Figure 4. The calibration curves of count ratio as a function of cement factor are constructed

Figure 4. Typical calibration curve (95 percent confidence limits).

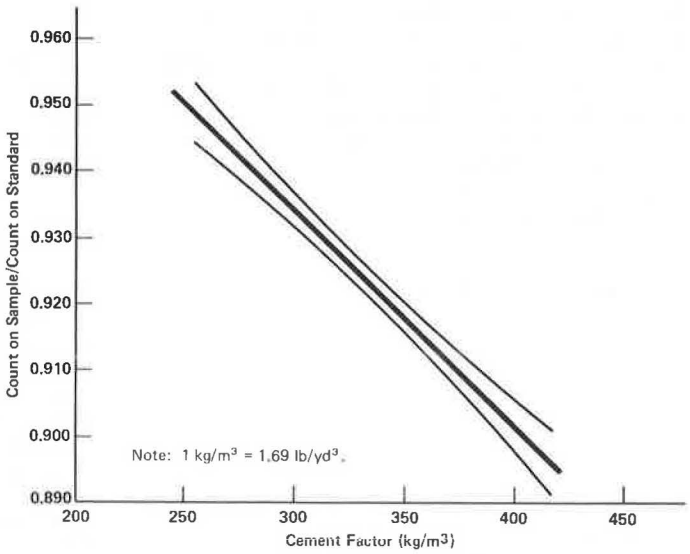

Figure 5. Calibration curves for two aggregates and three ratios of coarse to fine aggregates: state A.

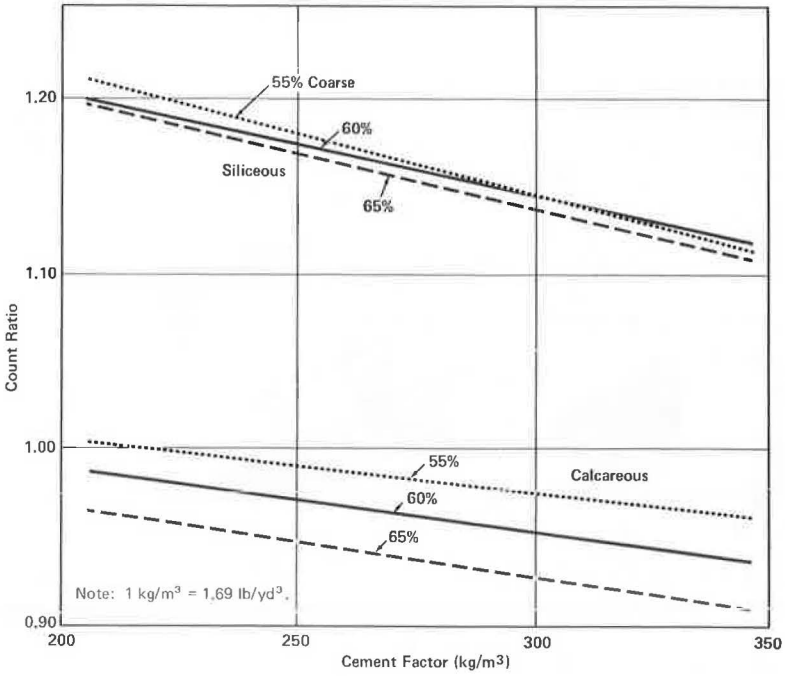

in the laboratory for each concrete job by using small, carefully controlled laboratory batches for which the actual cement factor can be established from the weights of the components.

That the response of the nuclear gauge depends not only on the calcium content but also on all of the elements in the mix (particularly those having a high Z-value) leads to the main limitation on its usefulness; i.e., whenever the aggregate composition is changed significantly, a new calibration curve is required. New calibration curves are required for each distinct aggregate source or combination, for each significant change in the ratio of coarse to fine aggregate when the two sizes are not chemically alike, and (possibly) for within-quarry chemical composition changes in a single aggregate.

Detailed information on the design and operation of the instrument is available in an operating manual (5).

LABORATORY EVALUATIONS

The first of two laboratory evaluations of the cement content gauge was completed at the Federal Highway Administration (FHWA) Fairbank Highway Research Station in 1973 (6).

Two coarse aggregates (25.4-mm maximum size) were used in the main part of the evaluation; one was siliceous (a river gravel) and had very little intrinsic high-Z material and the other was calcareous (a dolomitic limestone) and had more than 20 percent calcium. A siliceous fine aggregate (quartz grains) and a type 1 cement were used throughout. It was anticipated that concretes made with aggregates that had large quantities of calcium and other high-Z elements would have low count rates, reduced sensitivities (changes in count rate per unit change in cement content), and less accurate cement-content determinations.

Tests of mixes made with each of the two aggregates over a range of cement factors [270 to 400 kg/m^3 (450

Figure 6. Nuclear and gravimetric cement factors: project B-1.

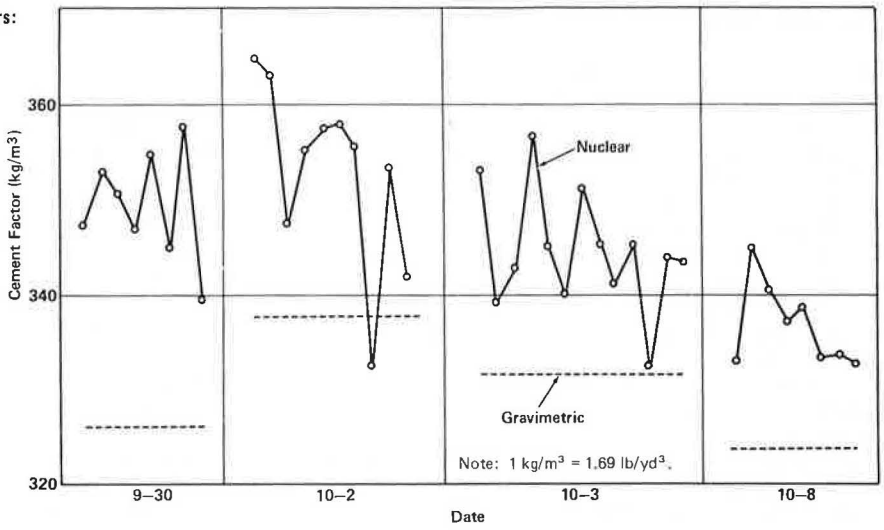

to 670 lb/yd^3)] and densities [2180 to 2400 kg/m^3 (136 to 150 lb/ft^3)] gave the following results (1 kg/m^3 = 1.69 lb/yd^3):

Type of Coarse Aggregate	N	Standard Error (kg/m^3)
Siliceous	45	13
Calcareous	90	18

(The standard error is the root-mean-square of the difference between the cement factor as determined by using the nuclear gauge and the actual cement factor of a batch as determined from the weights of the components.)

The effect of varying the proportions of coarse to the fine aggregates when the two components are distinctly different chemically was also noted in this evaluation. Data were obtained by using the calcareous coarse and the siliceous fine aggregates in two different proportions, 65 and 50 percent coarse. When the calibration curve for the 65 percent coarse-aggregate concrete was used to determine the cement content of samples in which this aggregate made up only 50 percent of the total aggregate volume, the resulting errors were found to average about 160 kg/m^3 (270 lb/yd^3). This shows that a specific calibration curve is required for each ratio of coarse to fine aggregates when the two fractions differ chemically.

Temperature was found to significantly affect the raw gauge counts, but the effect was eliminated when the count-ratio procedure was used with the PIC standard. The gauge geometry is such that its response is relatively independent of the concrete density over the range studied. The response also does not vary with either water or air contents over the usual range of those variables in highway concrete.

A second laboratory evaluation was undertaken in 1976 in state A, and the results were recently published (7). Two coarse aggregates were used, one siliceous (an alluvial gravel) and the other calcareous (a crushed limestone), in combination with a single siliceous fine aggregate and a type 1 cement. The cement factors ranged from 220 to 350 kg/m^3 (370 to 590 lb/yd^3).

The results of this evaluation are shown below (1 kg/m^3 = 1.69 lb/yd^3).

Type of Coarse Aggregate	N	Standard Error (kg/m^3)
Siliceous	84	8
Calcareous	84	17

These results also show that there is a considerable loss of accuracy when the aggregate matrix is calcareous; however, it is still possible to make valid measurements on concrete mixes that contain these aggregates (albeit at a lower level of accuracy).

The effect of varying the ratio of coarse to fine aggregates can be seen in Figure 5. Among the siliceous coarse-aggregate samples, the slight differences between the calibration curves suggest that the 60 percent coarse-aggregate curve could be used for samples anywhere in the range of 55 to 65 percent coarse. When this curve was used as the calibration curve for all 84 of the siliceous aggregate samples, regardless of the coarse-aggregate percentage, the standard error was ±14 kg/m^3 (±23 lb/yd^3).

Among the calcareous coarse-aggregate mixes, however, if the 60 percent curve were used for a sample that had 65 percent coarse aggregate, the resulting error in the cement factor would be greater than 70 kg/m^3 (120 lb/yd^3). This confirms the need for individual calibration curves for different ratios of coarse to fine aggregate. Even when the ratio is held constant, the gauge will be less accurate for calcareous aggregate than for siliceous aggregate mixes because of reduced sensitivity. For the calcareous aggregates, the gauge was approximately 40 percent less sensitive to changes in cement content; i.e., a given change in cement factor of calcareous aggregate mixes produced a 40 percent smaller change in count rate than did the same change in siliceous aggregate mixes.

The state A researchers also reported an overall estimation of the gauge precision: ±9 kg/m^3 (±15 lb/yd^3) for repeated measurements on the same sample. This value varies from material to material and is much higher for calcareous aggregate mixes than for siliceous aggregate mixes.

Thus, the two laboratory evaluations have shown that the nuclear gauge can be used to determine the cement factor of most siliceous aggregate mixes within 13 kg/m^3 (22 lb/yd^3) of the actual value (65 percent of the time) and of calcareous aggregate mixes within 18 kg/m^3 (31 lb/yd^3) of the actual value. When the coarse and fine aggregates are very different chemically (e.g., calcareous coarse and siliceous fine), these tolerances will apply only at constant ratios of coarse to fine aggregates. Brief laboratory evaluations by states B and C prior to their field tests yielded standard errors below the limiting values suggested here.

FIELD EXPERIENCE

Field trials of nuclear cement-content gauges were undertaken by states B and C during the 1974 construction season.

In state B, one of the prototype gauges was used on three Interstate projects, two of which involved pavements and the other bridge decks. The results were published in a recent FHWA report (8). All of the aggregates used in these projects were siliceous.

The coarse aggregate used on the first project (project B-1) was a 38.1-mm (1½-in) maximum-size crushed granite, the fine aggregate was a natural sand, and the cement was a type 1. Calibration curves were constructed for this and the other two state B projects in the laboratory. The batching plant was a portable paving plant that had an electronic balance-beam scale with overweight and underweight indicators. Concrete was transported in side dump trucks. Test samples were obtained from the concrete between the spreader and the slip-form paver. Field measurements were obtained on the concrete on 4 different days over a 9-day period.

The results of the 39 test measurements obtained on this project are shown in Figure 6, which also shows the gravimetric cement content for each sample, based on the batch-ticket cement content adjusted by periodic unit-weight measurements. All but one of the 39 nuclear measurements indicated cement factors higher than the gravimetric values; the average difference was 16 kg/m^3 (27 lb/yd^3).

The data for project B-1 are summarized below (1 kg/m^3 = 1.69 lb/yd^3):

		Cement Factor (kg/m^3)		
Project	N	Mean Gravimetric	Nuclear	SD of Nuclear
B - 1	39	330	346	9
B - 2	38	329	326	12
B - 3	46	409	403	17

For project B-1, the mean cement factor, as determined by the nuclear gauge, was 346 kg/m^3 (583 lb/yd^3) with a standard deviation of ±9 kg/m^3 (±15 lb/yd^3). The design cement factor for this concrete was 320 kg/m^3 (540 lb/yd^3) but, when adjustments were made for unit weight, the average gravimetric cement factor was 330 kg/m^3 (556 lb/yd^3). The nuclear data did not indicate any apparent quality-control problems with cement content on this project.

The coarse aggregate on the second pavement project (B-2) was also a 38.1-mm crushed granite, the fine aggregate was a manufactured sand from the same source, and the cement a type 1. The batch plant, transporting vehicles, and sampling procedures duplicated those used on project B-1. Field measurements were made on 3 different days in an 8-day period.

As shown above, the mean cement factor, as determined by the nuclear gauge, was 326 kg/m^3 (550 lb/yd^3) and the standard deviation was ±12 kg/m^3 (±20 lb/yd^3). The design cement factor was again 320 kg/m^3, but the mean of the gravimetric cement factors was 329 kg/m^3 (555 lb/yd^3), which is not significantly different from the nuclear-determined values. Again, there were no apparent quality-control problems.

The third project (B-3), several bridge-deck pours, used the same crushed-granite coarse aggregate used in project B-2 and a type 1 cement. The concrete came from a ready-mix plant that had electronic dial scales. The fine aggregate was a blend of a natural sand and the manufactured sand used in project B-2. The blend ratio was initially 80:20 (natural:manufactured) but during the field testing program was changed to 50:50. The chemical difference between the two fine aggregates necessitated the preparation of a new calibration curve when this ratio change was made. A third calibration curve was prepared later on, when the ratio of the coarse to fine aggregates was changed from 65:35 to 62:38 although, in retrospect, a new calibration curve was not necessary in this case; i.e., there was no significant difference in the calibration curves for these two ratios. Field measurements were made on 7 different days over a 1.5-month period.

For this project, the mean cement factor, as determined by the nuclear gauge, was 403 kg/m^3 (679 lb/yd^3) and the standard deviation was ±17 kg/m^3 (±29 lb/yd^3). The design cement factor was 400 kg/m^3 (675 lb/yd^3), and the mean of the gravimetric cement factors was 409 kg/m^3 (690 lb/yd^3). The nuclear-gauge results indicate that there were no apparent problems with the quality of the concrete.

To make conclusions about the quality of concrete in the field (in terms of absolute cement-content measurements), the user must rely on the values for the gauge accuracies established in the laboratory where the cement factors of samples are carefully controlled and known. This is also true for other new methods for determining cement content, because there is no reliable standard of comparison in the field. Gravimetric cement factors based on batch-ticket weights with adjustments for unit weight are not good standards for comparison because they are subject to errors in the ticket weights themselves and to a variety of accidents and questionable practices in batching and mixing procedures.

Some of the conclusions that can be drawn about the concrete on the three state B projects from the nuclear-gauge data are very obvious. For example, on all three, the average of the nuclear-determined cement factors exceeded the design cement factor, a good quality sign from the purchaser's viewpoint. As shown by the standard deviations, the variability of the concrete in the ready-mix project (B-3) significantly exceeded the variability of the concrete in the centrally batched projects. (This is not intended as a general conclusion about the relative variability of concrete from the two types of plants, but merely as a statement showing the kind of information the cement-content gauge can provide.) With more data available (e.g., taking several samples from a single batch), mixer evaluations could be undertaken easily with the nuclear gauge.

State C used a second prototype gauge on two Interstate projects: The first was an overlay paving project that used a calcareous aggregate concrete, and the second was a bridge deck that used a lightweight aggregate.

On both projects, a chemical method was used to determine the cement content of a portion of the concrete used in each nuclear-gauge measurement. This state uses this method, which is based on SO_3 measurement, for cement-factor determinations on mixes in which the aggregates contain both calcium and silicates because such aggregates make ASTM C85 unreliable. The accuracy of the SO_3 procedure is estimated as ±10 percent.

The coarse aggregate used on the first state C project (C-1) was a 38.1-mm crushed limestone, the fine aggregate was a siliceous sand, and the cement was a type 1. The concrete was supplied from a job-site central-mix plant and transported in side dump trucks to the paving operation. Test samples were taken from the forms after placement by the spreader. Field measurements were made on 6 different days over a 1.5-month period.

The 41 nuclear-gauge-determined, the chemically determined, and the gravimetrically determined cement factors are shown in Figure 7. The chemically determined and the nuclear-gauge-determined cement factors

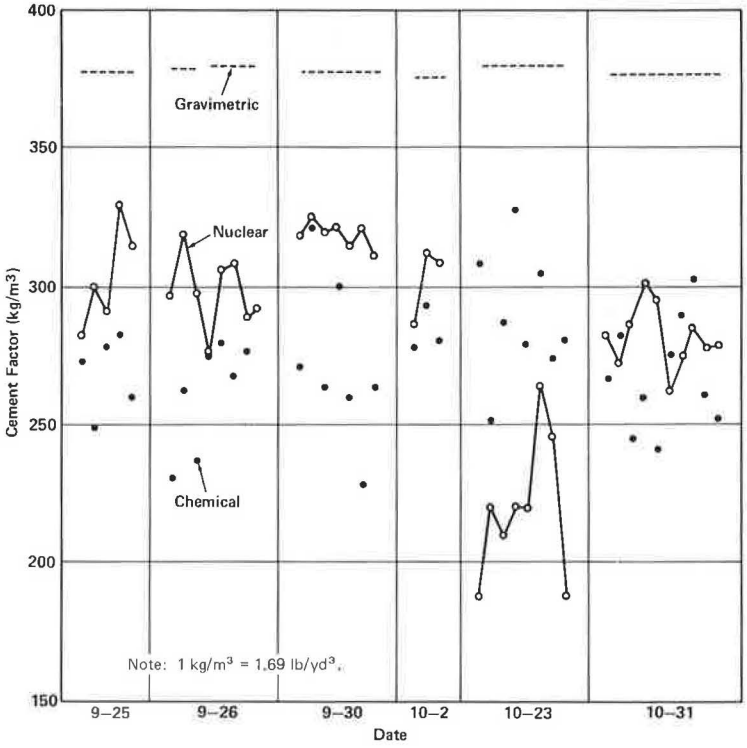

Figure 7. Nuclear, chemical, and gravimetric cement factors: project C-1.

are well below the gravimetric values. The mean cement factor, as determined by the nuclear gauge, was 283 kg/m^3 (477 lb/yd^3), and the standard deviation was 37 kg/m^3 (63 lb/yd^3). The SO_3 determinations showed a mean cement factor of 291 kg/m^3 (490 lb/yd^3) and a standard deviation of 26 kg/m^3 (43 lb/yd^3). These values contrast with the design cement factor of 362 kg/m^3 (610 lb/yd^3) and the average gravimetric factor of 375 kg/m^3 (632 lb/yd^3).

A number of efforts were made to establish the cause of the difference between the batch-ticket determinations and the results of the two test methods. Such items as the scales and gates at the batch plant were checked and found to be operating satisfactorily. The aggregate stockpiles were resampled, and the nuclear-gauge calibration curve was checked and verified. Flexure test specimens indicated that the concrete met minimum strength requirements. A sizable shift in the ratio of coarse to fine aggregate (63:37 to 58:42) would produce a 90 kg/m^3 (150 lb/yd^3) change in the nuclear readings but not in the SO_3 test results; the possibility of such a change was investigated and ruled out.

Early in 1976, some 18 months after placement, cores were taken from the pavement for further investigation. Three 100-mm (4-in) diameter cores were taken from concrete placed on each of the 4 d when the nuclear gauge had been in used. ASTM C85 was used to establish the cement factors of the cores although, as discussed above, the aggregates used in this concrete are a difficult combination for this test method. The results of this test showed cement factors of 294 to 425 kg/m^3 (496 to 716 lb/yd^3) with a mean value of 346 kg/m^3 (584 lb/yd^3); this was about 30 kg/m^3 (50 lb/yd^3) lower than the gravimetric cement contents, but not as low as the nuclear or chemically determined cement contents. The result of all of these investigations, then, was a standoff, and the questions remain unresolved. Sizable cement-content deficiencies were indicated by the nuclear and the SO_3 test procedures. At the same time, the ASTM cement-content test showed much smaller deficiencies, and a very thorough examination of the concrete-plant operations did not locate any cause for the discrepancies.

The coarse aggregate used on the second state C project (C-2) was a 38.1-mm lightweight fired slag, the fine aggregate was a siliceous sand, and the cement was a type 2. The lightweight concrete was supplied from a central-mix plant and transported in agitating trucks. The concrete was sampled randomly as it was discharged from the trucks. Cement-factor measurements were made on 9 different days over a 2.5-month period.

A total of 60 cement-factor determinations were made by each of the three methods: nuclear, chemical, and gravimetric. The mean cement factor, as determined by the nuclear gauge, was 411 kg/m^3 (693 lb/yd^3). This was substantially lower than the averages determined by the SO_3 tests [441 kg/m^3 (743 lb/yd^3)] and the gravimetric tests [444 kg/m^3 (748 lb/yd^3)]. However, the nuclear-gauge data also showed that the within-batch SD for three samples from each of the 10 batches was 5 kg/m^3 (8 lb/yd^3); this indicated very good reproducibility of the method with this aggregate.

Further examination of the nuclear results indicated that there was a distinct change (break) in the data midway through the testing. These results are summarized in Figure 8 in which the data are grouped according to these time periods, one the data taken before the change and the other after. For the first 22 samples, i.e., those taken before November 16, 1974, the two test methods were in good agreement with the gravimetric cement factors: The nuclear-gauge-determined values averaged 435 kg/m^3 (733 lb/yd^3). After the break, the average gauge-determined cement factor was 396 kg/m^3 (668 lb/yd^3). The respective SDs of the two groups were 11 and 13 kg/m^3 (19 and 21 lb/yd^3); these values are comparable to those shown elsewhere in this paper for aggregates that work well in the gauge, i.e., noncalcareous aggregates.

Attempts to locate the cause of the shift in nuclear-gauge readings were not successful, although most likely it was an undiscovered change in either the chemical composition of one of the concrete components or in

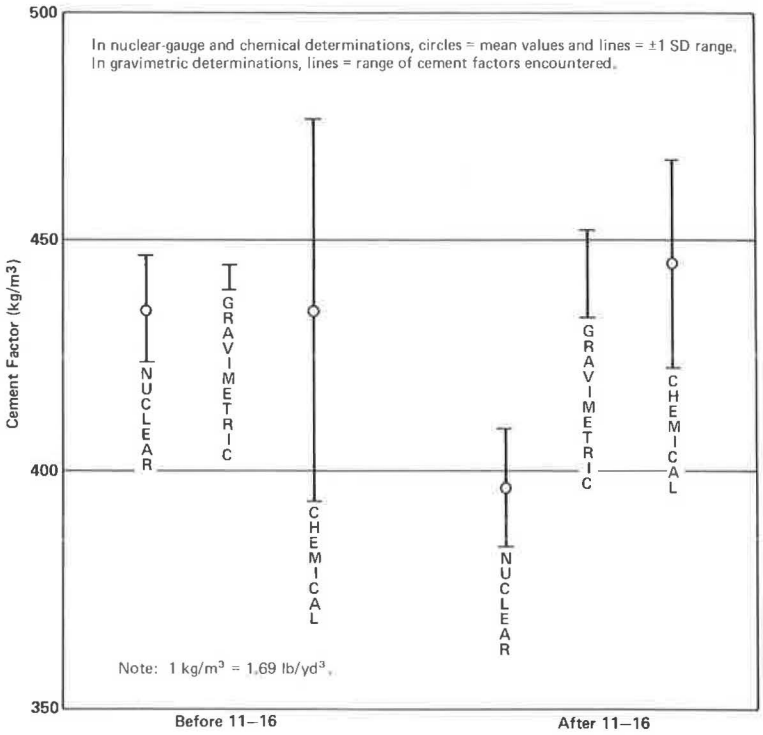

Figure 8. Distributions of nuclear, chemical, and gravimetric cement factors: project C-2 before and after November 16, 1974.

the nuclear-gauge electronics or geometry. The break did coincide with a large change in air temperature at the construction site, but subsequent laboratory tests, as well as the data developed during the laboratory evaluation in state A, rule temperature change out as the cause. The possibility of a change in the chemical composition of the slag aggregate was rejected when a calibration curve constructed by using aggregates sampled at the end of the project showed no significant difference from the curve constructed before testing began.

The break in the nuclear-gauge data limits any conclusions that can be drawn about the concrete quality on project C-2. However, all of the SD values indicate that the batching and mixing were well controlled.

CONCLUSIONS

1. The nuclear cement-content gauge is suitable for rapid field determinations of the cement content of plastic concrete. Possible applications include mixer studies, troubleshooting, and routine quality control.
2. The gauge measures the cement factors of most siliceous aggregate mixes to within ±13 kg/m^3 (±22 lb/yd^3) and of calcareous aggregate mixes to within ±18 kg/m^3 (±31 lb/yd^3) of the true cement content of the sample.
3. The major limitations of the gauge are (a) the necessity for recalibration when the aggregate source is changed or when the ratio of coarse to fine aggregates is changed and (b) its reduced accuracy for calcareous and certain siliceous aggregate concretes.
4. Nuclear-gauge determinations of cement factors agreed with calculated gravimetric cement factors (from batch tickets) on three of the five field projects discussed in this paper and a portion of a fourth. On the fifth project, the nuclear gauge and another cement-content test method showed cement factors that were more than 90 kg/m^3 (150 lb/yd^3) lower than the batch-ticket value.

ACKNOWLEDGMENT

I gratefully acknowledge the assistance of Leland Dong, who, during his tenure as a member of the Federal Highway Administration Implementation Division, developed and monitored the state evaluations of the nuclear cement-content gauge.

REFERENCES

1. T. M. Mitchell. Nuclear Gauge for Measuring the Cement Content of Plastic Concrete. Public Roads, Vol. 38, No. 4, 1974.
2. R. T. Kelly and P. J. Baldwin. The Kelly-Vail Technique for Water and Cement Content. Proc., Conference on Rapid Testing of Concrete, Construction Engineering Research Laboratory, Urbana-Champaign, IL, Rept. M-128, 1975, pp. 19-41.
3. J. A. Forrester. Cement Content by the Rapid Analysis Machine. Proc., Conference on Rapid Testing of Concrete, Construction Engineering Research Laboratory, Urbana-Champaign, IL, Rept. M-128, 1975, pp. 43-53.
4. J. H. Woodstrom and B. J. Neal. Cement Content of Fresh Concrete. California Department of Transportation, Rept. CA-DOT-TL-5149-1-76-55, 1976.
5. T. M. Mitchell. Nuclear Cement-Content Gauge: Instruction Manual. Federal Highway Administration, Rept. FHWA-RD-75-63, 1975.
6. T. M. Mitchell. A Radioisotope Backscatter Gauge for Measuring the Cement Content of Plastic Concrete. Federal Highway Administration, Rept. FHWA-RD-73-48, 1973.
7. S. C. Shah and J. L. Melancon. Nuclear Cement-Content Gauge Comparison Analysis (Louisiana). Federal Highway Administration, Rept. FHWA-TS-78-201, 1977.
8. W. Gulden. Nuclear Cement-Content Gauge Performance Evaluation (Georgia). Federal Highway Administration, Rept. FHWA-RD-75-525, 1975.

Publication of this paper sponsored by Committee on Curing of Concrete.